# Cell differentiation specific inhibition of cell division guarantees the formation of diploid spores during development of *Myxococcus xanthus*

**Dissertation**

zur Erlangung des akademischen Grades
des Doktors der Naturwissenschaften
(Dr. rer. nat.)

dem Fachbereich Biologie
der Philipps-Universität Marburg
vorgelegt

von
**Sabrina Huneke-Vogt**
aus Borchen

Marburg, Juni 2017

Die Untersuchungen zur vorliegenden Arbeit wurden von September 2013 bis April 2017 am Max-Planck-Institut für terrestrische Mikrobiologie in Marburg unter der Leitung von Prof. Dr. MD Lotte Søgaard-Andersen durchgeführt.

Vom Fachbereich Biologie der Philipps Universität Marburg

als Dissertation angenommen am 12.10.2017

Erstgutachter: Prof. Dr. MD Lotte Søgaard-Andersen

Zweitgutachter: Prof. Dr. Martin Thanbichler

Weitere Mitglieder der Prüfungskommission:

Prof. Dr. Torsten Waldminghaus

Dr. Gert Bange

Tag der mündlichen Prüfung: 02.11.2017

Zum Zeitpunkt der Einreichung dieser Dissertation wird die folgende Originalpublikation vorbereitet um die erzielten Ergebnisse zu veröffentlichen:

**Huneke-Vogt, S.** & Søgaard-Andersen, L. (2017). Cell differentiation specific inhibition of cell division guarantees the formation of diploid spores in *Myxococcus xanthus*. (in preparation)

*meinen Eltern*

# Table of contents

# 1. Abbreviations

| | |
|---|---|
| ATP/ADP | Adenosin tri-/diphosphate |
| AU | arbitrary units |
| bp | base pair |
| c-di-GMP | bis-(3´5´)-cyclic dimeric GMP |
| cDNA | complementary DNA |
| Ct | cyclic threshold |
| CTT | casitone Tris medium |
| DIC | differential interference contrast |
| DNA | deoxyribonucleic acid |
| EDTA | ethylenediaminetetraacetic acid |
| eYFP | enhanced yellow fluorescent protein |
| FACS | fluorescent activated cell sorting |
| FSC | forward-scattered light |
| h | hour |
| Km | kanamycine |
| l | litre |
| mCerulean | monomeric Cerulean (cyan fluorescent protein) |
| mCherry | monomeric Cherry (red fluorescent protein) |
| min | minute |
| kDa | kilodalton |
| m- | milli- |
| µ- | micro- |
| M | molarity (mol * $l^{-1}$) |
| pH | negative decimal logarithm of the hydrogen ion activity |
| (p)ppGpp | guanosine pentaphosphate or tetraphosphate |
| RNA | ribonucleic acid |
| SDS-page | sodium dodecyl sulfate polyacrylamide gel electrophoresis |
| sec | second |
| SSC | side-scattered light |
| Strep | streptomycin |
| Tc | tetracycline |
| TEMED | *N*,*N*,*N*′,*N*′-Tetramethylethane-1,2-diamine |
| Tris | 2-Amino-2-hydroxymethyl-propane-1,3-diol |
| v/v | volume per volume |
| w/v | weight per volume |
| WT | wild type |

## 2. Abstract

In response to nutrient starvation, the soil bacterium *Myxococcus xanthus* initiates a complex developmental program resulting in the formation of fruiting bodies inside which the rod-shaped motile cells differentiate into environmentally resistant, spherical and diploid myxospores. Some cells, referred to as peripheral rods, remain as rod-shaped haploid cells outside of fruiting bodies. Replication is essential for fruiting body formation and sporulation. During vegetative conditions, cells grow asynchronously with respect to the cell cycle. The cells contain one to two chromosomes and initiation of replication proceeds immediately after cell division. Here we investigated the mechanism underlying the formation of diploid spores.

We confirmed the diploid chromosome content of mature spores by single cell and cell population analysis. Our results indicated that peripheral rods are cells in various stages of the cell cycle that are able to replicate. To address regulation of cell division, we focused on the key cell division protein FtsZ and its regulators PomX, PomY and PomZ. Experiments in which future myxospores and future peripheral rods were separated demonstrated that the protein levels of these four proteins decreased during development specifically in cells dedicated to become spores. In line with this, we showed that the presence of each of these proteins is not essential for fruiting body formation and sporulation. Transcriptional analysis revealed a decrease in transcript numbers of *ftsZ, pomX*, *pomY* and *pomZ* upon starvation. Moreover we observed that FtsZ is constitutively degraded during vegetative growth as well as during development and has the same half-life under these two conditions. We conclude that FtsZ proteolysis outperforms FtsZ synthesis during development resulting in elimination of FtsZ specifically in future spores. To address whether the decrease in FtsZ level in future spores causes the inhibition of cell division in these cells, we expressed *ftsZ* constitutively in developing cells. Remarkably, many of the spores formed by these cells contained one chromosome. Thus, the elimination of FtsZ in cells destined to become spores inhibits cell division and guarantees the formation of diploid myxospores. Most likely the ATP-dependent protease LonD is indirectly involved in FtsZ turnover but is not responsible for the transcriptional downregulation upon starvation.

Interestingly, sporulation did not depend on chromosome content however, chromosome content affects spore morphology. Cells which enter the developmental program with a chromosome content higher than WT cells form spores that are increased in average size and chromosome content. Although the decrease in FtsZ protein levels and *ftsZ* transcript numbers is specific to starvation, it seems to be independent of RelA and the stringent response. Additionally, regulation of FtsZ levels is independent of the global pool of the second messenger cyclic di-GMP which was shown to be an essential regulator of multicellular development in *M. xanthus*.

# 3. Zusammenfassung

Als Antwort auf nahrungslimitierende Bedingungen initiiert das im Boden lebende Bakterium *Myxococcus xanthus* ein komplexes Entwicklungsprogramm. Dieses führt zur Bildung von Fruchtkörpern in denen die stäbchenförmigen Zellen zu kugelförmigen, diploiden Myxosporen differenzieren, welche extreme Umweltbedingungen überdauern können. Einige Zellen, die als „*peripheral rods*“ bezeichnet werden bleiben haploid außerhalb der Fruchtkörper. Replikation ist essentiell für die Fruchtkörperbildung und Sporulation. Unter vegetativen Bedingungen wachsen die Zellen asynchron hinsichtlich ihres Zellzyklus. Sie enthalten ein bis zwei Chromosomen und auf Replikation folgt Zellteilung. In dieser Arbeit wurde der Mechanismus der zur Bildung von diploiden Sporen führt untersucht.

Wir bestätigten durch die Analyse einzelner Zellen sowie Zellpopulationen, dass Myxosporen zwei Chromosomen beinhalten. Unsere Ergebnisse wiesen darauf hin, dass sich „*peripheral rods*“ in verschiedenen Phasen des Zellzyklus befinden und in der Lage sind zu replizieren. Um die Regulierung der Zellteilung zu untersuchen haben wir uns auf das Haupt-Zellteilungsprotein FtsZ sowie dessen Regulatoren PomX, PomY und PomZ fokussiert. In Experimenten, bei denen zukünftige Sporen und „*peripheral rods*“ getrennt wurden, konnten wir zeigen, dass die Proteinlevel während des Entwicklungsprogramms spezifisch in künftigen Sporen abnehmen. Damit einhergehend war die Präsenz jedes dieser Proteine nicht essentiell für Fruchtkörperbildung und Sporulation. Transkriptionelle Analyse offenbarte eine Abnahme der Anzahl der Tranksripte von *ftsZ*, *pomX*, *pomY* und *pomZ* bei Nahrungslimitation. Zudem wird FtsZ kontinuierlich degradiert, sowohl während vegetativen als auch während nahrungslimitierenden Bedingungen. Wir folgerten, dass FtsZ Proteolyse die Synthese übertrifft, was zu einer Abnahme des Proteinlevels und der Inhibition von Zellteilung in künftigen Sporen führt. Konstitutive *ftsZ* Expression beeinflusste nicht den Sporulations-prozess, resultierte jedoch in die Bildung von Sporen die weniger als zwei Chromosomen beinhalteten. Folglich reicht die Eliminierung von FtsZ aus um Zellteilung zu inhibieren und diploide Sporen zu bilden. In diesen Vorgang, jedoch nicht in die transkriptionelle Regulation, ist wahrscheinlich die ATP-abhängige Protease LonD indirekt involviert.

Sporulation an sich ist unabhängig vom Chromosomengehalt, allerdings beeinflusst die DNA Menge die Morphologie der Sporen. Zellen die mehr Chromosomen als WT Zellen beinhalten und das Entwicklungsprogramm starten, formen Sporen, die eine höhere Durchschnittsgröße und einen höheren DNA Gehalt aufweisen. Obwohl die Abnahme von FtsZ und *ftsZ* Transkripten spezifisch während nahrungslimitierenden Bedingungen stattfindet scheint dies unabhängig von der „*stringent response*“ und RelA zu sein. Außerdem wird FtsZ unabhängig vom globalen Vorkommen des sekundären Botenstoffes zyklisches di-GMP reguliert, welches eine essentielle Rolle im multizellulären Verhalten von *M. xanthus* spielt.

# 4. Introduction

## 4.1. *Myxococcus xanthus* as a model for multicellular behavior of bacterial populations

In bacterial populations, cells sharing the same genetic material may differentiate into various cell types significantly different from one another in their properties and behaviors. These phenotypic variations provide important benefits to the whole group (Munoz-Dorado *et al.*, 2016) and mainly depend on regulation of gene expression in response to environmental changes or intercellular signaling (van Vliet & Ackermann, 2015). Different properties of individual cells is one feature of multicellular behavior (Lyons & Kolter, 2015). One example of multicellularity is the formation of biofilms, which is widespread among bacteria (Lyons & Kolter, 2015). It requires cell differentiation, intercellular communication and cooperation between individual cells (Lyons & Kolter, 2015, Claessen *et al.*, 2014, Lopez & Kolter, 2010). One of the bacterial groups displaying multicellular behavior are the Myxobacteria (Shimkets, 1990). As a member of this group, the Gram-negative soil bacterium *Myxococcus xanthus* has been studied intensively. The rod-shaped *M. xanthus* cells are capable of moving in swarms over solid surfaces (Kaiser, 1979). They prey as a “microbial wolfpack” on a variety of other bacteria to digest their contents (Berleman & Kirby, 2009). Upon nutrient starvation, they are able to build multicellular structures called fruiting bodies. Inside of fruiting bodies, cells differentiate into environmentally resistant myxospores (Kuner & Kaiser, 1982).

### 4.1.1. Development of *M. xanthus:* Differentiation into three distinct cell fates

As a response to carbon, nitrogen or phosphate deprivation, *M. xanthus* initiates a developmental program (Dworkin & Voelz, 1962). At the onset of development, *M. xanthus* cells starts to aggregate into multicellular mounds by regulated cell movement. The aggregation process takes approximately 24 h. These mounds develop into fruiting bodies inside which the cells differentiate into environmentally resistant myxospores.

Around 15% of the rod-shaped cell population, which enter the developmental program differentiates into myxospores (O'Connor & Zusman, 1991b) whose formation is completed after 72 h of starvation (Jelsbak & Sogaard-Andersen, 2003). Myxospores are resistant to heat, UV-irradiation, sonication, detergents and enzymatic digestion (Sudo & Dworkin, 1969). Differentiation into spores involves remodeling of the cell envelope, the synthesis of a rigid spore coat (Müller *et al.*, 2012), the synthesis of spore-specific lipid components (Ring *et al.*, 2006), massive reprogramming in gene expression (Müller *et al.*, 2010) and replication (Tzeng *et al.*, 2006, Tzeng & Singer, 2005).

Fruiting bodies are surrounded by peripheral rods, which are distinct from vegetative cells and spores. Their proportion amounts to 5%. Peripheral rods have been suggested to be cells scouting for food and to be able to survive in low nutrients that are insufficient to either promote growth or to induce germination of the spores inside the fruiting bodies (O'Connor & Zusman, 1991a, Lee *et al.*, 2012). In this respect, they may be similar to a persister state (Balaban, 2011, Higgs, 2014). Peripheral rods do not undergo cell divisions but they will respond rapidly to changing nutrient levels (O'Connor & Zusman, 1991a, Higgs, 2014). Although they experience the same starvation process, they do not engage in fruiting body formation and do not differentiate into spores (Hoiczyk *et al.*, 2009). While peripheral rods are formed during the developmental program, it is not yet clear which regulatory mechanisms control their production (Higgs, 2014). One model explains peripheral rod formation by their inability to make sufficient end-to-end contact to efficiently exchange signaling molecules due to their lower density. As a consequence, peripheral rods fail to express the late genes necessary for spore differentiation (Julien *et al.*, 2000).

The remaining 80% of cells undergo cell lysis. It was proposed initially that developmental cell lysis was a programmed event controlled by a toxin-antitoxin system consisting of MazF and MrpC (Nariya & Inouye, 2008). However, more recent findings showed that the endoribonuclease MazF is not solely necessary for developmental cell lysis (Lee *et al.*, 2012) but negatively regulates mRNA levels during development (Boynton *et al.*, 2013). The lysed cells have been suggested to serve as a nutrient source for the sporulating cell population (Wireman & Dworkin, 1977). Once nutrient conditions are improved, the spores are able to germinate into vegetative cells (Figure 1).

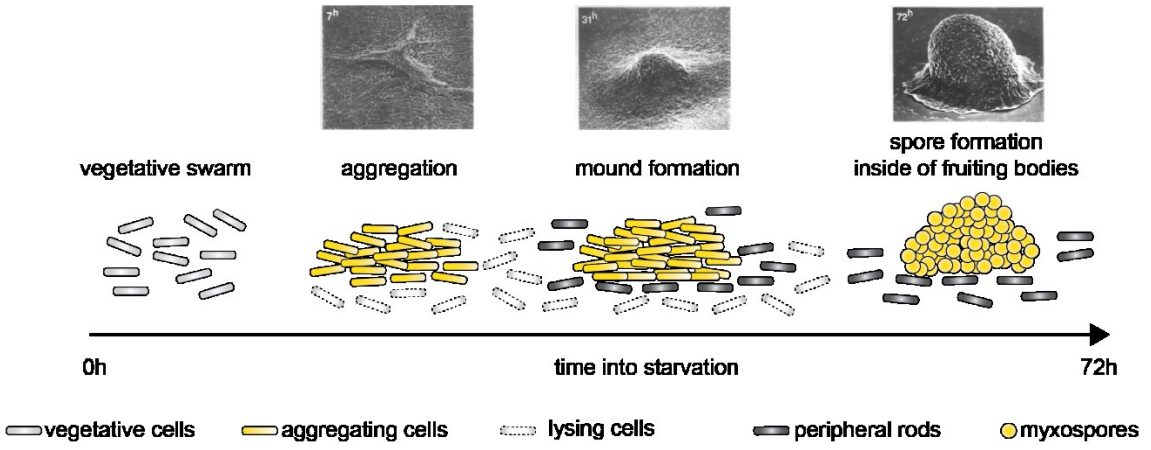


**Figure 1: The life cycle of *Myxococcus xanthus***
Scanning electron micrographs showing *M. xanthus* fruiting body formation (Kuner & Kaiser, 1982) and scheme of the developmental program. Upon nutrient starvation, vegetatively growing cells start to aggregate to form mounds or lyse. Mounds develop into fruiting bodies inside which cells differentiate into environmentally resistant myxospores. Peripheral rods surround fruiting bodies. Arrow indicates time of starvation. Modified from (Higgs, 2014).

### 4.1.2. Regulation of gene expression during fruiting body formation

Fruiting body formation is a highly organized developmental program which depends on regulation of complex processes. As a response to specific signals, transcription factors control the timing of specific gene expression. These transcription factors act sequentially in cascades and some of them combinatorially (Rajagopalan, 2014) to build a gene regulatory network (Kroos, 2017). In total, around 10% of all genes are either up- or downregulated during development (Huntley *et al.*, 2011). The gene regulatory network was described as four modules that partly depend on signaling pathways. Each module involves key transcription factors. One module depends on the NtrC-like activator (Nla)24, one depends on MrpC, one on FruA and one on a enhancer binding protein (EBP) cascade (Kroos, 2017).

Starvation triggers the stringent response, which involves the accumulation of the second messenger (p)ppGpp synthesized by the (p)ppGpp synthase RelA as a reaction to elevated levels of uncharged tRNAs (Singer & Kaiser, 1995, Harris *et al.*, 1998, Boutte & Crosson, 2013). The accumulation of (p)ppGpp is both necessary and sufficient for *M. xanthus* to initiate the developmental program (Harris *et al.*, 1998). Two (A and C) of the five (A-E) intercellular signal programs depend on (p)ppGpp (Manoil & Kaiser, 1980b, Manoil & Kaiser, 1980a, Harris *et al.*, 1998, Crawford & Shimkets, 2000a, Crawford & Shimkets, 2000b). All of them are essential to successfully complete the developmental program. Out of the five, the A-, C-signal are the ones which have been characterized in detail.

The A-signal consists of peptides and amino acids that are generated by extracellular proteolysis (Kuspa *et al.*, 1992b, Kuspa *et al.*, 1992a). When the extracellular concentration of the A-signal reaches a certain threshold due to high cell density, the A-signal is sensed and new proteins necessary for fruiting body formation and sporulation are synthesized (Kuspa *et al.*, 1992b) and A-signal-dependent genes will be expressed (Kaiser, 2004).

The C-signal involves a proteolytic cascade activated by nutrient starvation (Konovalova *et al.*, 2012, Rolbetzki *et al.*, 2008). A 25 kD precursor protein encoded by *csgA* is cleaved by the protease PopC to a smaller protein p17 which functions as the C-signal (Lobedanz & Sogaard-Andersen, 2003, Rolbetzki *et al.*, 2008) and accumulates at the surface of starving cells (Shimkets & Rafiee, 1990). PopC is thought to accumulate in the cytoplasm of vegetative growing cells and to form a complex with PopD, which inhibits PopC secretion and protease activity. Upon nutrient starvation, (p)ppGpp accumulates in a RelA-dependent manner and causes the degradation of PopD. Although the ATP-dependent protease $FtsH^D$ was thought to be involved in the degradation of PopD (Konovalova *et al.*, 2012), recent results suggest, that $FtsH^D$ is not participating in C-signaling. Instead, LonD, also an ATP-dependent protease is involved in degradation of PopD (Magdalena Polatynska, MPI Marburg). Once PopD is

degraded, PopC is released to cleave p25 to p17 (Konovalova *et al.*, 2012, Rolbetzki *et al.*, 2008). C-signal transmission is cell-cell contact dependent and p17 is thought to be recognized by a hypothetical C-signal sensor on neighboring cells, but a receptor has not been identified. Expression of genes depending on the C-signal starts 6 h after starvation (Kroos & Kaiser, 1987). Transmission of the C-signal was thought to cause a phosphorylation cascade inside the cell, which results in the phosphorylation of the response regulator FruA, which is essential for fruiting body formation (Ellehauge *et al.*, 1998). However, a histidine kinase for FruA was not identified so far. Recent results suggest that FruA might function without being phosphorylated (Mittal & Kroos, 2009) and that it acts a transcriptional activator (Ueki & Inouye, 2005a, Ueki & Inouye, 2005b, Viswanathan *et al.*, 2007). Nevertheless, the molecular mechanism by which the C-signal activates FruA is unknown.

Activated FruA and the output of the Mrp module (MrpC) (Figure 2, green and yellow) are thought to regulate late genes important for completion of development (Mittal & Kroos, 2009). MrpC is a transcription factor that appears to activate transcription of *fruA* (Ueki & Inouye, 2003) and to regulate a large number of genes important for development including *csgA*, encoding the precursor for the C-signal (Robinson *et al.*, 2014). MrpC and FruA regulate the transcription of genes cooperatively (Mittal & Kroos, 2009). Both transcriptional regulators were found to accumulate in higher levels in aggregating cells than in cells outside of aggregates, emphasizing their important role for aggregation and sporulation (Lee *et al.*, 2012).

The EBP cascade module (Figure 2, blue) is initiated early during development. EBPs activate transcription by $\sigma^{54}$ RNA polymerase (Bush & Dixon, 2012). Several developmentally regulated genes in *M. xanthus* have been shown to have $\sigma^{54}$ – dependent promoters (Garza *et al.*, 1998, Keseler & Kaiser, 1995, Romeo & Zusman, 1991). The EBPs Nla4 and Nla18 impact (p)ppGpp accumulation (Diodati *et al.*, 2006, Ossa *et al.*, 2007). Often, two or more EBPs combinatorially regulate their targets (Giglio *et al.*, 2011). EBPs were shown to be involved in regulating A-signaling, C-signaling, activation of FruA and the Mrp module (Jelsbak *et al.*, 2005, Giglio *et al.*, 2015, Gronewold & Kaiser, 2001, Rajagopalan, 2014).

Recent studies point out, that the second messenger c-di-GMP acts as an important signaling molecule during *M. xanthus* development. The guanylate cyclase DmxB is responsible for the increasing global pool of c-di-GMP during starvation. Nla24 (Figure 2, red) was discovered to be a c-di-GMP receptor and is thought to be involved in induction of genes important for exopolysaccharide production, which is necessary for fruiting body formation (Skotnicka *et al.*, 2016).

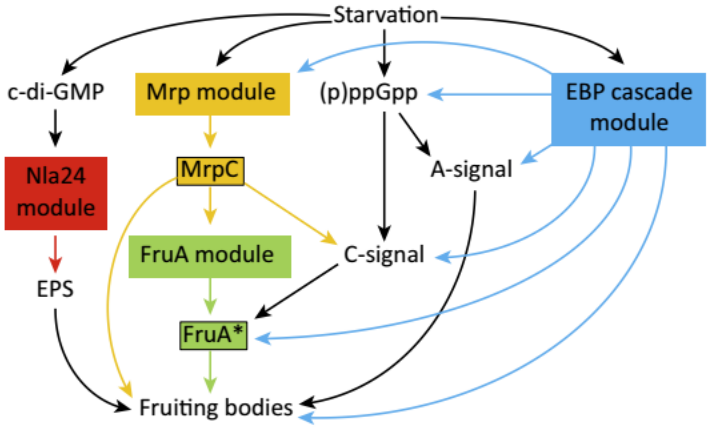


**Figure 2: Overview of the gene regulatory network during *M. xanthus* fruiting body formation**
During starvation, the Nla24 module (red), Mrp module (yellow). FruA module (green) and enhancer binding protein (EBP) cascade module (blue) build a network of transcriptional regulators to govern fruiting body formation. This network involves the second messengers (p)ppGpp and c-di-GMP and the A- and C-signaling pathways. More details see text. Figure was obtained from (Kroos, 2017).

## 4.2. Cell cycle during vegetative growth

In order to generate viable progeny with equal size and chromosome content, bacterial cells tightly coordinate replication and segregation temporally with cell division (Thanbichler, 2010). The coordination of cell cycle events are modified during sporulation in *Bacillus subtilis* (see 4.3.2), *Streptomyces coelicolor* (see 4.3.3) and *M. xanthus* (see 4.4.3). In order to understand the regulation of the cell cycle during spore formation, the coordination of these processes during vegetative growth needs to be understood in detail. An overview of the most important events to coordinate the cell cycle will be given in the following chapters.

### 4.2.1. Replication, segregation and cell division

In order to produce viable progeny, bacterial cells need to replicate their DNA, segregate the sister chromosomes and regulate and position its division machinery. These events summarized as the cell cycle is a set of parallel processes that overlap (Nordstrom *et al.*, 1991) (Figure 3).

The replication process can be divided in three phases: initiation, elongation and termination. Most bacteria have one origin of replication where the $AAA^+$ ATPase DnaA binds to facilitate separation of the single strands thereby allowing the assembly of the replisome components in the correct place at the correct time (Reyes-Lamothe *et al.*, 2012, Mott & Berger, 2007). During elongation, the replisomes proceed bi-directionally around the chromosome (Pomerantz & O'Donnell, 2007). When the two replication forks meet at the terminus region, the replisomes disassemble. Subsequently, the last replicated regions are accessible to chromosome processing including decatenation and chromosome dimer resolution (Reyes-

Lamothe *et al.*, 2012). During the whole replication process, the chromosome remains highly organized (Bravo *et al.*, 2005).

Bacterial chromosome segregation occurs in parallel to replication. Shortly after duplication, the two origins of replication move away from the division plane (Sherratt, 2003). In slow growing *B. subtilis* and *E. coli* cells, the two origins of replication move and remain near cell quarters (Berkmen & Grossman, 2006, Lau *et al.*, 2003, Li *et al.*, 2002). The remaining regions of the chromosome separate to follow their respective origin. In *Caulobacter crescentus*, chromosome replication, segregation and cell division is restricted to one of the two distinct cell types. After the asymmetric cell division event, a stalked and a swarmer cell are born (Shapiro & Losick, 1997). Just the stalked cell is able to enter the next round of the cell cycle immediately. Replication in the swarmer cell is arrested until its transition to the stalked cell stage (Domian *et al.*, 1997). DNA replication initiates during the swarmer-to-stalked-cell transition. After cell division, this results in two progeny each containing one single chromosome. In *C. crescentus*, one origin is found at the old cell pole in a new born cell. Once the origin is duplicated, the second copy is segregated to the opposite cell pole. When replication ends, the two copies of the terminus are observed near the division plane at midcell (Jensen & Shapiro, 1999) (Figure 3).

The segregation process is guaranteed by the ParAB system in concert with *parS* sequences in many bacteria (Livny *et al.*, 2007, Ptacin & Shapiro, 2010, Fogel & Waldor, 2006, Marston & Errington, 1999, Jakimowicz *et al.*, 2005, Harms *et al.*, 2013). Several bacteria lack a ParABS system, suggesting alternative segregation mechanisms exist. Best studied ParABS systems are the chromosomal system of *C. crescentus* (Ptacin & Shapiro, 2010) and the not essential Soj/Spo0J system of *B. subtilis* (Marston & Errington, 1999).

ParA ATPases of chromosome segregation systems have low intrinsic ATPase activity (Lim *et al.*, 2014). Their ATPase activity is stimulated by ParB. ParB also binds to *parS* sequences located close to the origin of replication. In *C. crescentus* ParA forms a cloud-like structure that extents from the pole over the nucleoid until it reaches a duplicated ParB/*parS* complex. Binding of this complex results in a retracting ParA structure which “pulls” on the ParB/*parS* complex (Ptacin & Shapiro, 2010). Therefore, the complex follows the retracting ParA structure, leading to migration of the duplicated origins. ParA function depends on its ability to bind DNA as well as on its ATPase activity (Ptacin & Shapiro, 2010).

Once the chromosome is duplicated and segregated cell division can take place. In rod-shaped bacteria division occurs generally at midcell by binary fission. As the first event of cell division, the tubulin homologue FtsZ (**f**ilamentous **t**emperature **s**ensitive) polymerizes into a ring-like structure, the Z-ring, at the future cell division site (Bi & Lutkenhaus, 1991). FtsZ is crucial for the recruitment of other cell division proteins. Together, they build a multiprotein complex, the

divisome that executes cytokinesis (Adams & Errington, 2009) (Figure 3). FtsZ has been intensively studied and shown to be a target for regulation of cell division. An overview will be given in the following chapters.

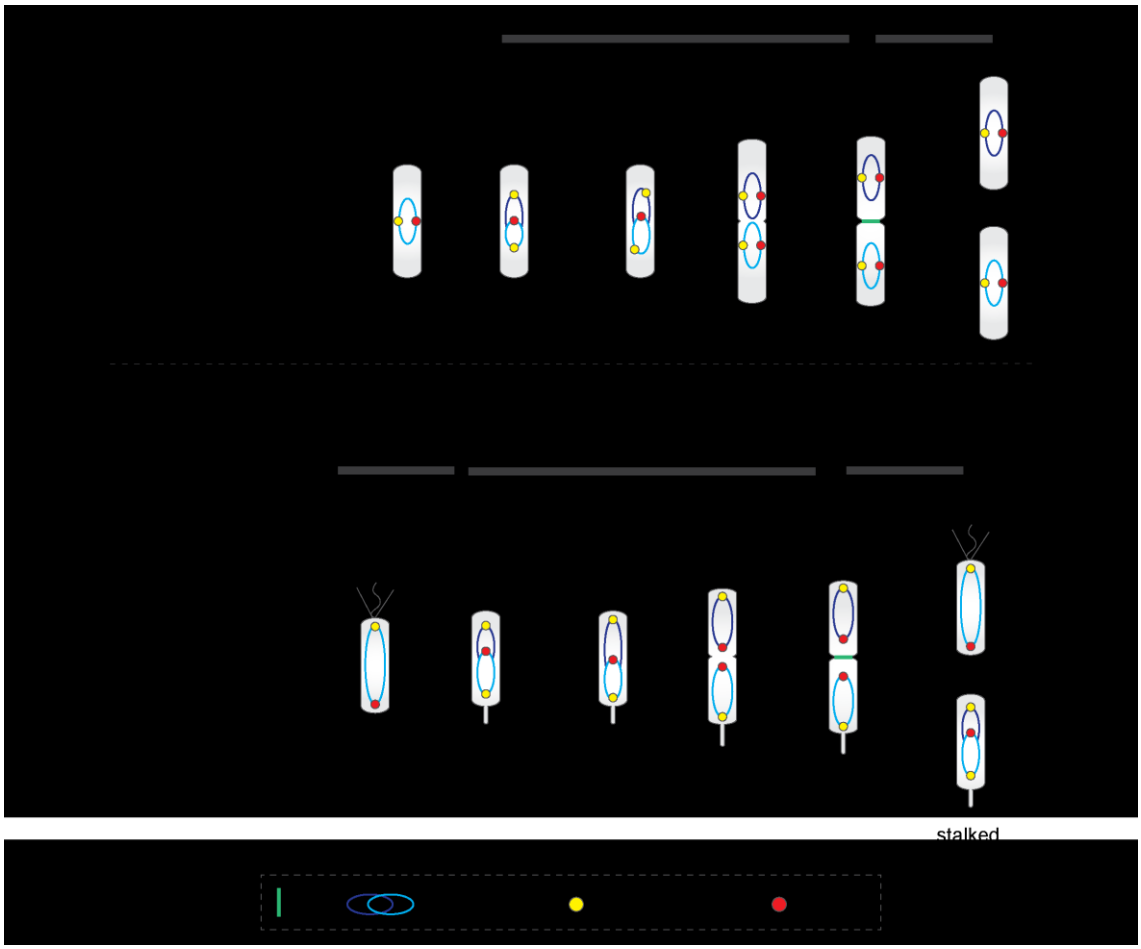


**Figure 3: Schematic representation of the cell cycle of rod shaped bacteria**
Bacteria coordinate DNA replication, segregation and cell division in order to produce progeny having each one chromosome. During the cell cycle the chromosome remains highly organized. Shown is the schematic overview of slow growing *B. subtilis* and *E. coli* cells. *C. crescentus* undergoes an asymmetric cell division event giving birth to two distinct cell fates: a non-replicative swarmer and a stalked cell which can immediately enter the division cycle. The positions of the origin of replication (yellow) and termini (red) are indicated. More details see text.

### 4.2.2. The cell division protein FtsZ

Generally, the first event during cell division is the polymerization of the cytoplasmic protein FtsZ into a ring-like structure at the division site. Subsequently, the Z-ring serves as the scaffold to recruit downstream proteins to build the multiprotein complex essential for cytokinesis, the divisome (Adams & Errington, 2009). It persists throughout division to guide synthesis, location and shape of the division septum (Addinall & Lutkenhaus, 1996). FtsZ is an essential and highly conserved GTPase (RayChaudhuri & Park, 1992, de Boer *et al.*, 1992a) related to eukaryotic tubulin (Nogales *et al.*, 1998). *In vitro*, FtsZ assembles into protofilaments (Figure 4) that form tubules, sheets and minirings (Erickson *et al.*, 1996, Lu *et al.*, 2000). The

polymerization depends on GTP and FtsZ hydrolyses GTP in a cooperative and self-activating manner (Mukherjee & Lutkenhaus, 1994, Oliva *et al.*, 2004, Scheffers & Driessen, 2001). Each FtsZ monomer contains a N-terminal polymerization domain, a flexible unstructured linker region and a conserved C-terminus (Erickson *et al.*, 2010). The conserved C-terminal tail mediates interactions with itself (Buske & Levin, 2012) and auxiliary proteins, which are involved in divisome assembly and disassembly (Shen & Lutkenhaus, 2009, Haney *et al.*, 2001, Singh *et al.*, 2007, Camberg *et al.*, 2009). Electron microscopy of *E. coli* and *C. crescentus* FtsZ revealed that bundles of FtsZ that are 5–10 filaments wide are probably building the structure known as the Z-ring (Szwedziak *et al.*, 2014). However, the precise molecular structure of the Z-ring remains unknown. As shown by FRAP experiments, it is a highly dynamic structure that undergoes constant remodeling (Anderson *et al.*, 2004, Stricker *et al.*, 2002). Recently, *in vitro* treadmilling of FtsZ filaments has been reported (Loose & Mitchison, 2014). Also *in vivo*, FtsZ filaments were found to treadmill around the division site. Treadmilling is thought to guide and organize septal wall synthesis. These findings imply that FtsZ and the cell wall synthesis machinery work together to facilitate constriction. A model was proposed, suggesting that FtsZ filaments organize a moving synthesis machinery in a ring that provides new cell wall material inside of old material thereby closing the septum (Bisson-Filho *et al.*, 2017, Yang *et al.*, 2017).

Regulation of FtsZ polymerization into the Z-ring is very complex and occurs on all levels: spatially and temporally, assembly and disassembly, synthesis and degradation. In the next chapters, regulation mechanisms will be described.

### 4.2.3. Positive regulation of Z-ring formation and dynamics

A variety of proteins was identified to be involved in regulating FtsZ function. Dysregulation leads to defects in cell division and cell death. Positive regulators are important in recruitment and stabilization of the Z-ring. Proteins that are shown to positively influence FtsZ function are for example FtsA and ZipA. Both these proteins recruit FtsZ to the membrane (Pichoff & Lutkenhaus, 2005, Pichoff & Lutkenhaus, 2002, Hale & de Boer, 1997, Liu *et al.*, 1999). The protein SepF was identified in *B. subtilis* and is conserved throughout the Gram-positive bacteria. SepF tethers the Z-ring to the inner membrane and overlaps with the role of FtsA in Z-ring assembly (Ishikawa *et al.*, 2006, Hamoen *et al.*, 2006, Fadda *et al.*, 2003).

The first identified regulator which positively controls positioning of the Z-ring was reported in *Streptomyces* (Willemse *et al.*, 2011). Here, FtsZ is directly recruited by the membrane - associated SsgB protein. At the onset of sporulation, SsgB forms foci along the aerial hyphae that in the later stages of cell division colocalize with FtsZ in a ladder-like structure (Schwedock *et al.*, 1997, Willemse *et al.*, 2011). Localization of FtsZ depends on SsgB presence, which in

turn in is correctly localized by SsgA. SsgB promotes FtsZ polymerization *in vitro*, suggesting that SsgB is not just important for FtsZ positioning at the incipient cell division site but also stimulates Z-ring formation (Willemse *et al.*, 2011). In *Streptococcus pneumoniae*, the protein MapZ or LocZ was identified independently by two groups to be a spatial regulator for Z-ring formation. The absence of MapZ results in cell division and morphology defects. Z-rings are still formed at WT frequency but are not positioned correctly, resulting in the formation of anucleate minicells (Fleurie *et al.*, 2014, Holeckova *et al.*, 2014). Direct interaction to FtsZ via the N-terminal domain of MapZ was demonstrated *in vitro* and *in vivo*. It was suggested that phosphorylation of MapZ by two kinases causes FtsZ relocation to the incipient cell division site (Fleurie *et al.*, 2014). MapZ does not stimulate FtsZ polymerization into filaments and does not stimulate Z-ring formation *in vivo.* Thus, MapZ is suggested to be only a spatial regulator (Fleurie *et al.*, 2014).

### 4.2.4. Negative regulation of Z-ring formation and dynamics

Negative regulators prevent FtsZ assembly into the Z-ring to control its dynamics and positioning. As an example, the integral membrane protein EzrA of *B. subtilis* was shown to negatively influence Z-ring formation. Lack of EzrA increases Z-ring formation and induces formation of multiple Z-rings. Deletion in *ezrA* lowers the critical FtsZ concentration needed for Z-ring formation (Levin *et al.*, 1999). In line with this, overexpression of *ezrA* blocks Z-ring formation and EzrA interferes with FtsZ filament formation *in vitro*. It is thought to prevent aberrant Z-ring formation at the cell poles through *de novo* FtsZ assembly and to maintain proper FtsZ assembly within the medial FtsZ ring (Haeusser *et al.*, 2004). In *B. subtilis*, ClpX, the substrate recognition subunit of the ATP-dependent protease ClpXP is an inhibitor of FtsZ assembly. ClpX inhibits Z-ring formation *in vivo* and FtsZ assembly in a ClpP- and ATP-independent manner *in vitro* (Weart *et al.*, 2005). Also in *E. coli*, ClpX disassembles FtsZ polymers presumably by blocking reassembly of FtsZ. It has been suggested, that ClpX modulates FtsZ polymer dynamics in an ATP-independent fashion. Crucial for this function is the interaction of ClpX N-terminal domain to FtsZ monomers or oligomers (Sugimoto *et al.*, 2010).

Well studied are the negative regulators involved in positioning of the incipient cell division site. In *E. coli* and *B. subtilis*, the Min system in concert with nucleoid occlusion positions FtsZ. The Min system works around the FtsZ inhibitor MinC. The cytoplasmic protein MinC was shown to inhibit FtsZ polymerization into Z-rings without inhibiting its GTPase activity leading to a destabilization of FtsZ filaments (Hu *et al.*, 1999). Overexpression *in vivo* leads to a block in cell division (Hu *et al.*, 1999). MinC on its own inhibits cell division over the whole cell body (de Boer *et al.*, 1992b) but is sequestered to the membrane by the ParA ATPase MinD (de Boer *et al.*, 1991). MinD is associated with the membrane by its amphipathic helix in the C-terminus

(Szeto *et al.*, 2002, Szeto *et al.*, 2003). The so called topology factor MinE is recruited to the membrane by MinD-ATP and stimulates ATP hydrolysis of MinD This leads to MinD dissociation from the membrane together with MinC. Subsequently MinCD associates at the opposite cell pole and recruits MinE. This behavior results in a pole-to-pole oscillation of MinCDE leading to the highest concentration of the MinC inhibitior at the cell poles. Hence, the lowest MinC concentration is at midcell and allows Z-ring formation at this place (Raskin & de Boer, 1999, Hu & Lutkenhaus, 2001, Hu *et al.*, 1999). The Min system in *B. subtilis* also inhibits polar cell divisions, but in contrast to MinCDE in *E. coli* it lacks a MinE homolog. Instead, DivIVA and the connector protein MinJ are part of the system (Bramkamp *et al.*, 2008, Marston *et al.*, 1998). DivIVA binds to negatively curved membranes and recruits MinCD to the cell poles via MinJ (Lenarcic *et al.*, 2009, van Baarle & Bramkamp, 2010). Thus, in contrast to pole-to-pole oscillation of the MinCD in *E. coli*, MinCD in *B. subtilis* are attached to the poles to inhibit cell division (Bramkamp *et al.*, 2008, Edwards & Errington, 1997, Marston & Errington, 1999). Recent results indicate that MinC predominantly localizes at the future cell division site. It was suggested that MinC does not prevent cell divisions at the poles but rather prevents multiple cell divisions at midcell by promoting divisome disassembly (Gregory *et al.*, 2008, van Baarle & Bramkamp, 2010). In concert with the Min system, the nucleoid occlusion system prevents Z-ring formation over the nucleoid to position Z-ring assembly. The nucleoid occlusion proteins SlmA and Noc were identified in *E. coli* and *B. subtilis*, respectively (Bernhardt & de Boer, 2005, Wu & Errington, 2004). SlmA binds to specific DNA sequences to inhibit cell division over the nucleoid by causing disassembly of FtsZ protofilaments independently of its GTPase activity (Cabre *et al.*, 2015). Although no direct interaction of Noc and FtsZ could be demonstrated so far it is thought to be involved in the nucleoid occlusion mechanism. DNA bound Noc multiprotein complexes recruit DNA to the cell membrane and are thought to decrease the space between nucleoid and membrane resulting in a physical block of Z-ring formation over the nucleoids (Adams *et al.*, 2015).

In *C. cresenctus,* the ParA ATPase MipZ is the spatial regulator of division site placement. It has been shown to directly interfere with FtsZ polymerization by enhancing its GTPase activity (Thanbichler & Shapiro, 2006). MipZ is recruited to the stalked cell pole by its interaction to ParB (Thanbichler & Shapiro, 2006). ParB is bound to *parS* sequences near the origin of replication. Due to replication and segregation the origin of replication moves to the opposite cell pole (Mohl & Gober, 1997). MipZ follows ParB and localizes at both cell poles. Of note, MipZ forms a gradient with the highest concentration at the cell poles (Thanbichler, 2010, Kiekebusch *et al.*, 2012). The details leading to this mechanism were described (Kiekebusch *et al.*, 2012). Monomeric ADP-bound MipZ is recruited to the cell poles by its ParB interaction. Dimerization of ATP-bound MipZ is thought to be stimulated by ParB. Dimeric MipZ has low affinity to ParB leading to a release off the ParB/*parS* complex and association with the

nucleoid. MipZ ATPase affinity is stimulated by the nucleoid. This leads to a MipZ gradient along the nucleoid with decreasing MipZ concentration depending on the distance to the cell pole. (Kiekebusch *et al.*, 2012). Thus, the MipZ/ParB/*parS* system directly couples cell division to chromosome replication and segregation (Thanbichler & Shapiro, 2006, Kiekebusch *et al.*, 2012).

FtsZ assembly has also been shown to be coupled to nutrient availability and growth rate. The terminal sugar transferase UgtP of *B. subtilis* and the glycosyltransferase OpgH from *E.coli* inhibit cell division in a growth rate dependent fashion (Weart *et al.*, 2007, Hill *et al.*, 2013). In *C. cresentus*, the NAD-dependent glutamate dehydrogenase GdhZ and the oxireductase-like KidO interfere with FtsZ polymerization by stimulating its GTPase activity and destabilizing its lateral interactions between protofilaments, respectively. Thus, they couple cell division to nutrient availability (Beaufay *et al.*, 2015).

As part of the DNA-damage induced stress response, the division inhibitor SulA is synthesized in *E.coli*. SulA inhibits Z-ring formation and promotes its disassembly once formed by blocking the C-terminal domain that is crucial for FtsZ self-interaction (Cordell *et al.*, 2003, Huisman *et al.*, 1984, Justice *et al.*, 2000, Trusca *et al.*, 1998). YneA is the functional counterpart to SulA in *B. subtilis*. Although it is structurally and phylogenetically unrelated, it is also responsible for cell division suppression during the SOS response (Kawai *et al.*, 2003). At the onset of development of aerial hyphae in *S. coelicolor*, the expression of CrgA, an integral membrane protein, peaks. Overexpression leads to inhibition of Z-ring formation and proteolytic turnover of FtsZ. CrgA is thought to be involved in dynamics of the Z-ring (Del Sol *et al.*, 2006). MciZ, the mother cell inhibitor of FtsZ was identified as an inhibitor of Z-ring assembly during *B. subtilis* sporulation (Handler *et al.*, 2008). *In vitro*, MciZ binds specifically to FtsZ and prevents FtsZ polymerization, by reducing its GTPase activity. Artificial expression of *mciZ* during vegetative growth prevents Z-ring assembly (Handler *et al.*, 2008).

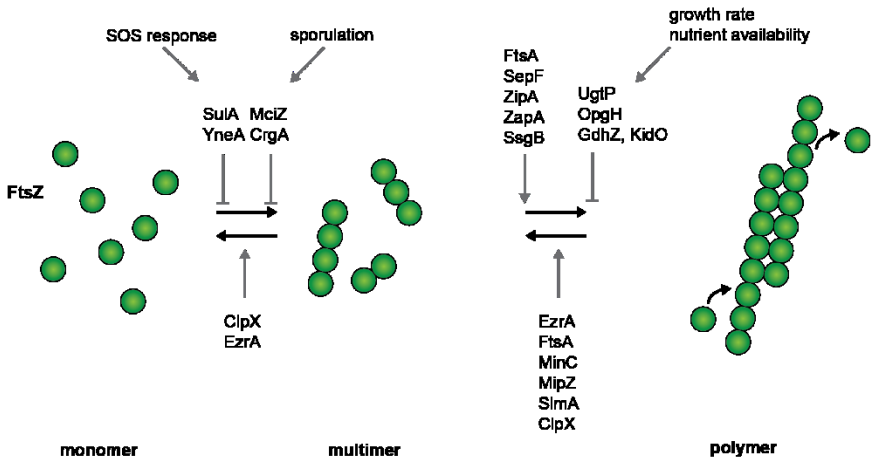


**Figure 4: Regulation of FtsZ polymerization by accessory proteins**
The cytoplasmic pool of FtsZ monomers polymerizes into multimers and polymers at the incipient restriction site as the first event of cell division. A large number of accessory proteins act in concert to regulate cell division at several levels of FtsZ assembly. The SOS response, sporulation or nutrient availability together with growth rate are features that influence this process. Detailed explanations see in the text. Figure modified from (Adams & Errington, 2009).

### 4.2.5. Proteolysis of FtsZ

In addition to regulators interfering with FtsZ ability to hydrolyze GTP, to form polymers or to assemble into the Z-ring, FtsZ concentration *in vivo* was shown to play an important role for function. Depletion of FtsZ in rod-shaped bacteria results in the formation of long, filamentous cells due to continuous growth of cells that are no longer dividing (Dai & Lutkenhaus, 1991, Treuner-Lange *et al.*, 2013). Cocci-shaped bacteria, such as *S. aureus*, increase in volume up to 8-fold when depleted for FtsZ (Pinho & Errington, 2003). Although FtsZ levels remain constant during one complete cell cycle in *E. coli* (Rueda *et al.*, 2003), the correct FtsZ concentration has been shown to be important for correct cell division. A 10-fold overexpression of FtsZ or FtsA inhibits cell division. This inhibition can be relieved by the simultaneous overexpression of FtsZ and FtsA (Dai & Lutkenhaus, 1992, Dewar *et al.*, 1992).

ClpX or ClpA, which possess ATP-dependent protein remodeling activities, interact with their proteolytic partner ClpP to form the ATP-dependent proteases ClpXP or ClpAP (Kirstein *et al.*, 2009). ClpP proteases were shown to be involved in FtsZ turnover in various organisms (Feng *et al.*, 2013, Williams *et al.*, 2014, Camberg *et al.*, 2009). In line with this, the overexpression of ClpX or ClpXP leads to a block in cell division and a filamentous phenotype (Camberg *et al.*, 2009, Weart *et al.*, 2005, Sugimoto *et al.*, 2010). In *E. coli*, ClpXP degrades approximately 15% of total FtsZ per cell cycle. *In vitro*, ClpXP degrades both FtsZ monomers and polymers (Camberg *et al.*, 2009). Degradation of FtsZ happens more rapidly in the presence of GTP, which promotes FtsZ assembly into polymers (Camberg *et al.*, 2009, Camberg *et al.*, 2014). Recently it was shown that two regions of FtsZ, one outside of the polymerization domain in the unstructured linker and one at the C-terminus are important for recognition and degradation

by ClpXP (Camberg *et al.*, 2014). Interestingly, ZipA was shown to stabilize FtsZ and preventing proteolysis by ClpXP by its binding to the C-terminal region of FtsZ (Pazos *et al.*, 2013). It was reported that *clpX* or *clpP* deletion mutants or protease defective mutants are forming normal shaped Z-rings. FRAP experiments revealed a reduced fluorescence recovery time of a region of the Z-ring in these mutants, leading to the conclusion that ClpXP is a regulator of Z-ring dynamics in *E. coli* (Viola *et al.*, 2017).

In *C. crescentus*, it was reported that FtsZ is degraded just before cell division but maintained at low levels specifically in the daughter stalked cell (Kelly *et al.*, 1998) and that FtsZ is a substrate of the ClpP protease (Bhat *et al.*, 2013). It was shown that FtsZ is a substrate of both ClpXP and ClpAP *in vivo* and *in vitro* and the localization of ClpX to the division site depends on FtsZ. ClpXP and ClpAP specifically degrade FtsZ in the non-replicative swarmer cells, suggesting that ClpXP and ClpAP activity is differently regulated in the two cell types. Mutations in the FtsZ C-terminus led to a stabilizing effect *in vivo*, suggesting, that the C-terminus is important to be recognized as a substrate (Williams *et al.*, 2014).

Interestingly, inhibition of Z-ring formation is a consequence of treatment with the natural compound ADEP (acyldepsipeptides) and explains its antibacterial activity. ADEP mimics a gain of function mutation (Ni *et al.*, 2016) and switches the ClpP peptidase from a regulated to an uncontrolled protease leading to proteolytic degradation of FtsZ in *B. subtilis*, *S. aureus* and *S. pneumoniae* (Sass *et al.*, 2011).

### 4.2.6. Regulation of *ftsZ* transcription

In addition to polymerization, GTPase activity and degradation to ensure the precise spatiotemporal regulation of cell division, FtsZ synthesis is also tightly regulated throughout the cell cycle and in response to environmental changes.

In various organisms, *ftsZ* expression is regulated by multiple promoters (Francis *et al.*, 2000, Letek *et al.*, 2007, Roy & Ajitkumar, 2005). In *E. coli*, six promoters distributed upstream of *ftsZ*, in the coding regions for *ftsA*, *ftsQ* and *ddlb* (three genes upstream of *ftsZ*) drive *ftsQAZ* transcription. The majority of *ftsZ* transcription is driven by promoters more than 6 kb upstream of the *ddlb* gene (Flärdh *et al.*, 1997, Dewar & Dorazi, 2000). Two promoters, out of the six promoters contributing to *ftsZ* transcription in the *ddlb-ftsZ* region, lying in the *ddlb* gene and drive almost 50% of *ftsZ* transcription (Flärdh *et al.*, 1997). One of them is strongly induced during fast growth and regulated by SdiA, a transcriptional activator (Wang *et al.*, 1991). The other one is induced at low growth rates and is positively regulated by the stationary growth phase sigma factor $\sigma^S$ (Sitnikov *et al.*, 1996). It was shown that *ftsZ* transcription is periodic in the cell cycle and mRNA levels reach a maximum at about the time DNA replication initiates, but are independent of the replication initiator DnaA (Garrido *et al.*, 1993).

Three promoters drive *ftsZ* transcription in *B. subtilis*, two of them are active during vegetative growth and depend on SigA, the major vegetative σ factor. One depends on SigH and its activity is increased three to four-fold at the onset of sporulation, when the organism divides asymmetrically resulting in two genetically identical haploid progeny: a large mothercell and a forespore. The expression of this promoter is under the control of the master transcription factors Spo0A and AbrB. In the absence of Spo0A, promoter activity was abolished. A *spo0A abrB* double mutant restored partially the *spo0A* background. Mutations in *abrB* led to increased promoter activity. These results suggested, that Spo0A relieves the negative effect of AbrB at the onset of sporulation (Gonzy-Treboul *et al.*, 1992). However, the absence of this promoter results in 30% of the normal sporulation rate, suggesting that the burst in *ftsZ* transcription is not an absolute requirement for asymmetric septum formation (Gonzy-Treboul *et al.*, 1992). Nevertheless, the asymmetric division depends, among others on an increase in FtsZ levels (Carniol *et al.*, 2005).

In *S. coelicolor*, three promoters driving *ftsZ* transcription were identified. One of them is constitutively active, the second one is active during vegetative growth and the third one is essential for spore formation (Flärdh *et al.*, 2000) when long aerial hyphae are formed and ladders of multiple Z-rings are ensure the production of hundreds of spores, each containing one chromosome (Chater, 2001, Flärdh & Buttner, 2009). Increased transcription from this promoter depends on the presence of any of the six developmental regulatory genes *whiA*, *B*, *G*, *H*, *I* and *J* (Flärdh *et al.*, 2000). WhiABGHIJ are thought to form a checkpoint system to correctly time the expression of *ftsZ* since sporulation can be restored in the *whi* mutants by expressing *ftsZ* from a constitutive promoter (Willemse *et al.*, 2012).

In *C. crescentus*, FtsZ only accumulates in stalked cells, which immediately initiate a new round of DNA replication after cell division. *ftsZ* transcription is driven by a single promoter and regulated temporally during the cell cycle in a manner that parallels the variation of FtsZ concentration and DNA replication. Transcription of *ftsZ* is repressed by the global regulator CtrA and decreases rapidly after the beginning of cell division (Kelly *et al.*, 1998). Activation of *ftsZ* transcription is promoted by the cell cycle regulated DNA methyltransferase CcrM. The *ftsZ* promoter shows highest activity when the conserved CGACTC motif in its promoter region is fully methylated (Gonzalez & Collier, 2013).

Taken together, FtsZ is a highly regulated protein at all levels. To perform a successful cell division at the right place and time, its synthesis, ability to assemble into the Z-ring, turnover and positioning are tightly coordinated. A large number of proteins targeting these properties are known. Furthermore its activity is adjusted due to growth rate, cell cycle, environmental conditions and cell fate.

## 4.3. Cell cycle regulation during sporulation

### 4.3.1. Sporulation as a strategy to survive unfavorable conditions

Several bacteria have evolved mechanisms to survive unfavorable environmentally conditions by differentiation into dormant spores. Commonly, spores are round or oval and the cell surface is covered with a spore coat, but the process of sporulation itself displays major differences, e.g. in the most extensively studied organisms *B. subtilis*, *S. coelicolor* and *M. xanthus* (Figure 5).

*B. subtilis* forms endospores in response to nutrient limitation and high cell density by an asymmetric cell division event (Errington, 1993, Piggot & Hilbert, 2004). The process of endosporulation can be categorized into four major stages. First, a polar septum is elaborated. Second, the prespore is engulfed by the mother cell. The third stage is characterized by spore coat assembly followed by the fourth step, lysis of the mother cell and release of the mature spore into the environment (Tan & Ramamurthi, 2014).

*S. coelicolor* grows as branching hyphae that form a vegetative mycelium containing 50 or more copies of the chromosome. The organism disperses through spores that form on reproductive structures called aerial hyphae. In response to nutrient depletion and other signals, aerial hyphae, which display a long chain of prespore compartments, grow into the air. Up to a hundred haploid spores are formed simultaneously by multiple synchronous cell divisions (Flärdh & Buttner, 2009, Chater, 2001).

In contrast, diploid myxospores are formed by rearrangement of the rod shaped cell into a spherical spore independent of a septation event (Higgs, 2014, Tzeng & Singer, 2005).

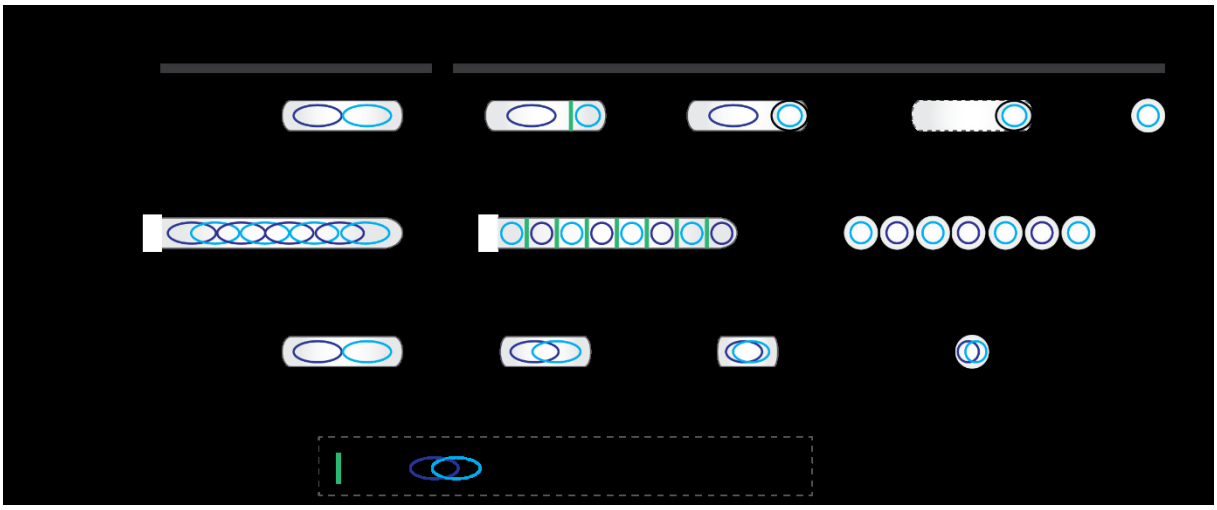

**Figure 5: Schematic representation of spore formation in *B. subtilis*, *S. coelicolor* and *M. xanthus***
The process of spore formation displays major differences in various organisms. Shown are general schemes of the sporulation process of *B. subtilis*, *S. coelicolor* and *M. xanthus*. Please note that it is unclear if cells that differentiate into myxospores contain two chromosomes at the onset of sporulation. Details see text.

The modification of basic cell cycle processes like chromosome replication, segregation and cell division play a crucial role during the sporulation processes of *B. subtilis*, *S. coelicolor* and *M. xanthus*. The coordination of these events ensures the formation of spores containing a distinct amount of chromosomes. In the following, an overview of cell cycle regulation during *B. subtilis* and *Streptomyces* sporulation will be given.

### 4.3.2. Cell cycle regulation during *B. subtilis* endosporulation

Endosporulation of *B. subtilis* has been studied intensively. Starvation conditions trigger the activation of the transcriptional master regulator Spo0A. Spo0A is activated by a phosphorelay system governed by five histidine kinases (KinA-E) that are partially redundant (LeDeaux *et al.*, 1995). High levels of Spo0A~P and the sigma factor $\sigma^H$ are required to enter the sporulation program (Hilbert & Piggot, 2004). Endosporulation is characterized by an asymmetric division, producing two distinct cells with very different fates and each one chromosome. The differentiation process is controlled by compartmentalized gene expression (Hilbert & Piggot, 2004). Immediately after asymmetric cell division, the sigma factor $\sigma^F$ becomes active exclusively in the prespore followed by activation of $\sigma^E$ in the mother cell (Piggot & Hilbert, 2004). $\sigma^G$ is synthesized in the prespore before engulfment and becomes active when engulfment is complete (Serrano *et al.*, 2004). Subsequently, the late mother cell sigma factor $\sigma^K$ is activated (Piggot & Hilbert, 2004). The sigma factors initiate distinct programs of gene expression in the mother cell and prespore, respectively (Piggot & Hilbert, 2004).

Before sporulation, the nucleoids of the vegetative cell are remodeled into a continuous structure called the axial filament, which stretches from one pole to the other (Ryter *et al.*,

1966). This organization is ensured by the RacA protein, which anchors the two chromosomes to the cell poles (Ben-Yehuda *et al.*, 2003, Wu & Errington, 2003). RacA recognizes GC-rich inverted repeats which are located near the origin (Ben-Yehuda *et al.*, 2005) and interacts with DivIVA, which mediates its localization to the cell poles. DivIVA, in turn, finds the poles by recognizing highly negatively curved membranes (Lenarcic *et al.*, 2009, Ramamurthi & Losick, 2009). Recently, the sporulation protein SirA was shown to be also required to capture the *ori* in the forespore in 10% of cells together with the ParA protein Soj (Duan *et al.*, 2016).

During sporulation both cell types inherit a single copy of the chromosome. The correct chromosome number was shown to be tightly regulated via at least three proteins: SirA (sporulation inhibitor of replication A), Sda (suppressor of *dnaA1*) and Spo0A~P. Entry of sporulation triggers the accumulation of high Spo0A~P levels, which controls *sirA* transcription. SirA binds to DnaA to inhibit its binding to the origin of replication. This prevents the initiation of additional rounds of replication during sporulation (Rahn-Lee *et al.*, 2011). Additionally Spo0A~P plays a more direct role since it is able to bind to sites around the origin of replication, inhibiting active DNA replication during sporulation, thereby regulating chromosome copy number (Boonstra *et al.*, 2013). Sda binds to the major histidine kinase KinA during active DNA replication and in response to DNA damage and replication defects, preventing Spo0A from getting phosphorylated (Cunningham & Burkholder, 2009). This mechanism restricts entry into sporulation to periods between DNA replication (Veening *et al.*, 2009, Burkholder *et al.*, 2001). Thus, more than one mechanism ensures the right chromosome number during *B. subtilis* endosporulation.

During sporulation, *B. subtilis* switches the position of the Z-ring from the midcell area to sites near both poles (Ben-Yehuda & Losick, 2002, Levin & Losick, 1996). Only one of these Z-rings will form a division septum, whereas the other is disassembled (Rudner & Losick, 2001), and separates the developing cell in a mother cell and forespore compartment. The switch from a medial to an asymmetric septum is crucial during endosporulation and depends on two factors: an increase in levels of FtsZ and the production of SpoIIE protein, the function of which is not completely understood (Carniol *et al.*, 2005). SpoIIE has a second function and is involved in activation $\sigma^F$ in the forespore. $\sigma^F$ is held in an inactive state until after completion of asymmetric division (Duncan *et al.*, 1995). At the time of asymmetric division, only approximately one-third of a chromosome is present in the forespore, but the remaining two-thirds is rapidly pumped in by the DNA translocase SpoIIIE (Bath *et al.*, 2000). Furthermore, MciZ was identified to prevent inappropriate Z-ring formation in the mother cell. The 40 amino-acid peptide is produced under the transcriptional control of $\sigma^E$ (Handler *et al.*, 2008).

### 4.3.3. Cell cycle regulation in *Streptomyces* sporulation

During *Streptomyces* vegetative growth chromosomes remain uncondensed and their replication is not followed by cell division. This mode of growth leads to the formation of elongated multigenomic compartments, which are not physically separated. Chromosome segregation and cell division occur during sporulation, when fundamental cell cycle processes are reorganized (Flärdh & Buttner, 2009). Gene products of the so called *bld* and *whi* genes have been shown to play important roles in regulation of sporulation (Flärdh & Buttner, 2009, Chater, 2001).

During the initial state of aerial hyphae development a long, non-septated, apical compartment develops: the sporogenic cell (Flärdh & Buttner, 2009). By a fluorescent fusion to the DNA polymerase III subunit DnaN it was shown, that the sporogenic cell displays a high level of DNA replication leading to the presence of 50 or more chromosome copies in each of them (Ruban-Osmialowska *et al.*, 2006). Involved in regulation of replication is the transcriptional regulator AdpA (Higo *et al.*, 2012). Binding of AdpA to the *oriC* region decreases access of the initiatior protein DnaA to prevent initiation of replication. A model was suggested in which the dissociation of AdpA from *oriC*, to permit binding of DnaA and initiation of replication, is associated with the formation of an aerial hyphae. Binding of AdpA to *oriC*, leading to replication inhibition is thought to be required during conversion of multigenomic aerial hyphae into chains of haploid spores (Wolanski *et al.*, 2012).

Responsible for segregation of multiple chromosomes in the aerial hyphae of *Streptomyces* are ParA and ParB (Kim *et al.*, 2000, Jakimowicz *et al.*, 2002). The *parAB* operon is under the control of two promoters including one that depends on several *whi* genes (Jakimowicz *et al.*, 2006). During sporulation ParA extends along the hyphae and ParB forms an array of regularly spaced complexes (Jakimowicz *et al.*, 2002, Jakimowicz *et al.*, 2007). One single ParB complex is found in every prespore that positions the chromosome between nascent septa. Lack of ParA and/or ParB from *S. coelicolor* interferes with chromosome segregation and leads to the formation of anucleate spores (Jakimowicz *et al.*, 2007). Furthermore, the absence of ParAB affects sporulation septation, suggesting that the distribution of chromosomes determines septa positioning (Jakimowicz *et al.*, 2007). Using time-lapse microscopy, the timing of hyphae elongation, sporulation as well as ParA and FtsZ appearance showed that the initiation of septation and chromosome segregation is synchronized with hyphal growth completion. It was shown, that segregation proteins affect Z-ring formation in *Streptomyces*, since the absence of ParB led to irregular shapes of the Z-ring. In conclusion, it is thought that the segregation proteins are involved in checkpoints to synchronize hyphae elongation and division (Donczew *et al.*, 2016).

To initiate the sporulation specific cell division, FtsZ assembles into long filaments in the aerial hyphae to subsequently build a ladder of Z-rings (Schwedock *et al.*, 1997, Grantcharova *et al.*, 2005, Willemse & van Wezel, 2009). The formation of Z-ladders depends on the SsgB protein. In turn, SsgB localization is mediated by SsgA. SsgB directly recruits FtsZ and promotes its polymerization (Willemse *et al.*, 2011). Recently, SepG was identified to be involved in coordination of sporulation specific cell division by ensuring the correct localization of SsgB and consequently also in the recruitment of FtsZ. Furthermore, SepG is required for nucleoid compaction in the prespore (Zhang *et al.*, 2016). The integral membrane protein CrgA was suggested to be an inhibitor of Z-ring formation leading to the correct frequency of Z-rings in sporogenic cells (Del Sol *et al.*, 2006).

## 4.4. Cell cycle regulation during vegetative growth and development of *M. xanthus*

In the last years, major progress has been made in order to understand the basic cell cycle processes during vegetative growth in *M. xanthus* (Harms *et al.*, 2013, Schumacher *et al.*, 2017, Treuner-Lange *et al.*, 2013). More experiments give insights how these events are coordinated during fruiting body formation with myxospore differentiation (Rosario & Singer, 2007, Rosario & Singer, 2010, Tzeng *et al.*, 2006, Tzeng & Singer, 2005).

### 4.4.1. Chromosome replication and segregation in *M. xanthus*

New born *M. xanthus* cells contain one circular chromosome arranged along a longitudinal axis. The origin of replication is located in the subpolar region close to the old cell pole, whereas the terminus region is located in the subpolar region close to the new cell pole. The two replisomes assemble at the origin of replication immediately prior to cell division and slowly move towards the terminus region (*ter*), which is moving in parallel towards the middle of the cell. Splitting and merging of one and two Ssb (single strand binding protein) clusters, used as a proxy for the replisomes, indicates that two replisomes move independently of each other. Replication initiates once per and takes about 70% of the cell cycle, which is approximately 210 min (Harms *et al.*, 2013). To segregate its chromosomes, *M. xanthus* uses a ParA/ParB/*parS* system like most bacteria. This system is essential since in-frame deletions of ParA and ParB could not be obtained and ParB depletion results in strong chromosome segregation defects and cell division over the nucleoid (Harms *et al.*, 2013). ParB binds specifically to *parS* sequences near the origin of replication. ParA forms a polar patch in the subpolar region that extends from the extreme pole up to the ParB/*parS* complex. Upon duplication of the ParB/*parS* complex, the ParA cloud extents from the (new) cell pole to the ParB/*parS* complex. The ParA structure retracts and is followed by the ParB/*parS* complex until it reaches the subpolar position. Thus, during the replication process one *ori* stays at the

old pole and one *ori* moves to the new cell pole. At the same time, the terminus region is relocated to the middle of the cell, where it is finally replicated. Immediately after replication and segregation and before cell division the chromosomes are arranged in an *ori-ter-ter-ori* organization (Harms *et al.*, 2013). Once the chromosome is segregated, cells are prepared to divide to produce two daughter cells, each containing one chromosome (Figure 6).

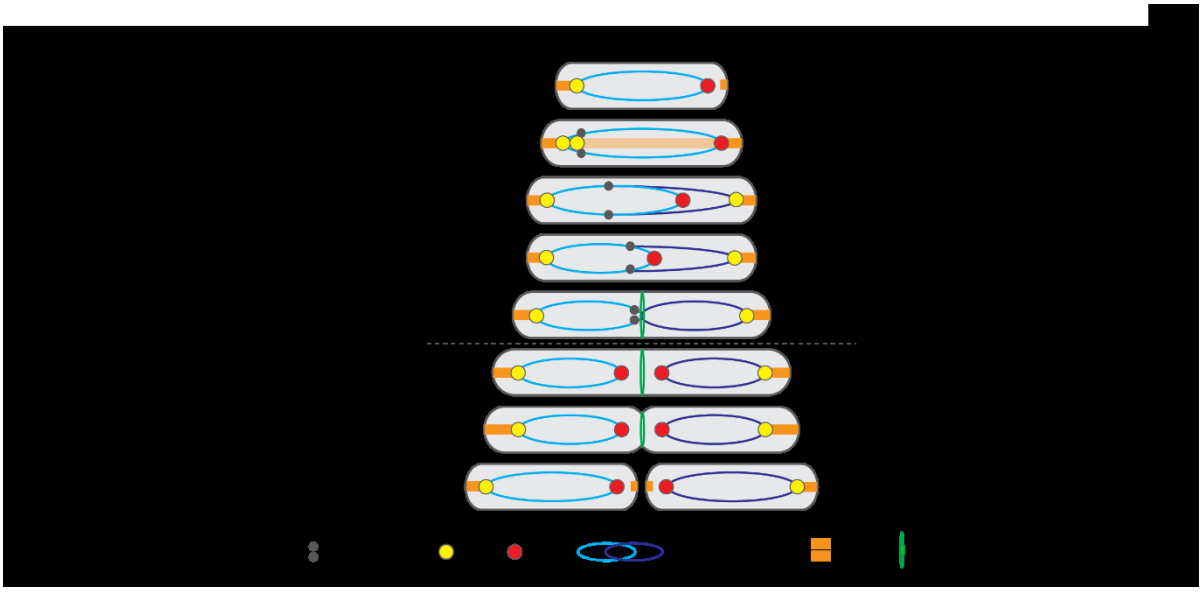

**Figure 6: Chromosome arrangement and dynamics in *M. xanthus***
The cartoon illustrates a cell through several stages of chromosome replication and segregation during one cell cycle. Details see text. Figure modified from (Harms *et al.*, 2013).

### 4.4.2. Cell division site placement in *M. xanthus*

*M. xanthus* uses the positive regulators PomX, PomY and PomZ to regulate FtsZ positioning and cell division frequency. The absence of one of the *pom* genes results in the formation of filamentous cells containing multiple chromosomes and anucleated minicells, fewer cell division constrictions and an aberrant formation and localization of Z-rings (Schumacher *et al.*, 2017, Treuner-Lange *et al.*, 2013). PomX, PomY and PomZ form a complex in the off-center position and move by biased random motion. This complex is associated with the nucleoid and translocates on the nucleoid towards the mid-nucleoid, which coincides with midcell before the nucleoids have segregated. The complex arrives at midcell before and independently of FtsZ. At the mid-nucleoid the PomXYZ complex displays constrained motion, and therefore remains at midcell (Figure 7). The dynamic localization pattern depends on the ATPase activity of the ParA ATPase PomZ, which is activated by PomX as well as by PomY and nonspecific DNA binding. ATP and nucleoid bound PomZ dimers interact with a complex of PomX and PomY and tether it to the nucleoid. A model was suggested that proposes a flux-based mechanism for the positioning of the PomXYZ complex by PomZ. PomZ displays diffusive random dynamics on the nucleoid. These dynamics result in diffusive flux of PomZ on the nucleoid from either side into the PomXYZ cluster. The PomZ fluxes into the cluster from the two sides

scale with the length of the nucleoid to the left or right side of the cluster. The flux difference creates a local PomZ concentration gradient across the PomXYZ complex with the highest concentration on the side facing most of the nucleoid. If the PomXYZ complex preferentially moves in the direction of highest PomZ flux, then the complex has a bias to move to the midnucleoid, which coincides with midcell. Here, PomZ fluxes equalize leading to an almost symmetric distribution of PomZ over the cluster. Therefore cluster motion is constrained to midcell. PomY and PomZ in the PomXYZ complex directly interact with FtsZ, suggesting that they stimulate Z-ring formation and positioning and promote cell division at midcell (Schumacher, 2016, Schumacher *et al.*, 2017).

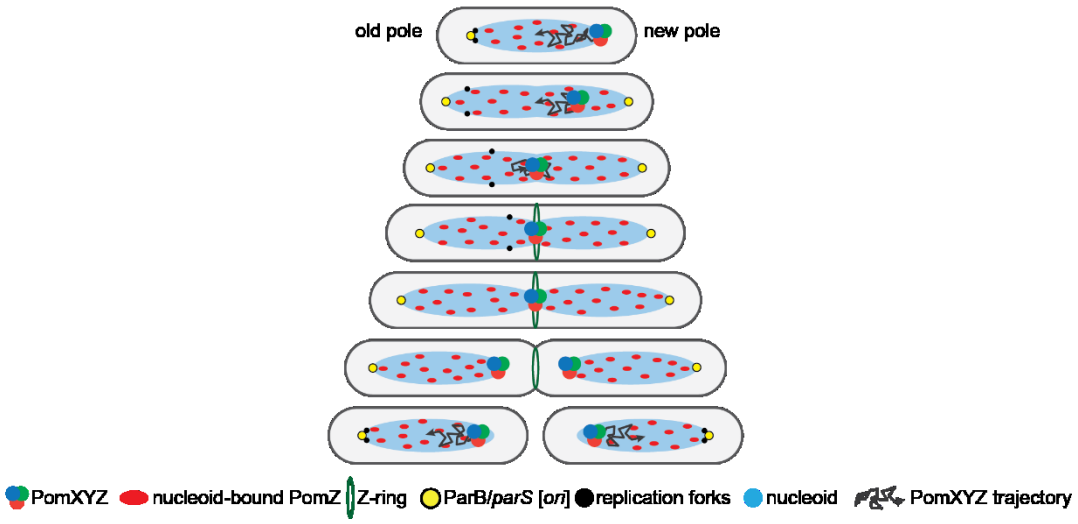


**Figure 7: PomXYZ complex translocates to midcell over the nucleoid**
Localization of the PomXYZ complex in a cell immediately after division (top) and during the cell cycle. Trajectories indicate biased motion of off-center complexes towards and constrained motion at midcell. Figure obtained from (Schumacher *et al.*, 2017).

### 4.4.3. Cell cycle and DNA synthesis during sporulation in *M. xanthus*

The first studies on replication during sporulation were performed in spores formed in response to glycerol treatment (Rosenberg *et al.*, 1967, Zusman & Rosenberg, 1968). In the presence of 0.5 M glycerol *M. xanthus* can be artificially induced to form spores. Almost all cells form spores after 2 – 8 h under these conditions (Dworkin & Gibson, 1964). Importantly, glycerol-induced spores differ from starvation induced spores with respect to the spore coat and protein composition (Kottel *et al.*, 1975, Inouye *et al.*, 1979b, Inouye *et al.*, 1979a, McCleary *et al.*, 1991). After glycerol addition, a 19% increase in DNA content was noted (Rosenberg *et al.*, 1967). A model was proposed, suggesting that upon sporulation, ongoing rounds of replication are completed but no initiation of replication occurs, leading to glycerol induced spores containing 1 – 4 chromosomes (Rosenberg *et al.*, 1967, Zusman & Rosenberg, 1968). In recent studies glycerol induced spores were analyzed by flow cytometry and showed that these spores contained one, two or even more chromosome copies. Furthermore, differences in

chromosome content of myxospores formed in fruiting bodies and glycerol induced spores were shown. Flow cytometry with purified myxospores formed in response to starvation was performed and these spores were found to contain two chromosomes. This result was confirmed by fluorescent in situ hybridization. It was suggested that the *ori* and *ter* regions are associated with the peripheral regions of the myxospore. By contrast, peripheral rods are thought to contain one chromosome (Tzeng & Singer, 2005). This finding raised questions regarding the cell cycle during fruiting body formation.

To address the role of replication during development, cells were treated with replication inhibitors like hydroxyurea, nalidixic acid or novobiocin at different time points. Addition of these compounds after 12 h does not cause a defect in fruiting body formation or sporulation, whereas earlier treatment does. It was concluded, that the developmental process becomes independent of replication after 12 h. This corresponds morphologically to the transition between aggregation phase and mound formation. In conclusion, replication occurs during the aggregation phase and is essential for sporulation and fruiting body formation (Tzeng *et al.*, 2006). Further insights were gained by investigation of a temperature sensitive mutant of *dnaB* ($DnaB^{A116V}$). Vegetative growth at the non-permissive temperature leads to cells containing one chromosome, since cells are able to complete ongoing rounds of replication but are deficient in initiating new rounds. Cells incubated at the non-permissive temperature 12 h before and during starvation were blocked in sporulation and fruiting body formation, although cells aggregated. Of note, cells of the $DnaB^{A116V}$ mutant did not show a development defect, when they were grown at the permissive temperature before starvation, but then shifted to the non-permissive during development. Also cells grown at the non-permissive temperature for 12 h and incubated on starvation media at the permissive temperature were able to form fruiting bodies. Although these fruiting bodies were misshaped, the sporulation frequency was comparable to WT cells. Moreover, despite experiencing starvation conditions for up to 24 h, when cells were shifted to permissive conditions that allow DNA replication (either removal of replication inhibitors or shift to permissive temperature), they were able to proceed with the developmental program. This led to the notion that DNA replication is required in order to form fruiting bodies and to differentiate into myxospores (Rosario & Singer, 2007).

In line with this, *dnaA* expression has been shown to be tightly regulated during nutrient depletion. *dnaA* encodes DnaA, a universally conserved ATPase responsible for initiation of DNA replication (Messer, 2002, Mott & Berger, 2007). Immediately upon starvation *dnaA* expression drops to approximately 30% of the vegetative level. Then, *dnaA* transcript numbers transiently increase between 4 and 6 hours of starvation reaching around 50% compared to vegetative growth before they decrease again. This expression peak depends on several early developmental regulators such as *relA*, *sigD* and *sdeK* and is consistent with DNA replication during the aggregation phase. (Rosario & Singer, 2010). Based on these observations, it was

suggested that *M. xanthus* uses a checkpoint mechanism at the early aggregation stage that couples replication to fruiting body formation.

Still unanswered are the questions how diploid myxospores and haploid peripheral rods arise during development and if all cells have to undergo a round of replication during development. The findings so far lead to the idea that, if all cells undergo a round of replication during development, the formation of myxospores must depend on an inhibition of cell division. By contrast, cell division must be allowed in cells becoming peripheral rods. Also, if initiation of replication is restricted to those cells becoming spores, cell division must be inhibited specifically in these cells (Treuner-Lange, 2014).

# 5. Scope of this study

Upon nutrient starvation, *M. xanthus* initiates a developmental program that culminates in the formation of multicellular structures called fruiting bodies inside which the rod-shaped cells differentiate into spherical myxospores containing two chromosomes. Fruiting bodies are surrounded by haploid cells referred to as peripheral rods. Development depends on DNA replication occurring during the aggregation phase before 12 h of starvation. Up to now, it is not clear if all cells have to undergo a round of replication during development or if replication is restricted to cells becoming spores. In both cases, it appears that cell division must be inhibited in sporulating cells.

In this study, we address replication and cell division during starvation induced cell differentiation in *M. xanthus*.

# 6. Results

If not mentioned otherwise, the wild type (WT) DK1622 (Kaiser, 1979) was used for all experiments performed in this study.

## 6.1. Myxospores contain two chromosomes

Previous results obtained by flow cytometry and fluorescent in situ hybridization showed that myxospores contain two chromosomes whereas peripheral rods are thought to contain one chromosome (Tzeng & Singer, 2005). To confirm these results, we performed flow cytometry. This method provides a snapshot of the distribution of the number of cells in a population that contain a distinct amount of DNA.

First, we investigated the chromosome content of WT cells during vegetative, exponential growth to confirm previous results. Under these conditions a distribution of cells in several stages of the cell cycle was observed (Tzeng & Singer, 2005, Harms *et al.*, 2013). As a standard, we used cells in the stationary growth phase, since they were shown to contain one single chromosome (Tzeng & Singer, 2005). The DNA content of cells was examined by staining the chromosome with 10 µM Vybrant® DyeCycle™ Orange for 40 min. The fluorescence intensity which is proportional to the DNA content was subsequently quantified by flow cytometry.

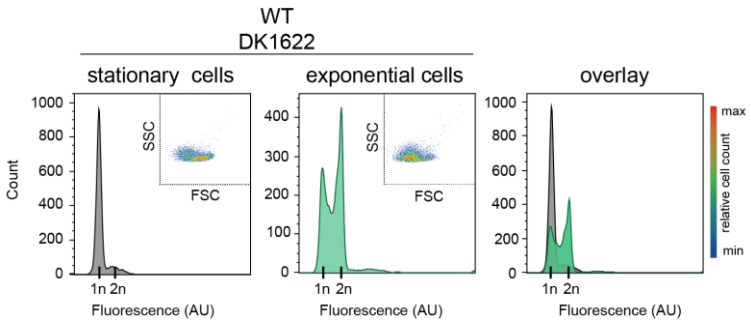


**Figure 8: Exponentially growing WT cells are in various stages of the cell cycle**
Flow cytometry profile of stationary (grey) and exponentially (green) growing WT cells. Stationary and exponentially cells were collected at $OD_{600}$ 1.75 and 0.6, respectively and stained with Vybrant® DyeCycle™ Orange. The x-axis represents arbitrary fluorescence intensity and the y-axis represents cell count. Each experimental run consisted of analysis of 10.000 individual cells. Tick marks represent the expected positions of fluorescent intensities corresponding to one and two copies of the chromosome based on the fluorescence of stationary cells. Correlated measurements of side-scattered (SSC) and forward-scattered light (FSC) are presented in a scatter plot to differentiate cell populations by their size and internal complexity, respectively. The color scale shows relative cell count from lowest (blue) to highest (red) in the scatter plots.

Flow cytometric analysis of stationary cells revealed one single peak, which was used as a standard for the expected fluorescence intensity corresponding to the presence of one chromosome (1n) (Tzeng & Singer, 2005). The presence of two chromosomes (2n) was expected to be represented by a peak which is doubled in fluorescence intensity. Exponentially growing cells reveal two single peaks corresponding to 1n and 2n content. These two peaks

are not separated completely, representing cells, which are in various stages of the replication process. In total, more cells had two chromosomes as the 2n count is higher (Figure 8). These data match results demonstrating that a population of vegetatively growing *M. xanthus* cells contains an average of 1.7 chromosomes per cell (Zusman & Rosenberg, 1970).

Correlated measurements of SSC (side-scattered light) and FSC (forward-scattered light) allow the differentiation of cell types in a heterogeneous cell population. SSC is proportional to internal cell complexity, whereas FSC is proportional to cell-surface area or size. Based on these parameters, stationary and exponentially grown cells display one homogenous cell population (Figure 8 insets). Since these results confirmed that exponentially growing cells are a mixture of asynchronous cells, which are in various stages of the cell cycle, having either one or two chromosomes or undergo replication, these cells were used as a standard in following flow cytometry experiments.

In the next step, we analyzed the flow cytometry profile of cells, which are differentiated into spores and peripheral rods. WT cells were grown to exponential growth phase and subsequently spotted on TPM agar to induce starvation. After 120 h cells were harvested and imaged on 1% agarose buffered with TPM at 32°C. Furthermore, they were resuspended in TPM buffer and their nucleoid was stained with 10 µM Vybrant® DyeCycle™ Orange for 40 min before the DNA content was quantified by flow cytometry. As a standard, exponentially growing cells were analyzed as described before.

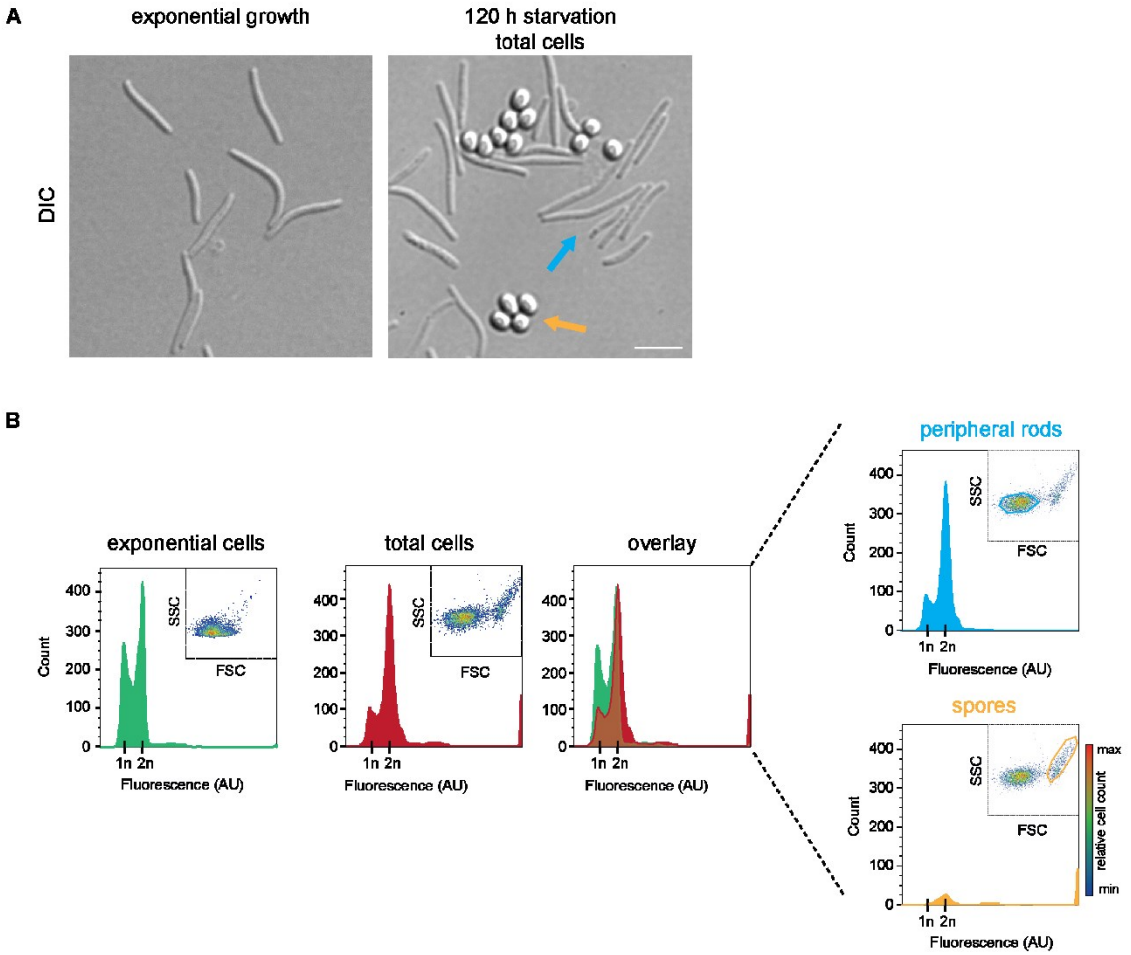


**Figure 9: Flow cytometry profile of peripheral rods and spores**
**(A)** Exponentially growing WT cells or WT cells starved on TPM agar for 120 h were imaged on 1% agarose buffered with TPM at 32 °C. Orange arrow points to spores, blue arrow to peripheral rods. Scale bar 5 µm. **(B)** Flow cytometry profile of WT cells starved on TPM agar for 120 h (red) compared to exponentially growing cells (green). Cells were stained with Vybrant® DyeCycle™ Orange. The x-axis represents arbitrary fluorescence intensity and the y-axis represents cell count. Each experimental run consisted of analysis of 10.000 individual cells. Tick marks represent the expected positions of fluorescent intensities corresponding to one and two copies of the chromosome based on the fluorescence of exponentially growing cells. Correlated measurements of SSC and FSC are presented in scatter plots and allow separate analysis of distinct cell populations. The analysis of cells having the same properties as vegetative cells (peripheral rods/encircled in blue) and the additional cell population detectable during development (spores/encircled in orange) are presented individually. The color scale shows relative cell count from lowest (blue) to highest (red) in the scatter plots.

Flow cytometric analysis of total cells starved for 120 h on TPM agar revealed two peaks corresponding to 1n and 2n content, based on the profile of exponentially growing cells. Less cells seem to contain one chromosome in comparison to vegetative growth, since the peak corresponding to 1n is smaller than the 1n peak of exponentially growing cells. Moreover, the number of cells which are “in between” the 1n and 2n peak decreases, suggesting that less cells are in the replication process (Figure 9).

Based on SSC and FSC measurements, we observe one cell population, which appears to have the same properties as vegetative cells. Additionally, a second cell population is present which reflects just a small fraction of all cells. This population is increased in both, SSC and

FSC values (Figure 9 insets). Since this population is not detectable in vegetative cells, we conclude that these cells represent the spores, whereas the first cell population represents the peripheral rods. Inspection of both cell populations individually revealed a different flow cytometric profile for each of them. Whereas cells coincident with SSC and FSC properties of vegetative cells, the peripheral rods, display two peaks corresponding to 1n and 2n, the second cell population, the spores, displays one peak corresponding to 2n. The observed peak appears to be very small in comparison to the peaks for peripheral rods, suggesting that the spore population is much smaller than the population of peripheral rods.

This flow cytometric analysis supports previous results indicating two chromosomes in myxospores (Tzeng & Singer, 2005). The population of peripheral rods is diverse in its chromosomal content, having one or more often two chromosomes and contains some cells which seem to undergo replication. This result differs from previous observations since peripheral rods were thought to contain one chromosome (Tzeng & Singer, 2005).

## 6.2. Low speed centrifugation can separate two distinct populations of cells

During the developmental program of *M. xanthus*, cells differentiate into three cell fates: Aggregation into fruiting bodies, followed by differentiation into spores, cell lysis or cells become peripheral rods and stay outside of fruiting bodies. In this study, we want to examine future spores and future peripheral rods separately. To be able to distinguish between aggregating cells (future spores) and non-aggregating cells (future peripheral rods) in our experiments we used a previously established method (O'Connor & Zusman, 1991b, Lee *et al.*, 2012, Lee *et al.*, 2011). Cells were starved in submerged culture using MC7 buffer or on TPM agar, harvested at different time points during the developmental program and separated by low speed centrifugation (50 x g, 5 min). This results in the separation of aggregating cells in the pellet and the non-aggregating cells in the supernatant. To test if this method was working properly in our hands, we checked for accumulation of ProteinC in both fractions in WT cells. ProteinC is a 31 kDa fragment of the extracellular protease FibA, which is exclusively produced in aggregating cells. Therefore it can be used as a marker for the distinct cell populations (Lee *et al.*, 2011).

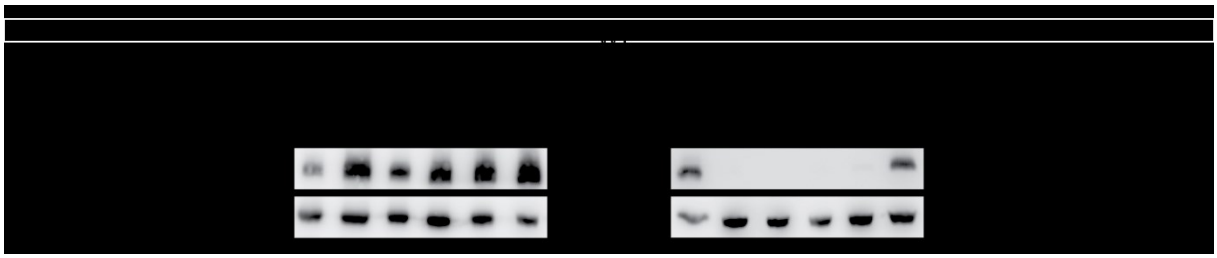

**Figure 10: ProteinC accumulates mainly in aggregating cells**
Immunoblot analysis to confirm separation of specific cell populations differentiated during development. WT cells were starved in submerged culture using MC7 buffer. Samples were taken at indicated time points. Aggregating and non-aggregating cells were separated by low speed centrifugation (50 x g, 5 min). Cell lysates were probed with specific α-ProteinC, (Lee *et al.*, 2011) and α-PilC antibodies (Bulyha *et al.*, 2009) to detect ProteinC (31 kDa) and PilC (45.2 kDa).

ProteinC accumulates in aggregating cells during the time course up to 24 h of development. In non-aggregating cells, the protein does not accumulate up to 12 h of starvation. After 24 h, ProteinC is detectable in this cell fraction, but at lower levels compared to the amount of protein in aggregating cells. As loading control, we checked for the accumulation of PilC which is detectable up to 24 h in both cell fractions (Figure 10). PilC is an inner membrane protein and part of the pilus machinery in *M. xanthus* (Bulyha *et al.*, 2009). Of note, earlier results regarding the accumulation of PilC in aggregating and non-aggregating cells suggested a decrease in both cell populations but considerably more rapidly in the aggregating cells (Lee *et al.*, 2012). However, our analysis could not support these observations. In fact, we found that PilC levels do not significantly change until 24 h in non-aggregating or aggregating cells (see also 6.4.2). Previous results concerning the accumulation of PilC or ProteinC have been aquired in the *M. xanthus* wild type DZ2 and showed no accumulation of ProteinC in the non-aggregating cell fraction from 0 h to 36 h of starvation in submerged culture, but by 48 h it was also observed in future peripheral rods (Lee *et al.*, 2012). The observed differences concerning the accumulation of ProteinC in the wild types DZ2 and DK1622 can be explained by the fact that DK1622 is faster in its developmental program, i.e. after 24 h of starvation, DK1622 cells have already formed dense aggregates whereas DZ2 forms dense aggregates after 36 h - 48 h (Lee *et al.*, 2012). The different WT background might also explain the different accumulation patterns of PilC.

Taken together, the distinct accumulation of ProteinC shows, that we can distinguish aggregating from non-aggregating cells by low speed centrifugation.

## 6.3. Cell cycle status of distinct cell fates early and late during development

Previous work showed that mature *M. xanthus* spores and peripheral rods have a different chromosomal content. Using flow cytometry and FISH (fluorescent *in situ* hybridization) on fixed cells, Tzeng and Singer concluded that myxospores contain two fully duplicated genomes, whereas peripheral rods were suggested to contain one chromosome (Tzeng & Singer, 2005). In addition, replication during the first 12 h of development is essential for fruiting

body formation and sporulation (Tzeng *et al.*, 2006, Rosario & Singer, 2007). Using flow cytometry, we confirmed that myxospores contain two chromosomes. Our results suggest that peripheral rods are diverse in their chromosomal content, having one or two chromosomes and might undergo replication (Figure 9/6.1).

Recently investigated tools to visualize different chromosome regions and the replisome in vegetatively growing cells allow single cell analysis in living cells (Harms *et al.*, 2013). On one hand, these tools will be used to confirm existing data about the chromosome content and organization in myxospores and peripheral rods and to analyze the chromosome content of cells early during development. On the other hand, these tools allow to address if replication is restricted to one cell fate during fruiting body formation and if DNA synthesis is happening exclusively during the first 12 h of starvation. These additional experiments allow to examine living cells early and late during development and give the possibility to address how replication and chromosome organization are coupled to cell fate during fruiting body formation. Furthermore, by investigation of single cells we will be able to verify if peripheral rods undergo replication as suggested by the flow cytometry profile (Figure 9/6.1)

### 6.3.1. Aggregating and non-aggregating cells have the same chromosome content after 24 h of starvation

To analyze the chromosome content of single developing cells, we used different fluorescent markers. Using a strain which expresses *parB-eYFP* under the control of the vanillate inducible promoter in the WT background (SA6144) enables to check for the number of origins of replication (*ori*), since ParB binds to the *parS* sequences near the *ori* in *M. xanthus* (Harms *et al.*, 2013). Additionally, we used FROS (fluorescent repressor operator system) to visualize different chromosomal loci. By insertion of a *tetO*-array at 192° (SA4194) or 33° (SA6143) and in parallel expressing *tetR-eYFP* under the control of the vanillate inducible promoter we were able to observe the terminus and origin region, respectively. FROS has been used previously to investigate the chromosome arrangement of vegetatively growing *M. xanthus* cells (Harms *et al.*, 2013).

The analysis of vegetatively growing or developing cells revealed a certain amount of cells showing no signal. However, during both conditions cells contained one or two ParB-eYFP or TetR-eYFP clusters in a reproducible pattern in the presence of 100 µM vanillate. Cells showing a signal were taken into account for the analysis. The localization patterns in strains expressing *tetR-eYFP* or *parB-eYFP* during vegetative growth conditions obtained in this study match the localization patterns, which were shown previously for each of them during vegetative growth (Harms *et al.*, 2013). ParB-eYFP forms two signals in the subpolar regions in 69% of cells, more specifically around 20% and 80% of cell length. A single ParB-eYFP

cluster is found at around 20% of cell length in 31% of cells. TetR-eYFP binding to the *tetO*-array inserted at 33° forms one cluster in 71% of cells at around 30% of cell length whereas in 29% of cells two signals are found. They are found around 30% and 70% of cell length. Two termini, represented by TetR-eYFP binding to the *tetO*-array inserted at 192° are visible in 6% of cells. In the remaining 94% we observe one signal. The clusters are found around 40 - 50% of cell length which is close to the middle of the cell. Cells show a diffuse signal when expressing *eYFP* in *M. xanthus* (SA6166) by using the same conditions (Figure 11A).

To examine the chromosome number during development, cells expressing *parB-eYFP* (SA6144) or FROS to visualize the origin region at 33° (SA6143) or the terminus region at 192° (SA4194) were grown to exponential growth phase in the presence of 100 µM vanillate and subsequently spotted on TPM agar plates supplemented with 100 µM vanillate. Under these conditions the strains were able to aggregate into fruiting bodies. After 120 h of starvation, the sporulation frequencies were comparable to WT cells (Figure 11B).

After 24 h cells were harvested, separated in aggregating and non-aggregating cell fractions (6.2) and imaged on 1% agarose buffered with TPM at 32°C. The analysis of the localization patterns in both cell fractions did not reveal a strong difference between the number of ParB-eYFP clusters or the number of TetR-eYFP foci binding to 33° or 192° of the chromosome. Two ParB-eYFP signals were found in 81% and 77% in non-aggregating and aggregating cells, respectively. In the remaining 19% and 23% of cells we observed one ParB-eYFP cluster. In both cell types, 60% of cells showed two and 40% one TetR-eYFP signal representing the origin region (33°). Furthermore, 62% of aggregating and 77% of non-aggregating cells showed one signal representing the terminus region (192°) whereas 38% and 23% of cells contained two TetR-eYFP foci, respectively. Expression of *eYFP* did not result in any foci formation (Figure 11C). These results did not reveal any differences in the chromosome status of aggregating and non-aggregating cells after 24 h of starvation. Most cells contained two origins of replication and one terminus region. In comparison to vegetative growth, the number of cells showing two foci for TetR-eYFP binding to the *tetO*-array at 33° and 192° increased, indicating that more cells have two chromosomes after 24 h of starvation.

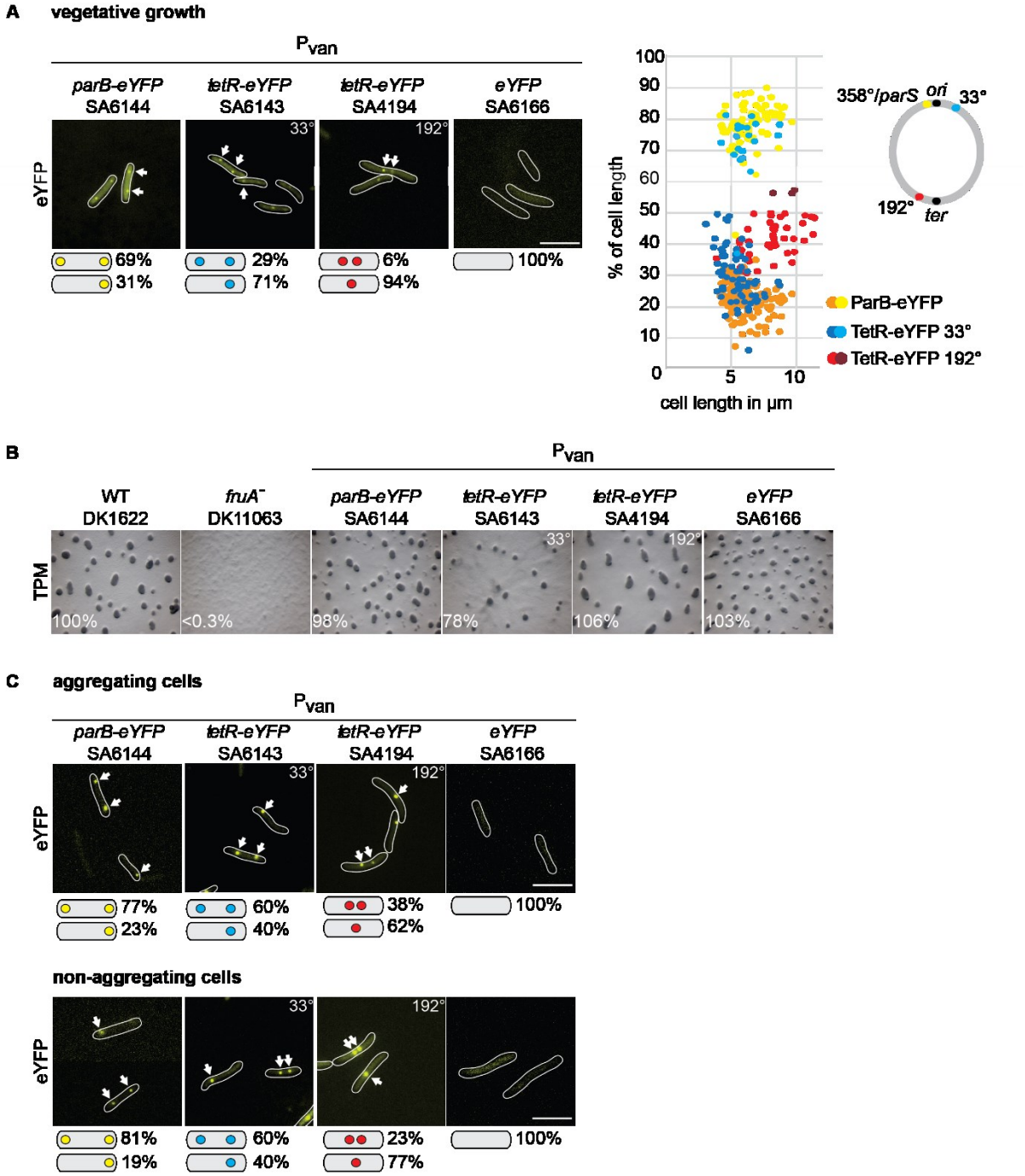


**Figure 11: After 24 h of starvation non-aggregating and aggregating cells show the same chromosome content.**

**(A)** Cells of indicated strains were grown to exponential growth phase in the presence of 100 µM vanillate to induce expression of fluorescent fusion proteins and imaged on 1% agarose buffered with TPM at 32 °C. Outline of representative cells was obtained from DIC pictures. Abundance of localization patterns is indicated by numbers. Scale bar 5 µm. The scatter plot depicts the position of one or two TetR-eYFP as well as ParB-eYFP clusters in the cells as % of cell length and as function of cell length (n>100). The cartoon represents the circular chromosome with the positions of *tetO*-arrays and *parS* sequence. **(B)** Cells were grown as described in (A) and starved for 120 h on TPM agar including 100 µM vanillate. Sporulation frequency is indicated by numbers. Scale bar: 500 µm. **(C)** Cells were grown as described in (A) and starved for 24 h on TPM agar containing 100 µM vanillate. Aggregating and non-aggregating cells were separated and imaged on 1 % agarose buffered with TPM at 32°C. Outline of representative cells was obtained from DIC pictures. Cartoons indicate occurrence of given localization patterns (n>150). White arrows indicate foci. Scale bar: 5 µm.

### 6.3.2. Aggregating and non-aggregating cells after 24 h of starvation actively replicate their chromosome

Previous results indicate that during the aggregation phase of the developmental program cells actively replicate their genome and that this crucial for efficient sporulation (Tzeng *et al.*, 2006). To understand how the cell cycle progresses during development in both cell fates in more detail we investigated replication on the single cell level in developing cells. To do so, we used a tool which has been used before to analyze replication in vegetative *M. xanthus* cells (Harms *et al.*, 2013). The fluorescent fusion protein Ssb-eYFP functions as a marker for the replication forks since Ssb binds to unwound DNA on the lagging strand during replication (Shereda *et al.*, 2008). In strain SA5831 *ssb-eYFP* is integrated at the native site and expressed under the control of its native promoter. Exponentially growing cells as well as cells starved on TPM agar for 24 h were analyzed for their number of foci. Cells were able to form fruiting bodies and to sporulate. After 120 h of starvation, the sporulation frequencies were comparable to WT cells, suggesting that the expression of *ssb-eYFP* did not lead to a developmental defect (Figure 12A). Aggregating and non-aggregating cells were separated as described (6.2) and cell fractions as well as vegetative cells were imaged on 1% agarose buffered with TPM at 32°C.

In 76% of vegetatively growing cells we detected one or two Ssb-eYFP signals indicating single stranded DNA at the replication forks (Figure 12B). This localization pattern was observed previously (Harms *et al.*, 2013) and the presence of a single cluster or two well separated clusters was suggested to reflect two replisomes that move independently of each other. One cluster represents two merging Ssb-eYFP clusters to form a single cluster because the replisomes are in close physical proximity (Harms *et al.*, 2013).

Cells which were starved for 24 h showed signals in 40% of both aggregating and non-aggregating cells (Figure 12C). Thus there is no difference between the cell fractions under these conditions. However, these observations do not allow to distinguish between ongoing replication in aggregating and non-aggregating cells and the presence of stalled replication forks, since Ssb-eYFP clusters can also be observed in vegetative cells which are blocked in replication by hydroxyurea for 8 h (Figure 12B). Treatment with hydroxyurea leads to depletion of deoxyribonucleotides by inhibition of the ribonucleotide reductase (Sinha & Snustad, 1972). In *M. xanthus*, the presence of 50 mM hydroxyurea leads to severe growth defects, suggesting replication is blocked (Schumacher *et al.*, 2017). To address the question if replication is ongoing in cells starved for 24 h, we used the nucleoside analog of thymidine EdU (5-ethynyl-2´-deoxyuridine). This component is incorporated into the DNA during active DNA synthesis. Exponentially growing WT cells or WT cells expressing *ssb-eYFP*, or WT cells that were starved on TPM medium for 24 h were incubated for 30 minutes at 32°C with shaking in CTT

or TPM buffer in the presence of 18.75 µg/ml EdU. Incorporation of EdU was detected by a click reaction using AlexaFluor594.

During exponential growth conditions, in 41% of WT cells a signal representing incorporation of EdU was detected, indicating active DNA synthesis in a subpopulation of cells. Treatment of the WT cells in the same way, but without addition of AlexaFluor594 during the click it reaction did not result in any signal formation. Furthermore no signals were formed when cells were incubated without EdU but applied to AlexaFluor594 during the click it reaction. This confirms that no unspecific foci are formed. In addition, Ssb-eYFP colocalized with the place of active DNA replication, since in essentially all cells showing a signal for both (36%), the signals overlapped. Moreover, we detected cells showing a signal for Ssb-eYFP but no EdU labeling (2%) and vice versa (11%), suggesting that a Ssb-eYFP foci does not guarantee active DNA replication and that Ssb-eYFP does not always form a cluster during replication (Figure 12D). After 24 h of starvation we observe foci in 38% of aggregating and 33% of non-aggregating cells, indicating active DNA replication in developing cells (Figure 12E).

In summary, aggregating and non-aggregating cells starved for 24 h do not show a difference regarding active replication.

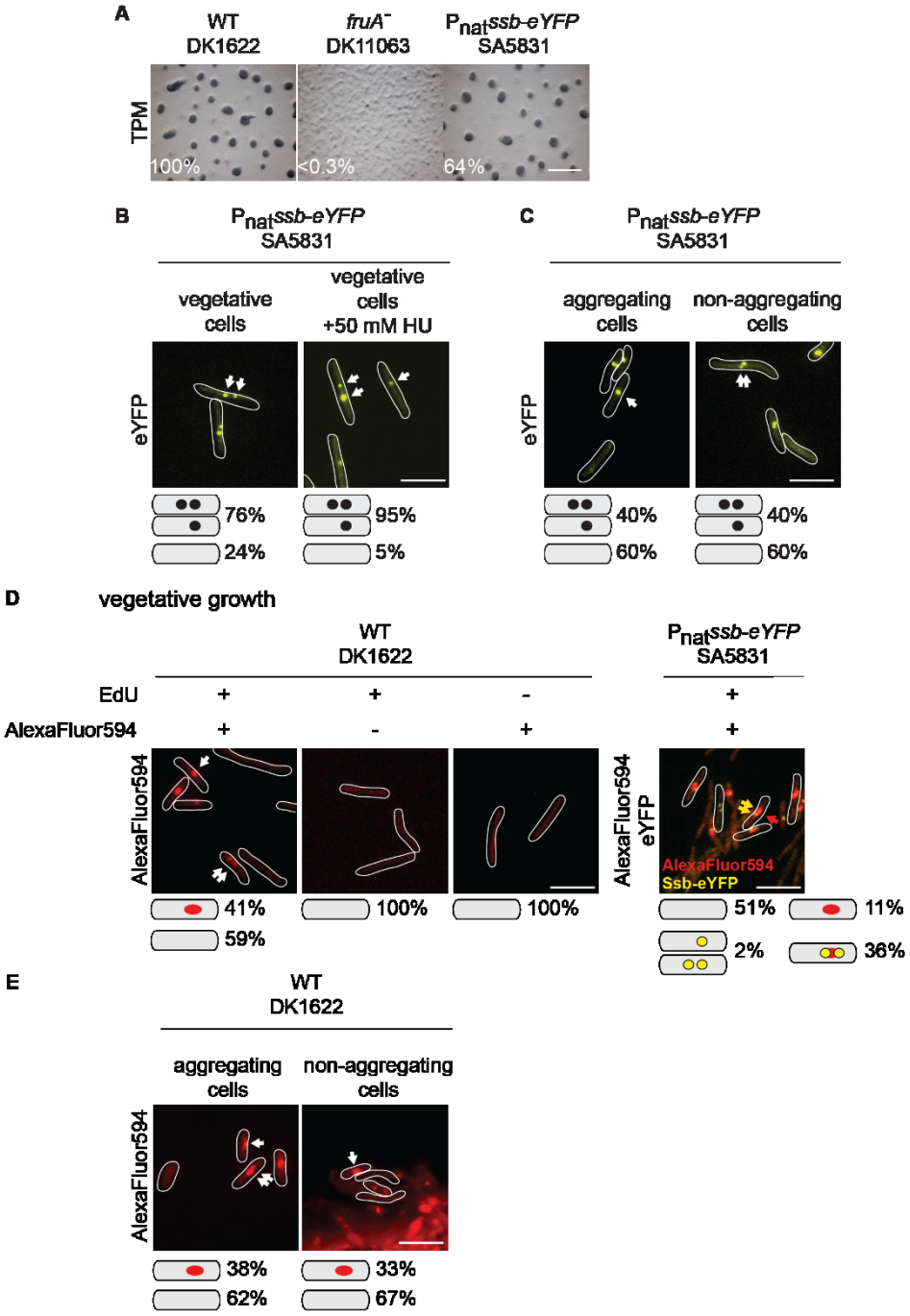


**Figure 12: Aggregating and non-aggregating cells replicate after 24 h of starvation**
**(A)** Cells of indicated strains were starved for 120 h on TPM agar. Sporulation frequency is indicated by numbers. Scale bar: 500 µm **(B)** Exponentially grown WT cells expressing *ssb-eYFP* with or without 50 mM hydroxyurea (HU) treatment for 8 h were imaged on 1% agarose buffered with TPM at 32 °C by fluorescence microscopy. Outlines of representative cells were obtained from DIC pictures. White arrows indicate foci. Cartoons indicate occurrence of given localization patterns (n>150). Scale bar: 5 µm. **(C)** Cells were starved for 24 h on TPM agar. Aggregating and non-aggregating cells were separated and imaged as described in (B). Cartoons are as in (B) (n>150). Scale bar: 5 µm. **(D)** Exponentially grown cells were incubated in the presence or absence of 18.75 µg/ml EdU for 30 min followed by a click it reaction. The experiment was performed in the presence (+) or absence (-) of EdU and with (+) or without (-) AlexaFluor594 as indicated. Cells were imaged as described in (B) Cartoons are as in (B). Scale bar: 5µm. **(E)** WT cells were starved for 24 h on TPM agar. Aggregating and non-aggregating cells were separated. EdU was applied, click it reaction was performed and cells were imaged as described in (B). Cartoons are as in (B) (n>100). Scale bar: 5µm.

### 6.3.3. Mature spores contain two origins of replication and two termini

To analyze the chromosome content of mature spores and peripheral rods at later stages during development, we used the same strains as described before (6.3.1) to visualize different chromosomal loci in single cells. Additionally, we constructed a strain expressing *parB-mCerulean* via the copper inducible promoter in parallel with *tetR-eYFP* under the regulation of the vanillate inducible promoter having the *tetO*-array inserted at 192°. This strain (SA6182) gives the opportunity to visualize the origin of replication as well as the terminus region simultaneously and enables to gain information about the *ori* and *ter* number in the same cell. The cells were grown to exponential growth phase in the presence of 100 µM vanillate or 100 µM vanillate and 150 µM $Cu^{2+}$ to express fluorescent fusion proteins and subsequently spotted on TPM agar plates containing 100 µM vanillate or 100µM vanillate and 150µM $Cu^{2+}$ to induce starvation. As shown for strains described earlier (Figure 11B), also SA6182 is able to form fruiting bodies and to sporulate at WT levels under the described conditions (Figure 13A). After 120 h spores were harvested and imaged on 1% agarose buffered with TPM at 32°C. To not miss any signals in the spherical spore, we performed Z-stacks with 0.15 µm intervals through the spores and analyzed the maximal projection of these pictures.

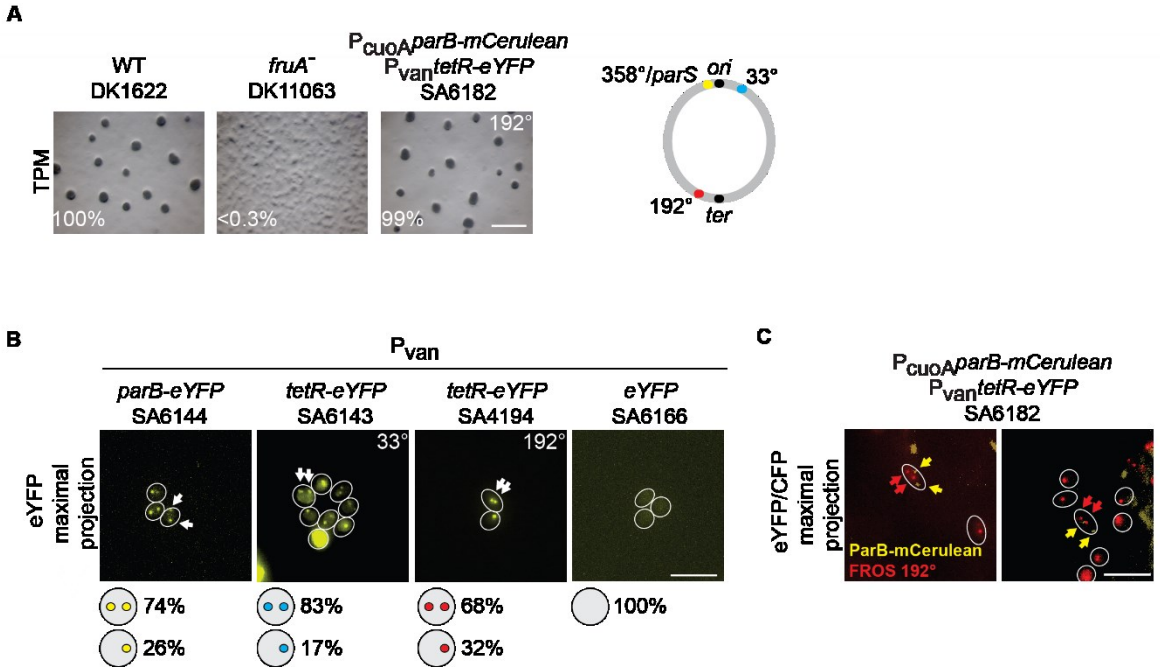


**Figure 13: Most myxospores contain two fully duplicated genomes**
**(A)** Cells of indicated strains were starved for 120 h on TPM agar containing 100 µM vanillate and 150 µM $Cu^{2+}$ to induce expression of fluorescent fusion proteins. Sporulation frequency is indicated by numbers. Scale bar: 500 µm. A cartoon shows the circular chromosome with the positions of the chromosomal markers in the genome of *M.xanthus*. **(B)** Cells of indicated strains were starved for 120 h on TPM agar containing 100 µM vanillate and 150 µM $Cu^{2+}$. After 120 h spores were harvested and imaged on 1 % agarose buffered with TPM at 32 °C. Z-stacks with 0.15 µm intervals were performed. Maximal projection of representative spores is shown. Outline was obtained from DIC pictures. Cartoons indicate occurrence of given localization patterns (n>100). Arrows indicate foci. Scale bar: 5 µm. **(C)** Cells of indicated strain were starved for 120h on TPM agar containing 100 µM vanillate and 150 µM $Cu^{2+}$. Images were taken as described in (B). Scale bar: 5 µm.

Analyzing mature spores expressing different fluorescent chromosomal markers revealed that 74% shows two ParB-eYFP foci representing the origin of replication. In the remaining 26% of spores we detected one ParB-eYFP cluster. Furthermore, we observed two signals for TetR-eYFP binding to the *tetO*-array at 33° in 83% of spores and two signals for TetR-eYFP binding to the *tetO*-array at 192° in 68% of spores. In 17% and 32% of spores one TetR-eYFP cluster is formed, respectively (Figure 13B). Thus, most mature spores contain two origins of replication and two termini regions. In addition, we visualized the two origins of replication by ParB-mCerulean and the two terminus regions by the FROS system in one spore (Figure 13C). Notably, ParB-mCerulean formed foci in very few vegetatively growing cells (data not shown) or spores, indicating it is not as stable as ParB-eYFP. It was suggested that the *ori* and *ter* regions are associated with the peripheral regions of the myxospore and appeared to be at opposite ends (Tzeng & Singer, 2005). However, our data do not support this observation, since the foci representing the *ori* and *ter* regions are also found in the middle of the spore and are not opposite to each other (Figure 13C).

Taken together, we were able to confirm previous results obtained by cell population analysis (Tzeng & Singer, 2005)(Figure 9B) and showed that mature spores mostly contain two fully duplicated genomes. Single cell analysis revealed that most spores contain two origins of replication and two termini regions.

### 6.3.4. Peripheral rods are diverse in their chromosomal content

To investigate the earlier proposed 1n chromosomal content of peripheral rods (Tzeng & Singer, 2005) and in addition to flow cytometric analysis (Figure 9B), we used our tools to examine the chromosome content in peripheral rods as well. The same strains and conditions as described above (6.3.3) were used and the cells were starved on TPM agar in the presence of 100 µM vanillate for 120 h. Cells were harvested, peripheral rods were separated (6.2) and imaged on 1% agarose buffered with TPM at 32°C.

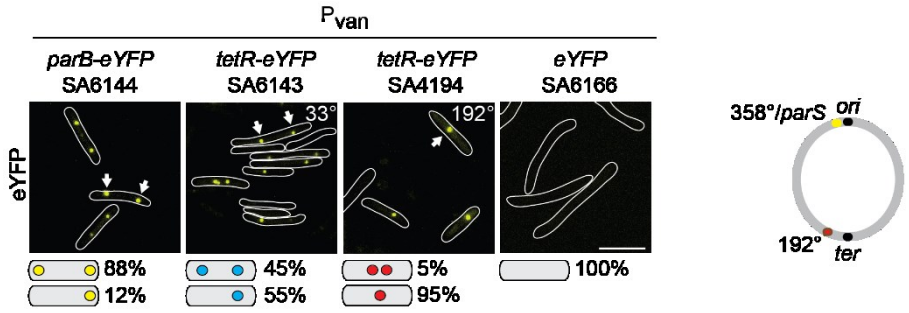


**Figure 14: Peripheral rods are diverse in their chromosomal content**
Cells of indicated strains were starved for 120 h on TPM agar containing 100 µM vanillate to induce expression of fluorescent fusion proteins. Peripheral rods were imaged on 1 % agarose buffered with TPM at 32 °C by fluorescence microscopy. Representative cells are shown and outlines were obtained from DIC pictures. Cartoons indicate occurrence of given localization patterns (n>100). White arrows highlight foci. A scheme represents the circular chromosome with the positions of the chromosomal markers in the genome of *M.xanthus* visualized by fluorescence microscopy. Scale bar: 5 µm.

In 88% of cells, we observed two ParB-eYFP foci, representing the origin of replication whereas in 12% one ParB-eYFP cluster was visible. Two TetR-eYFP foci, binding to the *tetO*-array at 33° of the chromosome were present in 45% of cells, representing the origin region. The remaining 55% of cells showed one TetR-eYFP signal. Additionally, we detected two TetR-eYFP foci in 5% and one TetR-eYFP cluster in 95% of the cells binding the *tetO*-array at 192° of the genome which represents the terminus region. The expression of eYFP did not result in any foci formation (Figure 14).

These data suggest, that peripheral rods do not contain one single chromosome as proposed previously (Tzeng & Singer, 2005). Instead, the chromosome content is comparable to exponentially growing cells (Figure 11A). Most cells contain two origins but one terminus, suggesting that they undergo replication. These data are in line with our flow cytometry data (Figure 9B).

### 6.3.5. Peripheral rods undergo replication

In cells starved for 24 h we were not able to detect a difference regarding the number of cells, which actively replicate their chromosome in the two cell fates. To explore if mature spores and peripheral rods undergo replication, we used Ssb-eYFP as a marker for the replication forks and EdU labeling to visualize newly synthesized DNA in cells, which had been starved on TPM agar for 120 h as described in 6.3.2.

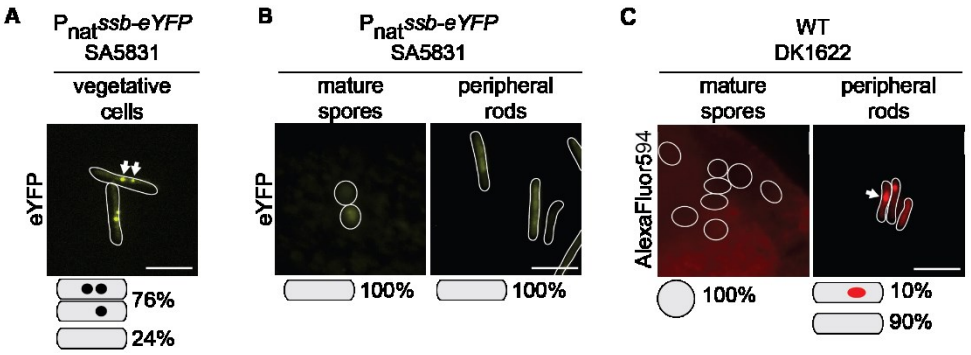


**Figure 15: Ssb-eYFP does not form clusters in mature spores or peripheral rods but peripheral rods replicate actively**
**(A)** Exponentially grown cells expressing *ssb-eYFP* (SA5831) were imaged on 1% agarose buffered with TPM at 32 °C. Outlines were obtained from DIC pictures. Please note, that same data as in Figure 12A are presented. **(B)** Cells expressing *ssb-eYFP* were starved for 120 h on TPM agar. Mature spores and peripheral rods were separated and imaged as described in (A). For spores, Z-stacks with 0.15 µm intervals were performed Maximal projection of representative spores is shown. **(C)** WT cells were starved for 120 h on TPM agar. Mature spores and peripheral rods were separated and cells were incubated in the presence of 18.75 µg/mL EdU for 30 minutes followed by a click it reaction with AlexaFluor594. Images were taken as described in (B). Cartoons indicate occurrence of given localization patterns (n>150). Scale bar 5 µm.

76 % of exponential growing cells (Figure 15A/Figure 12A) and 40% of aggregating or non-aggregating cells starved for 24 h (Figure 12B) show Ssb-eYFP foci, suggesting the presence of replication forks. Neither mature spores nor peripheral rods starved for 120 h showed any Ssb-eYFP focus (Figure 15B). We could not visualize EdU incorporation in mature spores, suggesting that spores were not replicating during the labeling process. The second possibility is that either EdU or AlexaFluor594 were not able to pass the spore coat. In peripheral rods, we observed active DNA replication in 10% of cells (Figure 15C).

In summary, aggregating and non-aggregating cells starved for 120 h show clear differences regarding their chromosomal content. Most mature spores have two origins of replication and two termini, suggesting they have two fully duplicated genomes. This is supported by flow cytometry analysis. Most likely, myxospores do not actively replicate. The majority of peripheral rods shows two origins of replication and one terminus, similar to the chromosome content of vegetatively growing cells. Also the flow cytometry of peripheral rods is comparable to vegetatively growing cells and includes cells that seem to undergo replication. In 10% of peripheral rods, we detected active DNA replication, indicating a reduction in cells which actively replicate their genome compared to vegetative growth conditions.

## 6.4. Analysis of proteins important for cell division during development

Analyzing the chromosome content of developing cells revealed and confirmed the presence of two fully duplicated genomes in myxospores. In vegetative cells, cell division follows upon chromosome duplication. These observations suggest that cell division is inhibited in cells dedicated to become spores. To test this hypothesis, we focused on analyzing proteins that are known to be important players in *M. xanthus* cell division (Schumacher *et al.*, 2017,

Treuner-Lange *et al.*, 2013). In the following chapters, experiments to explore the presence and need of the main cell division protein FtsZ and the regulators of cell division PomX, PomY and PomZ during development will be described.

### 6.4.1. FtsZ and PomXYZ levels decrease during development

To get an insight into regulation of cell division during development of *M. xanthus*, we analyzed if proteins, which are known to be important for cell division and its regulation during vegetative growth are present during development. To do so, we checked for the accumulation of FtsZ, PomX, PomY and PomZ in WT cells. Cells were starved in submerged culture using MC7 buffer, samples were taken at different time points and cell lysates were analyzed by immunoblot analysis with specific antibodies.

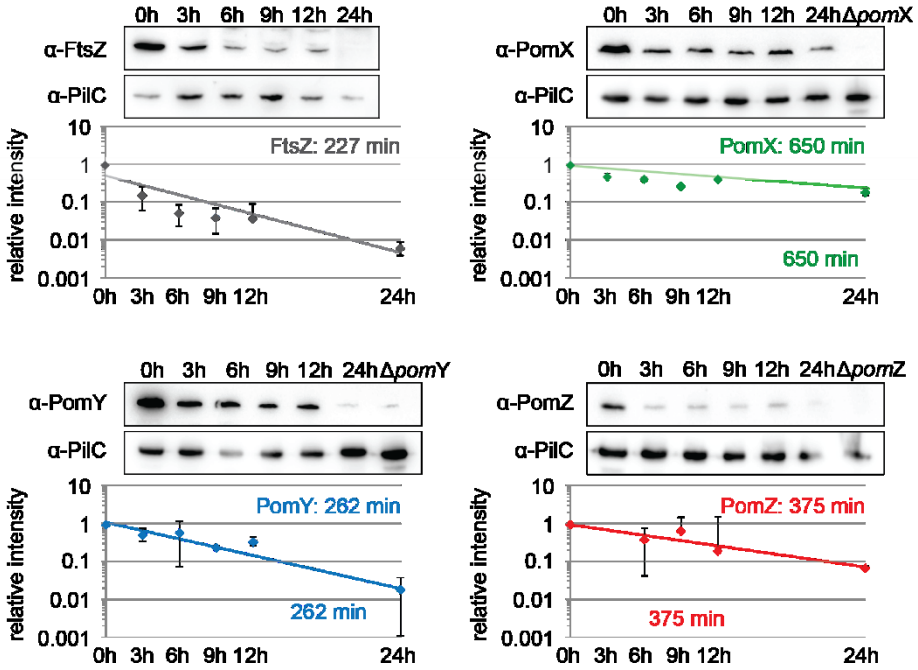


**Figure 16: FtsZ, PomX, PomY and PomZ decrease during development in total cells**
Immunoblot analysis of FtsZ (44.7 kDa), PomX (43.9 kDa), PomY (70.1 kDa) and PomZ (44.7 kDa) during development. WT cells were starved in submerged culture using MC7 buffer. Samples were taken at indicated time points. Blots were probed with specific α-FtsZ (grey), α-PomX (green), α-PomY (blue), α-PomZ (red) (Treuner-Lange *et al.*, 2013, Schumacher *et al.*, 2017) and α-PilC (45.2 kDa) antibodies (Bulyha *et al.*, 2009). Graphs were created by densitometry analysis of immunoblots to calculate the time to reduce to 50% of initial intensity which is indicated by coloured numbers. Data are presented as mean of two independent biological replicates relative to α-PilC loading control. Error bars indicate standard deviation.

The protein levels of FtsZ, PomX, PomY and PomZ decreased during development. To quantify this decrease in detail, we calculated the time until the level of each individual protein reduced to 50% of its level at the 0 h time point. FtsZ levels are reduced to 50% in 227 min. PomX is reduced to 50% in 650 min, PomY in 262 min and PomZ in 375 min (Figure 16).

### 6.4.2. FtsZ and PomXYZ decrease specifically in cells dedicated to become spores

To investigate if the accumulation of important cell division proteins is regulated differently in aggregating and non-aggregating cells we checked for the accumulation of FtsZ, PomX, PomY and PomZ in both cell fractions. To do so, we starved WT cells in submerged culture using MC7 buffer, harvested the cells at various time points and separated aggregating and non-aggregating cells as described earlier (6.2). Cell lysates were analyzed by immunoblot analysis with specific antibodies.

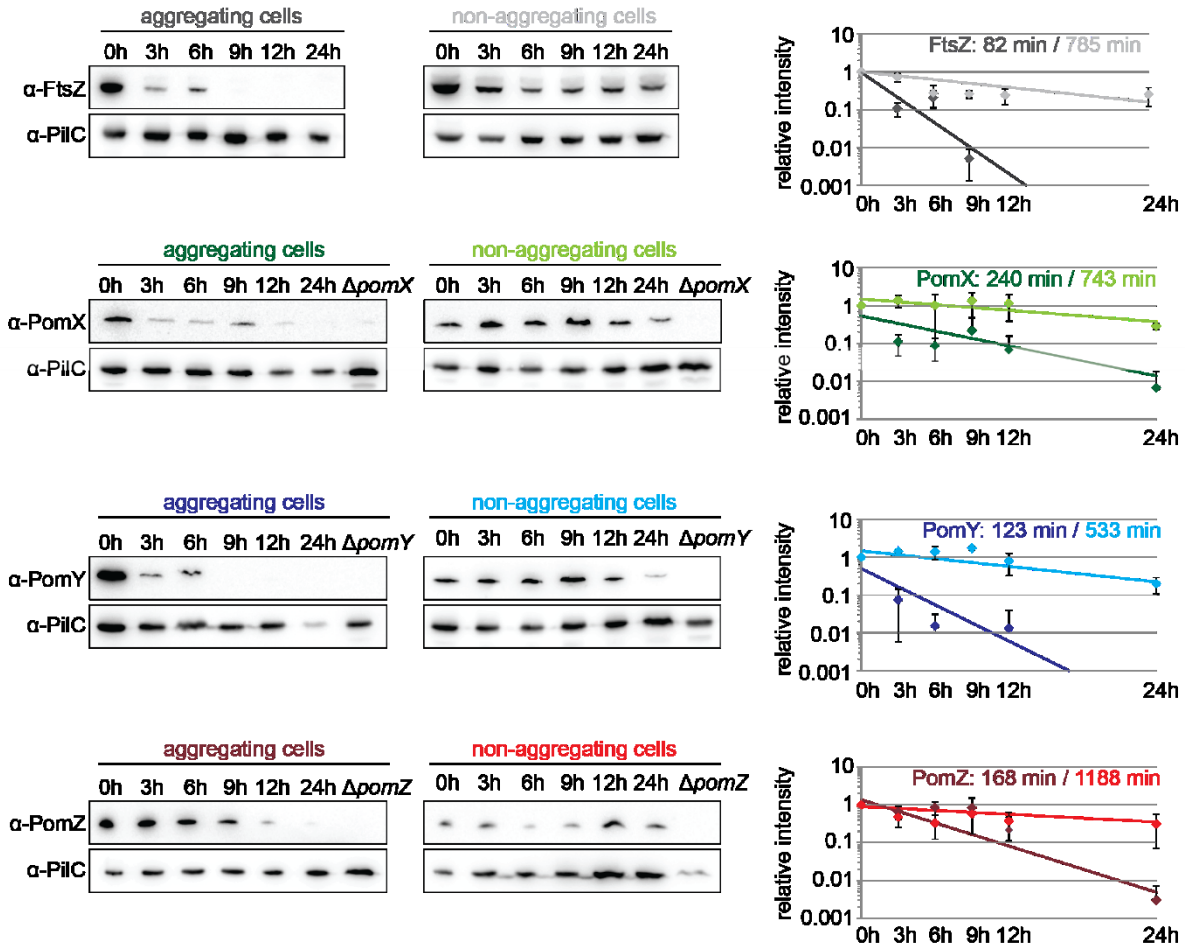


**Figure 17: FtsZ, PomX, PomY and PomZ decrease specifically in cells dedicated to become spores**
Immunoblot analysis of FtsZ (44.7 kDa), PomX (43.9 kDa), PomY (70.1 kDa) and PomZ (44.7 kDa) during development in specific cell fates. WT cells were starved in submerged culture using MC7 buffer. Samples were taken at indicated time points. Aggregating and non-aggregating cells were separated as described in 6.2. Blots were probed with specific α-FtsZ (grey), α-PomX (green), α-PomY (blue), α-PomZ (red) (Treuner-Lange *et al.*, 2013, Schumacher *et al.*, 2017) and α-PilC (45.2 kDa)) antibodies (Bulyha *et al.*, 2009). Graphs were created by densitometry analysis of immunoblots to calculate the time protein levels were reduced to 50% of initial intensity which is indicated by coloured numbers. Data are presented as mean of two independent biological replicates relative to α-PilC loading control. Error bars indicate standard deviation.

In the non-aggregating cell fraction, the decrease in protein levels of FtsZ, PomX, PomY and PomZ was much slower than in total cells (Figure 16). FtsZ levels were decreased to 50% in

785 min, PomX levels in 743 min, PomY levels in 533 min and PomZ levels in 1188 min. By contrast, the protein levels decreased more rapidly in the aggregating cell fraction. FtsZ levels decreased to 50% in 82 min, PomX levels in 240 min, PomY levels in 123 min and PomZ levels in 168 min.

In summary, protein levels decreased more slowly in the non-aggregating cell fraction than in the cells dedicated to become spores. This supports the hypothesis that cell division is inhibited in future spores. These data indicate that the accumulation of FtsZ, PomX, PomY and PomZ is regulated differently in both cell populations.

### 6.4.3. PomXYZ are dispensable for fruiting body formation and sporulation

The cell division regulators PomX, PomY and PomZ promote cell division and are essential to determine the future cell division site at midcell in growing cells (Schumacher *et al.*, 2017, Treuner-Lange *et al.*, 2013). To investigate if the cell division regulators are important for the developmental program of *M. xanthus*, we tested all three deletion mutants for their ability to form fruiting bodies and to sporulate. Cells were starved on TPM agar as well as in a submerged culture using MC7 buffer. As controls, WT cells and a *fruA* insertion mutant (DK11063), which is not able to aggregate into fruiting bodies and to sporulate, were used (Ellehauge *et al.*, 1998).

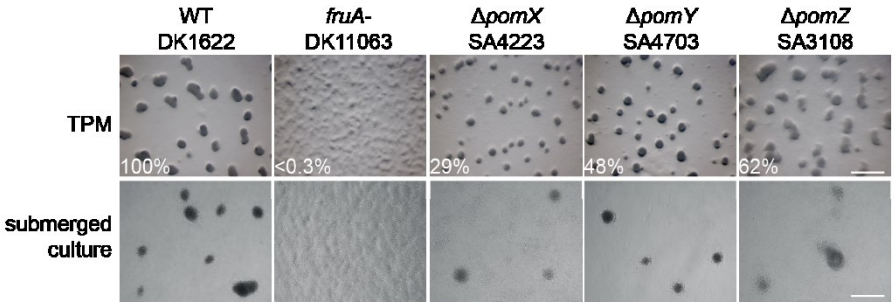


**Figure 18: PomXYZ are dispensable for development**
Development phenotype of Δ*pomX*, Δ*pomY* and Δ*pomZ* in-frame deletion mutants. Cells of indicated strains were starved on TPM agar plates or in submerged culture using MC7 buffer for 120 h. Number indicate sporulation frequency relative to WT determined from spores formed on TPM. Scale bar: 500 µm (TPM) and 100 µm (submerged culture).

WT cells were able to form fruiting bodies and to sporulate on TPM agar as well as in submerged culture. As expected, cells of the *fruA* insertion mutant, used as negative control were not able to form fruiting bodies or to sporulate. Cells of the three in-frame deletion mutants Δ*pomX*, Δ*pomY* and Δ*pomZ* formed fruiting bodies after 120 h. However, at earlier time points, Δ*pomX* and Δ*pomZ* cells were delayed in aggregation. Determining the spore frequency from fruiting bodies formed on TPM medium revealed, that cells of all three in-frame deletion mutants formed less spores than WT cells. For Δ*pomX* cells we counted 29% of heat and sonication resistant spores relative to WT. For Δ*pomY* cells the spore frequency amounts to

48% and for Δ*pomZ* cells to 62% (Figure 18). Nevertheless, the cells are able to aggregate and to sporulate, indicating that the regulators of cell division PomX, PomY and PomZ are dispensable for development.

### 6.4.4. FtsZ is dispensable for development

If cell division is inhibited in cells dedicated to become spores we would assume that not just the cell division regulators PomX, PomY and PomZ are dispensable for development but also FtsZ. Because FtsZ is an essential protein it cannot be deleted. To reduce the FtsZ protein level, we used a depletion strain expressing *ftsZ* under the control of the vanillate inducible promoter as the only *ftsZ* copy in the cell (SA6755). Cells were incubated under vegetative conditions in the presence of 25 µM vanillate resulting in FtsZ accumulation slightly higher in comparison to WT levels. After 9 h of incubation in the absence of vanillate, FtsZ is not detectable anymore via immunoblot (Figure 19A). At this time point, cells expressing *ftsZ* or had a cell length of 7.0 ± 1.7 µm. This is comparable to WT cells, since they were 8.8 ± 1.8 µm long. Cells depleted for FtsZ were elongated. They had an average cell length of 11.4 ± 3.0 µm (Figure 19B). Cells were spotted on TPM agar supplemented with or without vanillate.

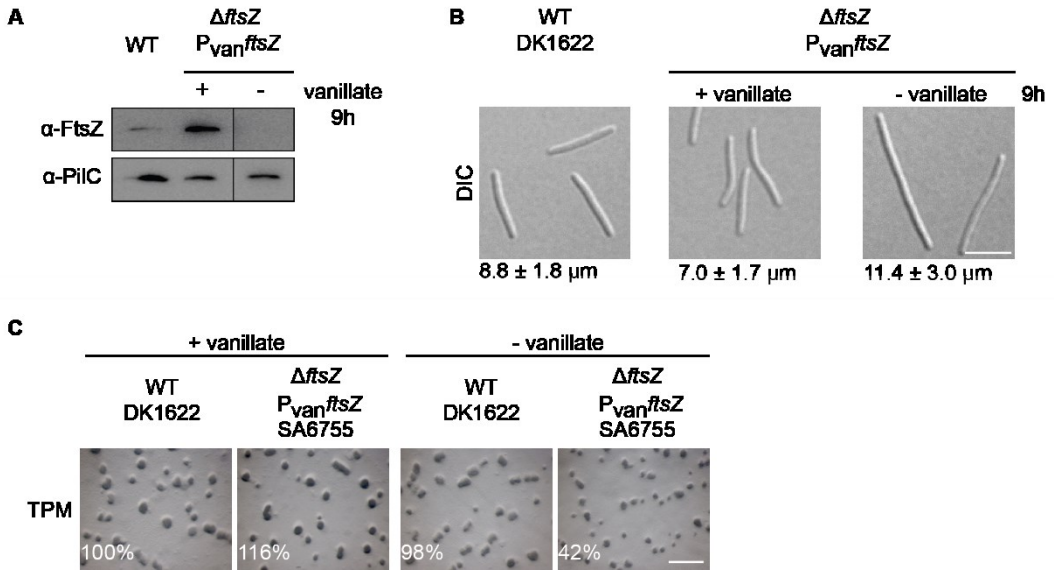


**Figure 19: FtsZ is dispensable for development**
**(A)** WT cells and SA6755 (Δ*ftsZ*/$P_{van}$ *ftsZ*) were incubated under vegetative conditions for 9 h in the presence (+) or absence (-) of 25 µM vanillate and cell lysates were checked for the accumulation of FtsZ (44.7 kDa) and PilC (45.2 kDa) via immunoblotting with specific antibodies (Treuner-Lange *et al.*, 2013, Bulyha *et al.*, 2009). **(B)** Cells described in (A) were imaged on 1% agarose buffered with TPM at 32°C. DIC pictures are shown. (n>150) Scale bar: 5 µm. **(C)** Cells described in (A) were spotted on TPM supplemented with or without 25 µM vanillate. Aggregation phenotype after 120 h is shown. Sporulation efficiencies are indicated by numbers. Scale bar: 500 µm.

After 120 h of starvation on TPM agar plates, WT cells as well as cells expressing *ftsZ* in a vanillate-dependent manner had aggregated into fruiting bodies. Cells depleted for FtsZ had also formed fruiting bodies after 120 h. WT cells and cells expressing *ftsZ* in the presence of

vanillate also differentiated into spores at a comparable frequency. When cells were depleted for FtsZ, the sporulation frequency dropped to 42 % (Figure 19B). Although the frequency is reduced, cells are still able to form spores. Hence, *M. xanthus* does not rely on the presence of the main cell division protein FtsZ to aggregate and sporulate.

## 6.5. Analysis of mechanisms to control the accumulation of cell division proteins during development

Analyzing proteins important for cell division during development revealed that the protein levels of FtsZ, PomX, PomY and PomZ decrease in cells dedicated to become spores but not in future peripheral rods (6.4.2) and that the presence of these proteins is not essential for *M. xanthus* to sporulate (6.4.3/6.4.4). These observations agree with our hypothesis, that cell division is specifically inhibited in cells becoming spores. In order to understand the reduction of protein levels in more detail, we aimed to investigate the mechanisms behind this regulation. Reduction of protein levels can be achieved by producing less protein or by specific degradation. In the following chapters, experiments to test these possibilities will be described.

### 6.5.1. *ftsZ* and *pomXYZ* mRNA levels decrease during development

To examine if the proteins important for cell division are regulated at the transcriptional level during starvation, we analyzed their mRNA levels. The mRNA levels of *ftsZ*, *pomX*, *pomY* and *pomZ* were determined via qRT-PCR at different time points during development. WT cells were starved in submerged culture using MC7 buffer and RNA samples were prepared. 1 µg RNA was used to generate cDNA and qRT-PCRs were performed.

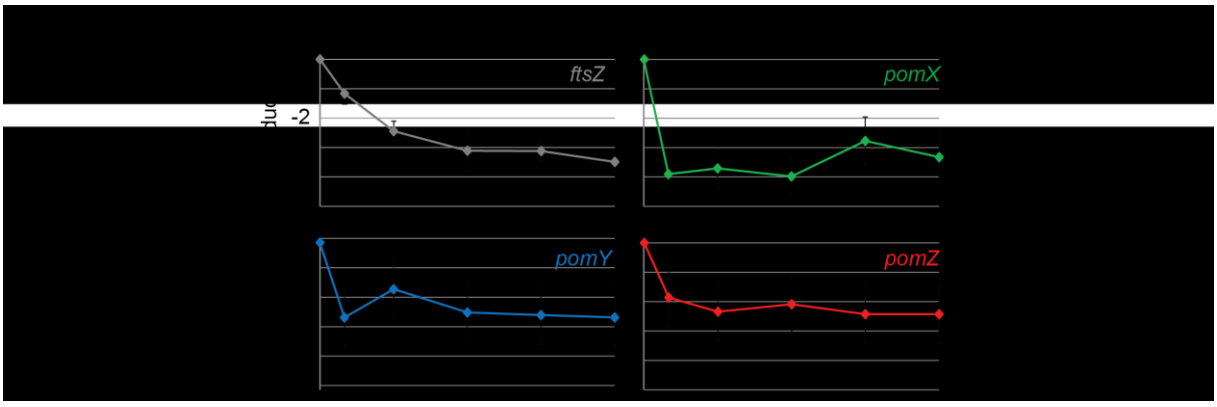


**Figure 20: mRNA levels of *ftsZ*, *pomX*, *pomY* and *pomZ* decrease during development in total cells**
Quantitative PCR analysis of *ftsZ*, *pomX*, *pomY* and *pomZ* expression during development. WT cells were starved in submerged culture using MC7 buffer. At indicated time points RNA samples were prepared and used to synthesize cDNA. Values at each time point represent the log2 change in total cells compared to 0 h time point. Values are an average of two independent biological replicates with each three technical replicates. Error bars indicate standard deviation.

Starvation resulted in an immediate decrease in the number of *ftsZ*, *pomX*, *pomY* and *pomZ* transcripts. *pomX* mRNA levels dropped 16-fold after 2 h of starvation and remained

approximately at this levels until 24 h. *pomY* and *pomZ* mRNA levels dropped approximately 6-fold after 2 h and also remained at the same level until 24 h. The number of *ftsZ* transcripts dropped 2-fold after 2 h. Until 12 h the *ftsZ* mRNA levels decreased continuously up to 6-fold and stayed at this level until 24 h (Figure 20). These results showed that transcription of the tested genes is downregulated during development. This might influence the protein level and contribute to the decreased protein levels we observed in total cells (Figure 16) and in future spores (Figure 17). The regulation is an early response to starvation, since we observed a change in transcription levels already after 2 h of starvation.

### 6.5.2. FtsZ and PomXYZ half-life does not change upon starvation

To test if FtsZ levels are controlled by regulated proteolysis upon initiation of development, we determined the half-life of FtsZ during vegetative growth and during development. Vegetatively grown cells or cells starved in submerged culture using MC7 buffer were treated with 25 µg/ml chloramphenicol. Chloramphenicol inhibits translation and leads to severe growth defects in *M. xanthus* (Konovalova *et al.*, 2012). Samples were taken every 30 min and cell lysates were subjected to SDS-PAGE and immunoblotting with specific α-FtsZ antibodies. The half-life was determined as the time until FtsZ is reduced to 50% of its initial level.

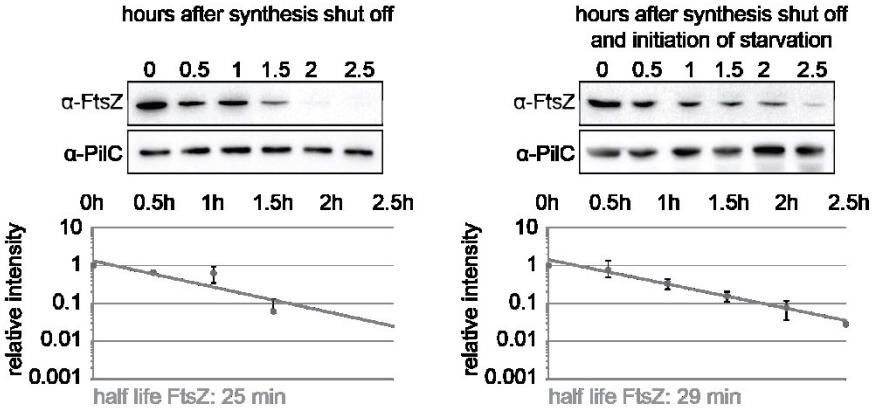


**Figure 21: Half-life of FtsZ during vegetative growth and development**
*In vivo* determination of FtsZ stability during vegetative growth **(A)** and development **(B)**. Samples were taken at indicated time points after addition of 25 µg/ml to vegetatively growing cells or to cells starving in submerged culture using MC7 buffer. Blots were probed with specific α-FtsZ (44.7 kDa) and α-PilC (45.2 kDa) antibodies (Treuner-Lange *et al.*, 2013, Bulyha *et al.*, 2009). Graphs were created by densitometry analysis of immunoblots to calculate the half-life of FtsZ indicated by grey numbers. Data are presented as mean of two independent biological replicates and at least two technical replicates, each and relative to α-PilC loading control. Error bars indicate standard deviation.

During vegetative growth, the half-life of FtsZ is 25 min. During development, we determined a half-life of 29 min for FtsZ. Since the half-life does not change between the two conditions, we assume that FtsZ is not specifically degraded upon starvation. In other organisms, proteases were identified to degrade FtsZ directly (Camberg *et al.*, 2009, Williams *et al.*, 2014). Accordingly, one possibility could be that FtsZ is constantly degraded during vegetative growth

and during development. However, when the developmental program is initiated protein levels are additionally controlled by transcriptional downregulation (6.5.1), resulting in decreasing protein levels (6.4.1). If this hypothesis is true, we predict that constitutive *ftsZ* expression should result in stabilization of FtsZ levels during development and that a protease would be involved in regulating FtsZ levels during vegetative growth and during development. Both of these predictions were tested and will be described in the following chapters.

### 6.5.3. Constitutive *ftsZ* expression stabilizes FtsZ levels during development

We predict, that bypassing the transcriptional downregulation would result in stabilization of FtsZ levels during development. To test this hypothesis, we took advantage of a strain expressing *ftsZ* in a vanillate-dependent manner as the only copy of *ftsZ* in the cell (SA6755). Exponentially growing cells were incubated in the presence of different vanillate concentrations for at least eight generations and subsequently starved in submerged culture using MC7 buffer or on TPM agar containing corresponding vanillate concentrations. To shut off *ftsZ* transcription during starvation, cells were incubated with 10 µM vanillate during vegetative growth and shifted to starvation media containing no vanillate.

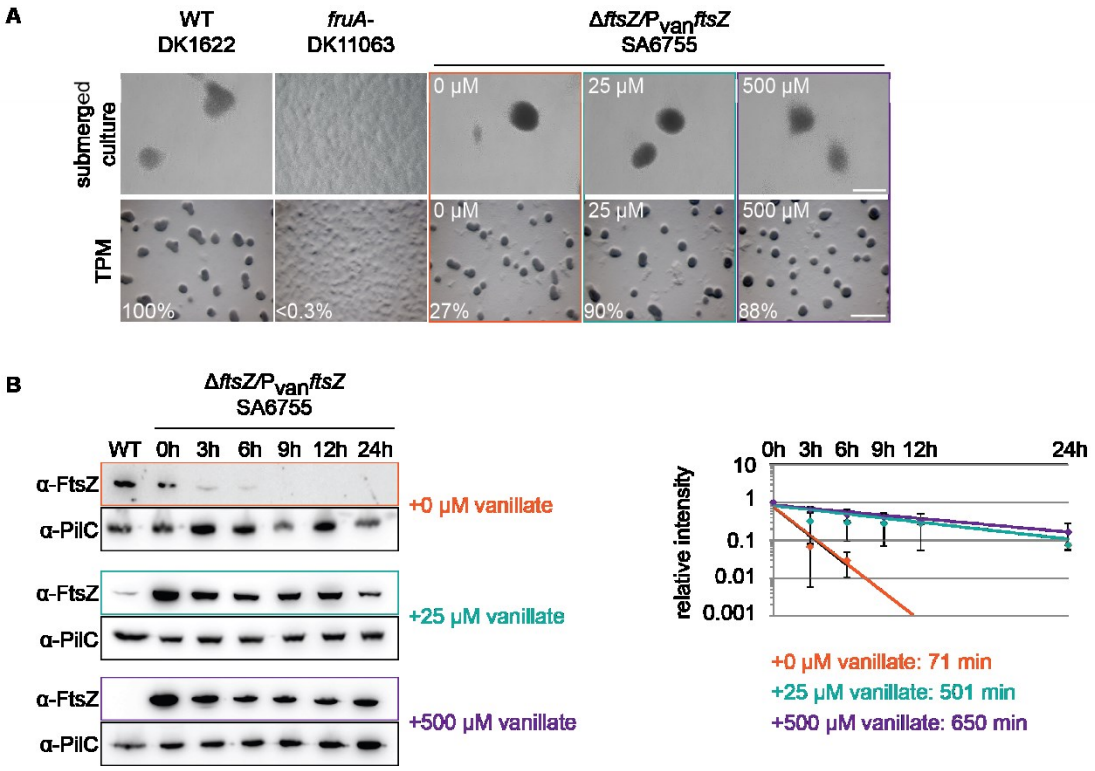


**Figure 22: Constitutive *ftsZ* expression leads to stabilization of FtsZ levels during development**
**(A)** Development phenotype of cells expressing *ftsZ* in a vanillate-dependent manner. Cells of indicated strains were grown in the presence of indicated vanillate concentrations for at least eight generations and subsequently starved on TPM agar plates or in submerged culture using MC7 buffer containing the indicated vanillate concentrations for 120 h. Cells grown in the presence of 10 µM vanillate were starved in the absence of vanillate. Numbers indicate sporulation frequency relative to WT determined from spores formed on TPM. Scale bar: 500 µm (TPM) and 100 µm (submerged culture) **(B)** Immunoblot analysis of FtsZ (44.7 kDa) during development in cells expressing *ftsZ* in a vanillate-dependent manner. Cells were starved in submerged culture using MC7 buffer in the presence of 0 µM (orange), 25 µM (cyan) and 500 µM (purple) vanillate. Samples were taken at indicated time points. Blots were probed with specific α-FtsZ (Treuner-Lange *et al.*, 2013) and α-PilC (45.2 kDa) antibodies (Bulyha *et al.*, 2009). Graphs were created by densitometry analysis of immunoblots to calculate the time the protein levels are reduced to 50% of initial intensity which is indicated by coloured numbers. Data are presented as mean of two technical replicates relative to α-PilC loading control. Error bars indicate standard deviation.

Constitutive *ftsZ* expression in the presence of 25 µM or 500 µM vanillate did not lead to a developmental defect. Under both conditions cells were able to form fruiting bodies on TPM agar plates as well as in submerged culture after 120 h. The sporulation frequencies were 90% and 88%, respectively. The incubation in the presence of 10 µM vanillate followed by a shift to 0 µM vanillate during starvation did not cause a defect in fruiting body formation. However, the sporulation frequency dropped to 27% (Figure 22A). To analyze FtsZ levels during starvation while *ftsZ* is constitutively expressed, samples were taken at different time points from submerged cultures and cell lysates were subjected to SDS-PAGE and immunoblot analysis with specific antibodies. In the presence of 25 µM and 500 µM vanillate, FtsZ levels were stabilized in the cells. We determined a time of 501 and 650 min during which the protein levels decreased to 50% of the initial intensity, respectively. In WT, the reduction to 50% took 227 min in total cells (Figure 16). In addition, the immunoblot analysis showed, that FtsZ was clearly

over accumulating in comparison to WT when expressed in the presence of 25 µM and 500 µM vanillate. The absence of vanillate in the starvation buffer led to a rapid decrease of FtsZ levels. Under these conditions, it took 71 min until FtsZ levels were decreased to 50% of the initial intensity (Figure 22B). This time is comparable to the FtsZ decrease in aggregating WT cells. Here, we determined a time of 82 min until the FtsZ level decreased to 50% (Figure 17).

In summary, these results support our idea that decrease of FtsZ during starvation is due to transcriptional downregulation, since we can bypass this decrease by constitutive *ftsZ* expression. This results in stabilization of FtsZ levels during development. Furthermore, we observed that the decrease of FtsZ levels is not essential for *M. xanthus* to form fruiting bodies or to sporulate. Spores are formed when FtsZ accumulates at higher levels compared to WT.

## 6.6. Decreasing FtsZ levels lead to inhibition of cell division and guarantee the formation of spores containing two chromosomes

We observed decreasing FtsZ levels specifically in cells dedicated to become spores (Figure 17). To test if the decrease in FtsZ levels is sufficient to inhibit cell division in aggregating cells we determined chromosome content in cells that constitutively express *ftsZ*, leading to accumulation of FtsZ during development (Figure 22).

### 6.6.1. Varying *ftsZ* expression during vegetative growth may lead to an increased average cell length and cells containing more than two chromosomes

A first step to understand spore formation when FtsZ levels are stabilized was to analyze the consequences of constitutive *ftsZ* expression during vegetative growth. It has been shown earlier, that the absence of FtsZ leads to a cell division defect accompanied by an increased cell length (Schumacher *et al.*, 2017, Treuner-Lange *et al.*, 2013). Overproduction of FtsZ did not interfere with Z-ring formation but resulted in an elongated average cell length (Treuner-Lange *et al.*, 2013).

We took advantage of a strain described earlier (6.4.4). In this strain *ftsZ* is expressed in a vanillate-dependent manner as the only *ftsZ* copy in the cell (SA6755). Cells were incubated in the presence of the indicated vanillate concentrations for at least eight generations, before cell lysates were subjected to SDS-PAGE and immunoblotting with specific antibodies. In the presence of 10 µM vanillate FtsZ accumulates in a slightly lower level than in WT cells. The incubation in the presence of 25 µM inducer results in FtsZ levels slightly higher than in WT. Inducing *ftsZ* with 500 µM vanillate leads to clear over accumulation (Figure 23A). To determine the cell lengths, cells were imaged on 1% agarose buffered with TPM at 32°C. Additionally, cells grown in the presence of different vanillate concentrations were stained for

40 min with Vybrant® DyeCycle™ Orange to analyze them according to their chromosome content via flow cytometry. Flow cytometry analysis showed two peaks for WT cells, revealing cells having one or two chromosomes. The WT had an average cell length of 7.5 ± 1.9 µm. *ftsZ* expression in the presence of 25 and 500 µM vanillate resulted in the same flow cytometry profile as for WT, indicating that also those cells containing one or two chromosomes. These cells were 7.0 ± 1.7 µm and 7.5 ± 1.8 µm long which was equivalent to WT cells. In the presence of 10 µM vanillate, we could observe a peak corresponding to one and two chromosomes as well. Additionally two small peaks which matched the presence of three and four chromosomes were visible. Expression of *ftsZ* with 10 µM vanillate did not complement the cell division defect completely, since the cells were elongated in comparison to WT cells. We determined an average cell length of 10.7 ± 3.5 µm. Correlated SSC and FSC measurements in parallel to flow cytometry revealed that cells grown in all conditions are one homogenous cell population (Figure 23B).

As a second approach, we checked the chromosome content by using fluorescent markers as described earlier (6.3.1). We took advantage of ParB-eYFP and FROS visualizing the terminus region of the chromosome (192°). *parB-eYFP* (SA6152) and *tetR-eYFP* binding to the *tetO*-array at 192° (SA6158) were expressed in the *ftsZ* depletion background via a copper inducible promoter. Cells were incubated in the presence of corresponding vanillate concentrations to induce *ftsZ* expression and 150 µM $Cu^{2+}$ to induce expression of fluorescent fusion proteins for at least eight generations before the cell lysates were analyzed by SDS-PAGE and immunoblotting with specific antibodies. The immunoblots showed that the presence of 10 µM vanillate led to FtsZ accumulation at a slightly lower level than in WT cells. The incubation in the presence of 25 µM inducer resulted in slightly higher FtsZ levels than in WT. Inducing *ftsZ* with 500 µM vanillate led to over accumulation in both strains, as also observed in the background strain (SA6755) (Figure 23C). Additionally, cells were imaged on 1% agarose buffered with TPM at 32°C. Determination of the cell lengths revealed that the presence of 25 or 500 µM vanillate for cells expressing *parB-eYFP* did not complement the cell length defect completely. The cell lengths amounted to 9.0 ± 2.5 and 9.3 ± 2.3 µm, respectively (Figure 23D). For both conditions, we observed the same distribution of ParB-eYFP signals. In 34% and 35% of cells we counted one and in 46% and 50% of cells two ParB-eYFP signals. On top of that, we could observe three (14% and 12%) or four (5% and 3%) signals in a fraction of cells (Figure 23D). This matched the WT distribution with the exception of cells showing more than two signals. In WT cells, which had a cell length of 7.5 ± 1.9 µm, we observed in one and two ParB-eYFP signals in 31% and 69% of cells. In the presence of 10 µM vanillate, the average cell length was 12.5 ± 3.5 µm, which was even more increased in comparison to WT. However, the distribution of ParB-eYFP signals was comparable to the conditions described before. In

21% of cells we counted one ParB-eYFP signal. 57% of cells showed two, 14% three and 8% four signals (Figure 23D).

Cells expressing *tetR-eYFP* to visualize the terminus region had a cell length of 9.3 ± 4.8 µm in the presence of 10 µM vanillate. Incubation with 25 µM vanillate led to an average cell length of 6.8 ± 1.7 µm and incubation in the presence of 500 µm vanillate led to 8.4 ± 2.0 µm length. Although cells in the presence of 10 µM and 500 µM were slightly elongated in comparison to WT cells, the average cell lengths were shorter than the same backgound strain expressing *parB-eYFP* (SA6152). In the WT background we observed in 6% of cells two TetR-eYFP signals representing the terminus region. In the remaining 94% of cells we counted one signal. Also in the strain expressing *ftsZ* in a vanillate-dependent manner, most of the cells showed one terminus region represented by a TetR-eYFP cluster. We observed in 65% of cells one TetR-eYFP foci in the presence of 10 µM, 82 % in the presence of 25 µM and 68% in the presence of 500 µM vanillate binding to *tetO* at 192°. In 28%, 18% and 31% of cells we counted two signals, respectively. Additionally, in 7% of cells we observed three TetR-eYFP signals in the presence of 10 µM vanillate. Incubation with 500 µM vanillate led to 1% of cells showing three signals representing the terminus region (Figure 23D).

These data showed that we can induce *ftsZ* in a vanillate-dependent manner. FtsZ accumulation lower than the WT level led to a cell length phenotype in the background strain (SA6755) accompanied by the presence of more than two chromosomes in the cells. FtsZ accumulation similar to or higher as the WT level led to normal cell length and two chromosomes in cells as in WT. Expression of *parB-eYFP* in parallel to vanillate-dependent *ftsZ* expression leads to a cell length phenotype even though FtsZ accumulates in higher levels than in WT. As a consequence of the increased cell length, cells tend to contain more than one or two ParB-eYFP signals, indicating more than one or two origins of replication in the cells. We observed the same phenomenon in cells expressing *tetR-eYFP* in parallel to vanillate-dependent *ftsZ* expression. FtsZ accumulated vanillate concentration dependent. If the average cell length is increased, we observed cells showing three signals representing the terminus. Furthermore, the number of cells having two termini increased, indicating two fully duplicated genomes. All in all, the number of chromosomes in the cell increases in a cell length dependent manner as shown before (Treuner-Lange *et al.*, 2013).

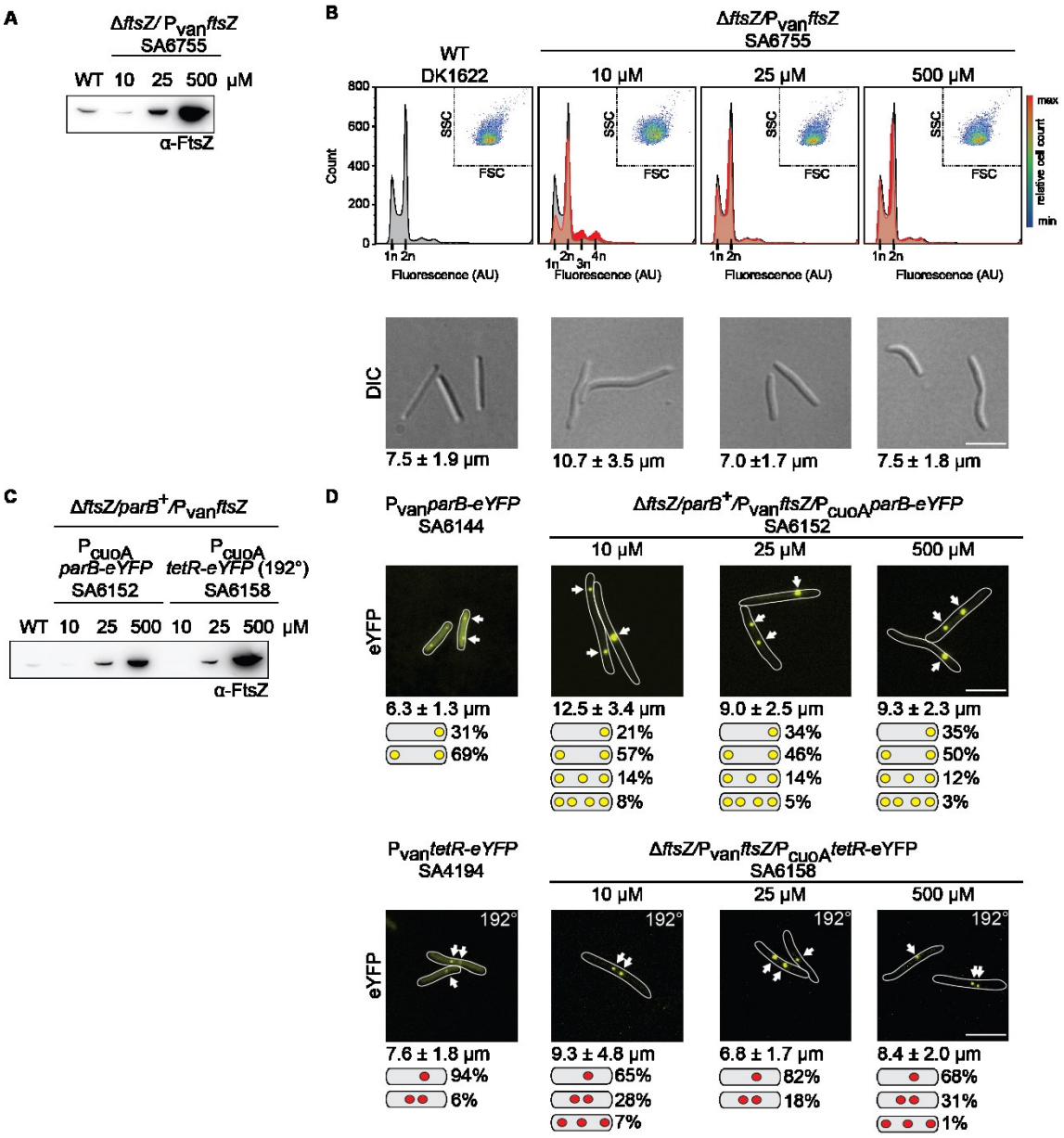


**Figure 23: Varying *ftsZ* expression leads to longer cells with more than two chromosomes**
**(A)** Immunoblot analysis of FtsZ (44.7 kDa), in cells expressing *ftsZ* in a vanillate-dependent manner (SA6755). Cells were grown for at least eight generations in the presence of shown vanillate concentrations. Cell lysates were probed with specific α-FtsZ antibodies. **(B)** Flow cytometric profile of exponentially growing WT cells and cells expressing *ftsZ* in a vanillate-dependent manner. Cells were grown in the presence of indicated vanillate concentrations to exponential growth phase and stained with Vybrant® DyeCycle™ Orange. The x-axis represents arbitrary fluorescence intensity and the y-axis represents cell count, whereby each experiment consisted of analysis of 10.000 individual cells. Tick marks represent the expected positions of fluorescent intensities corresponding to one and two copies of the chromosome based on the fluorescent intensity of exponentially growing WT cells. Correlated measurements of SSC and FSC are presented in a scatter plot. The color scale shows relative cell count from lowest (blue) to highest (red). Same cells were imaged on 1% agarose buffered with TPM. Cell length is indicated by numbers (n>150). Scale bar 5 µm. **(C)** Immunoblot analysis of FtsZ, when *ftsZ* is expressed in a vanillate-dependent manner and fluorescent fusion proteins are expressed via $Cu^{2+}$. Cells of indicated strains were grown to exponential growth phase in the presence of shown vanillate concentrations. Cell lysates were probed with specific α-FtsZ antibodies. **(D)** Exponentially growing cells of indicated strains were grown for at least eight generations in the presence of indicated vanillate concentrations and imaged as described in (A). Average cell length as well as abundance of localization patterns is indicated (n>150). Scale bar 5 µm.

### 6.6.2. Stabilization of FtsZ levels leads to spores containing less than two chromosomes

To analyze chromosome content in spores formed while FtsZ levels are stabilized (Figure 22), we used two approaches. To investigate the DNA amount of the distinct cell populations, we performed flow cytometry analysis. Cells expressing *ftsZ* in a vanillate-dependent manner (SA6755) were grown to exponential growth phase in the presence of different vanillate concentrations and subsequently spotted on TPM agar including the corresponding vanillate concentration to induce starvation. To shut off *ftsZ* transcription during starvation, cells grown with 10 µM vanillate were applied to starvation media supplemented with no vanillate. Under these conditions, cells are able to form fruiting bodies. The sporulation frequency of cells expressing *ftsZ* in the presence of 25 µM and 500 µM vanillate is comparable to WT. Cells that expressed *ftsZ* during vegetative growth in the presence of 10 µM and were starved on TPM agar without vanillate sporulated at a frequency of 27% (Figure 24A). After 120 h cells were harvested, resuspended in TPM buffer and their DNA was stained with 10 µM Vybrant® DyeCycle™ Orange for 40 min before the DNA content was quantified by flow cytometry. As a standard, exponentially grown cells were analyzed as described before (6.3.3).

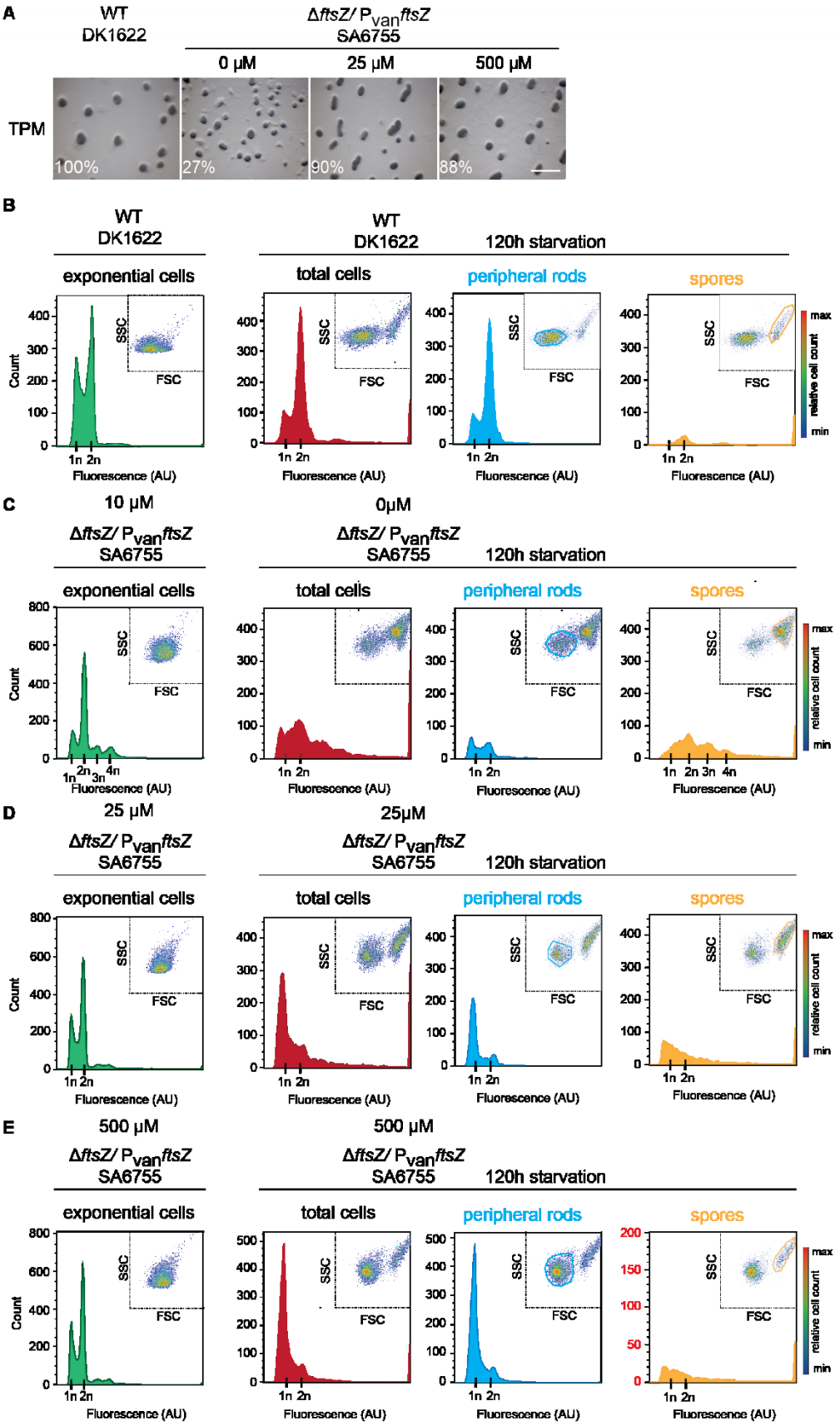


**Figure 24: Flow cytometry profile of spores formed when FtsZ levels are stabilized**
**(A)** Development phenotype of WT cells and cells expressing *ftsZ* in a vanillate-dependent manner. Cells were starved on TPM agar plates in the presence of indicated vanillate concentrations for 120 h. Cells starved in the absence of vanillate were incubated in the presence of 10 µM vanillate during vegetative growth. Number indicate sporulation frequency relative to

WT. Scale bar: 500 µm. **(B/C/D)** Total cells described in (A) were analyzed by flow cytometry (red). Flow cytometric profile of corresponding exponentially growing cells is also presented and the same data as in Figure 9 and Figure 23. Cells were stained with Vybrant® DyeCycle™ Orange. The x-axis represents arbitrary fluorescence intensity and the y-axis represents cell count, whereby each experiment consisted of analysis of 10.000 individual cells. Tick marks represent the expected positions of fluorescent intensities corresponding to one, two or more copies of the chromosome based on the fluorescent intensity of exponentially grown WT cells. Correlated measurements of SSC and FSC are presented in a scatter plot. The color scale shows relative cell count from lowest (blue) to highest (red). Based on correlated SSC and FSC measurements, cell populations were analyzed separately.

Flow cytometric analysis of exponentially growing WT cells and cells expressing *ftsZ* in the presence of 25 µM and 500 µM vanillate revealed two distinct peaks representing the presence of one and two chromosomes. Cells expressing *ftsZ* in the presence of 10 µM vanillate revealed two peaks corresponding to 1n and 2n, and two additional small peaks which corresponded to 3n and 4n. These cells have an increased average cell length. All vegetative cells shown here display one homogenous cell population (Figure 24, insets). The flow cytometry data regarding vegetative growth were described before (6.1/6.6.1). Furthermore, WT spores formed after 120 h on TPM agar show one single peak corresponding to 1n. The flow cytometric profile of peripheral rods displays two peaks corresponding to 1n and 2n as described before (6.1).

Cells that were incubated in the presence of 10 µM vanillate were subsequently starved without vanillate. The flow cytometric analysis of peripheral rods and spores formed under these conditions revealed two peaks corresponding to 1n and 2n, but also two additional not very clear peaks which corresponded to 3n and 4n. Correlated SSC and FSC measurement shows two cell populations. Peripheral rods appeared to have the same properties as vegetative cells. The spores are increased in both, SSC and FSC values (6.1). Both cell populations showed a different flow cytometric profile when analyzed separately. Whereas the profile of peripheral rods showed two peaks corresponding to 1n and 2n, the cytometric profile of the spores revealed one peak each corresponding to 2n, 3n and 4n (Figure 24C). Cells expressing *ftsZ* in the presence of 25 or 500 µM vanillate during development were also analyzed. The flow cytometric profile of peripheral rods and spores formed under these conditions showed two peaks corresponding to 1n and 2. Of note, the ratio of cells is shifted, since the 2n peak appeared to be much lower and the 1n peak much higher when compared to the profile of WT cells. Correlated SSC and FSC measurements allows to analyze both cell populations separately. The flow cytometric profile of peripheral rods showed that these cells contained either one or two chromosomes, but more cells than in WT contained only one. The profile of the spores formed while *ftsZ* is constitutively expressed in the presence of 25 µM vanillate showed one peak corresponding to 1n but also cells which contained more than one chromosome, although no distinct peak is visible. The profile of spores formed while *ftsZ* is constitutively expressed in the presence of 500 µM vanillate appeared to be very similar to this

profile. One peak corresponding to 1n was visible as well as cells which contained more than one chromosome, but no additional distinct peak was observed (Figure 24D/E).

Next, we analyzed the DNA content of spores formed while FtsZ levels were stabilized by visualizing different chromosomal loci in the single cells. We took advantage of strains described before (6.6.1). ParB-eYFP as marker for the origin of replication (SA6152) or TetR-eYFP binding to the *tetO*-array at 192° (SA6158), which represents the terminus region of the chromosome, were expressed via the copper inducible promoter in the strain expressing *ftsZ* in a vanillate-dependent manner. Cells were incubated in the presence of different vanillate concentrations to induce *ftsZ* expression and 150 µM $Cu^{2+}$ to express fluorescent fusion proteins for at least eight generations before the cells were spotted on TPM medium including the corresponding vanillate concentrations and 150 µM $Cu^{2+}$. To shut off *ftsZ* transcription during starvation, cells grown with 10 µM vanillate were applied to starvation media supplemented with no vanillate. Our previous results showed, that starvation in the presence of certain vanillate concentrations to express *ftsZ* leads to stabilization of FtsZ levels during development (Figure 22B). Cells were starved for 120 h and formed fruiting bodies under these conditions. The sporulation frequency was comparable to WT cells, except for cells developing in the absence of vanillate. Here, the sporulation frequency was reduced to 58% (cells expressing *parB-eYFP*) and 29% (cells expressing *tetR-eYFP*) (Figure 25A). Cells were harvested to image them on 1% agarose buffered with TPM at 32°C. To not miss any signals in the spherical spore, we performed Z-stacks with 0.15 µm intervals through the spores and analyzed the maximal projection of these pictures.

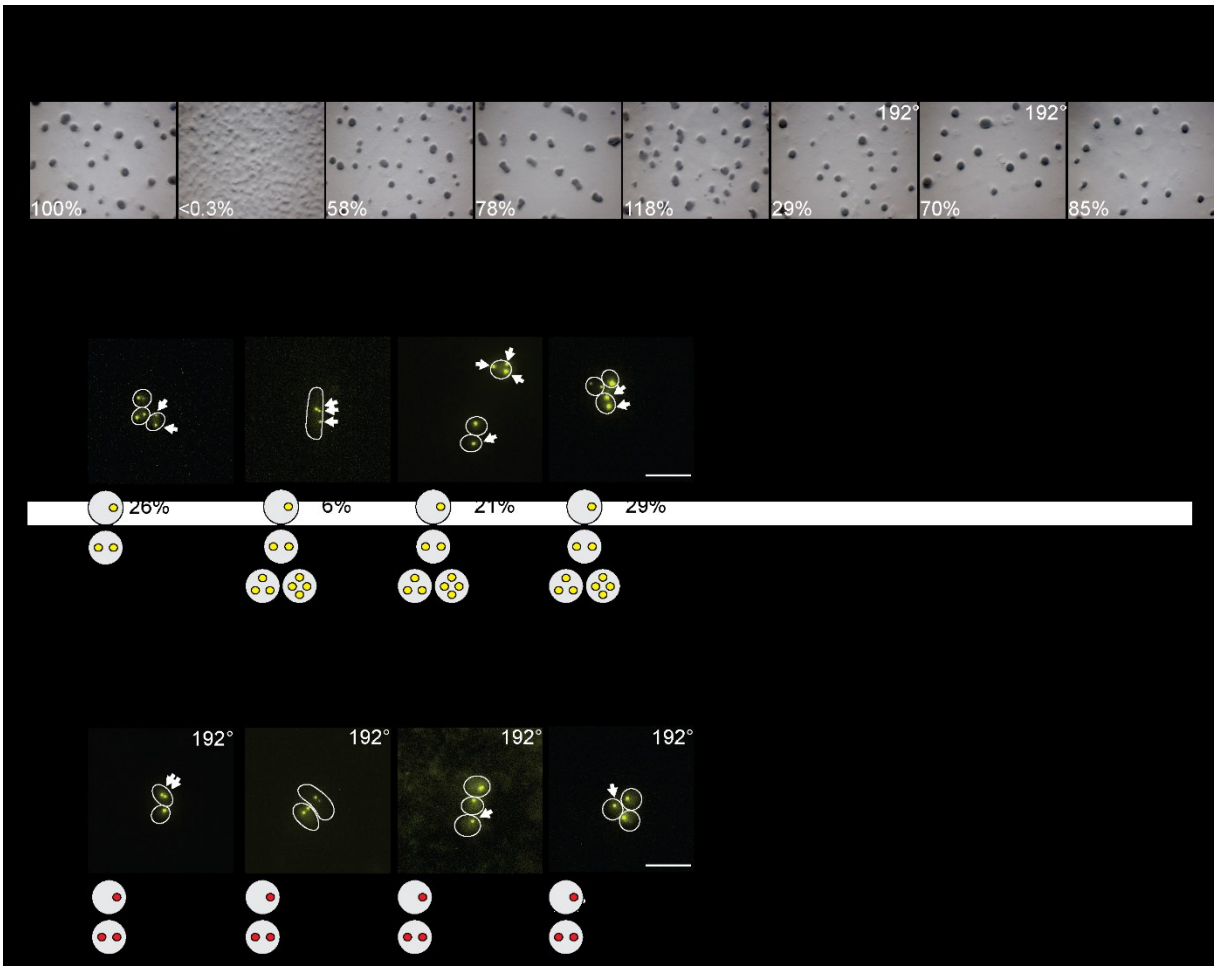


**Figure 25: Stabilization of FtsZ levels leads to spores containing less than two chromosomes**
**(A)** Development phenotype of cells expressing *ftsZ* in a vanillate-dependent matter together with *parB-eYFP* and *tetR-eYFP* via the copper inducible promoter. Cells of indicated strains were starved on TPM agar plates including the indicated vanillate concentrations and 150 µM $Cu^{2+}$ for 120 h. Cells starved in the absence of vanillate were incubated in the presence of 10 µM vanillate during vegetative growth. Numbers indicate sporulation frequency relative to WT. Scale bar: 500 µm. **(B)** Strains were treated and imaged as described in A. Z-stacks with 0.15 µm intervals were performed. Maximal projection of representative spores are shown. Outline was obtained from DIC pictures. Cartoons indicate occurrence of given localization patterns (n>100) Arrows indicate signals. Scale bar: 5 µm.

Cells expressing *ftsZ* in the presence of 10 µM vanillate during vegetative growth were subsequently spotted on TPM agar without vanillate to shut off *ftsZ* expression. Under these conditions, we observed one ParB-eYFP signal in 6% of spores. 46% of spores displayed two signals, whereas we observed in 48% of spores three or four ParB-eYFP signals. In the presence of 25 µM vanillate, we detected in 21% of spores one, in 62% two and in 17% of spores three or four ParB-eYFP signals. We were able to observe almost the same pattern for spores formed in the presence of 500 µM vanillate. Under this condition, one ParB-eYFP signal was visible in 29% of spores. 61% of spores displayed two signals and in 10% of spores we observed three or four signals. In WT background 74% of spores showed two and 26% of spores one ParB-eYFP signal (Figure 25B). To interpret the results obtained for the distribution of ParB-eYFP signals in heat and sonication resistant spores formed during varying *ftsZ* induction it is important to keep in mind earlier results. Of note, the strain expressing *ftsZ* in a

vanillate-dependent manner and *parB-eYFP* under the control of the copper inducible promoter (SA6152) shows a cell length defect, also in the presence of high vanillate concentrations during vegetative growth (Figure 23D). Furthermore, these longer cells tended to contain more than one or two ParB-eYFP signals, indicating more than two origins of replication in the cells. As a consequence, the cells enter the developmental program with a higher average chromosome number than WT cells. This might affect the chromosome content in spores (see also 6.8).

Cells that expressed *ftsZ* in the presence of 10 µM vanillate during vegetative growth and subsequently formed spores in the absence of vanillate showed two TetR-eYFP signals in 62% of spores. The signals represent the terminus region. The remaining 38% of spores displayed one signal. Spores formed in the presence of 25 µM vanillate showed two TetR-eYFP signals in 43% of all cases. In 57% of spores we detected one signal. The proportion of spores which showed one TetR-eYFP signal increased even more when formed in the presence of 500 µM vanillate. 87% of spores had one TetR-eYFP signal, whereas 13% of spores displayed two signals. In WT background, 68% of spores displayed two TetR-eYFP signals. In the remaining 32% of spores we observed one signal (Figure 25B). Visualizing the terminus region in the background of cells expressing *ftsZ* in a vanillate-dependent manner (SA6158) did not lead to an increased average cell length during vegetative growth in the presence of high vanillate concentrations (Figure 23D). We assumed that spore formation would not be influenced by vegetative cell morphology or aberrant chromosome content.

To sum up our results, two different approaches showed, that the number of spores containing two fully duplicated chromosomes decreased, when FtsZ levels were stabilized by vanillate induced *ftsZ* expression. Our flow cytometry data showed, that most spores formed contained one chromosome when *ftsZ* is constitutively expressed. Similarly the single cell analysis points into this direction. Particularly the results regarding the amount of termini regions in spores formed under these conditions indicate, that the number of spores containing two fully duplicated chromosomes decreases the higher the FtsZ level is. By artificially increasing FtsZ levels during starvation, we basically created the contrary situation in comparison to what happens to FtsZ levels in WT cells upon starvation. Since we observed that the proportion of spores containing one instead of two chromosomes was increased, we conclude that indeed, reduction of FtsZ levels is required and sufficient to inhibit cell division, which guarantees the formation of spores containing two chromosomes.

## 6.7. An ATP-dependent protease is involved in FtsZ degradation

We hypothesize, that in addition to transcriptional regulation, a protease is involved in constantly degrading FtsZ during vegetative growth and development (6.5.2). Regulated proteolysis during bacterial development often involves ATP-dependent proteases

(Konovalova *et al.*, 2014) and we can find seven of them in *M. xanthus* (Konovalova *et al.*, 2012).

### 6.7.1. FtsH$^D$ is not involved in degradation of FtsZ

One ATP-dependent protease found in *M. xanthus* is FtsH$^D$. To clarify if FtsH$^D$ is involved in FtsZ regulation, we checked for the accumulation of FtsZ during development. The in-frame deletion mutant is able to form fruiting bodies and to sporulate at WT levels on TPM agar and in submerged culture using MC7 buffer (Figure 26A). To prepare cell lysates, cells were starved in submerged culture using MC7 buffer. Samples were taken at different time points and cell lysates were subjected to SDS-page and immunoblotting with specific α-FtsZ antibodies.

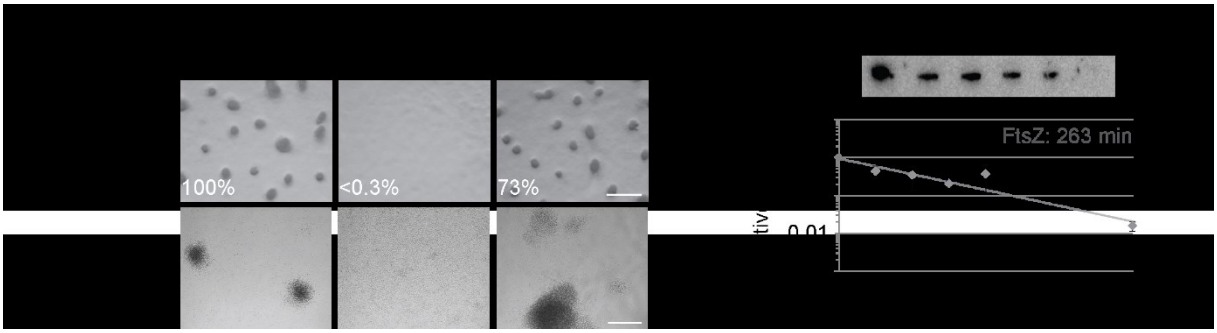


**Figure 26: FtsH$^D$ is not involved in FtsZ degradation**
**(A)** Development phenotype of cells of Δ*ftsH$^D$* in-frame deletion mutant. Cells of indicated strains were starved on TPM agar plates or in submerged culture using MC7 buffer for 120 h. Numbers indicate sporulation frequency relative to wild type determined from spores formed on TPM. Scale bar 500 µm (TPM) and 100 µm (submerged culture). **(B)** Immunoblot analysis of FtsZ (44.7 kDa) in the absence of FtsH$^D$ during development. Cells were starved in submerged culture using MC7 buffer. Samples were taken at indicated time points. Blots were probed with specific α-FtsZ antibodies (Treuner-Lange *et al.*, 2013). Graph was created by densitometry analysis of immunoblots to calculate the time FtsZ levels are reduced to 50% of initial intensity which is indicated by grey number. Data are presented as mean of two technical replicates. Error bars indicate standard deviation.

FtsZ levels decreased in Δ*ftsH$^D$* in-frame deletion mutant during development. In 263 min the protein level decreased to 50% (Figure 26B). This time is comparable to the decrease in the WT (227 min, 6.4.1) suggesting that FtsH$^D$ is not involved in FtsZ protein level regulation during development.

### 6.7.2. LonD is involved in FtsZ and PomXYZ degradation

To test if the ATP-dependent protease LonD is involved in regulating FtsZ, PomX, PomY or PomZ levels we checked for the accumulation of these proteins upon starvation. *lonD* insertion mutants are not affected during vegetative growth, but are not able to aggregate upon starvation and do not form spores (Tojo *et al.*, 1993b). A Δ*lonD* in-frame deletion mutant has a development defect and is not able to form fruiting bodies or to sporulate (Figure 27A). Cells

were starved in submerged culture and samples were taken at different time points. Cell lysates were subjected to SDS-PAGE and immunoblotting with specific antibodies.

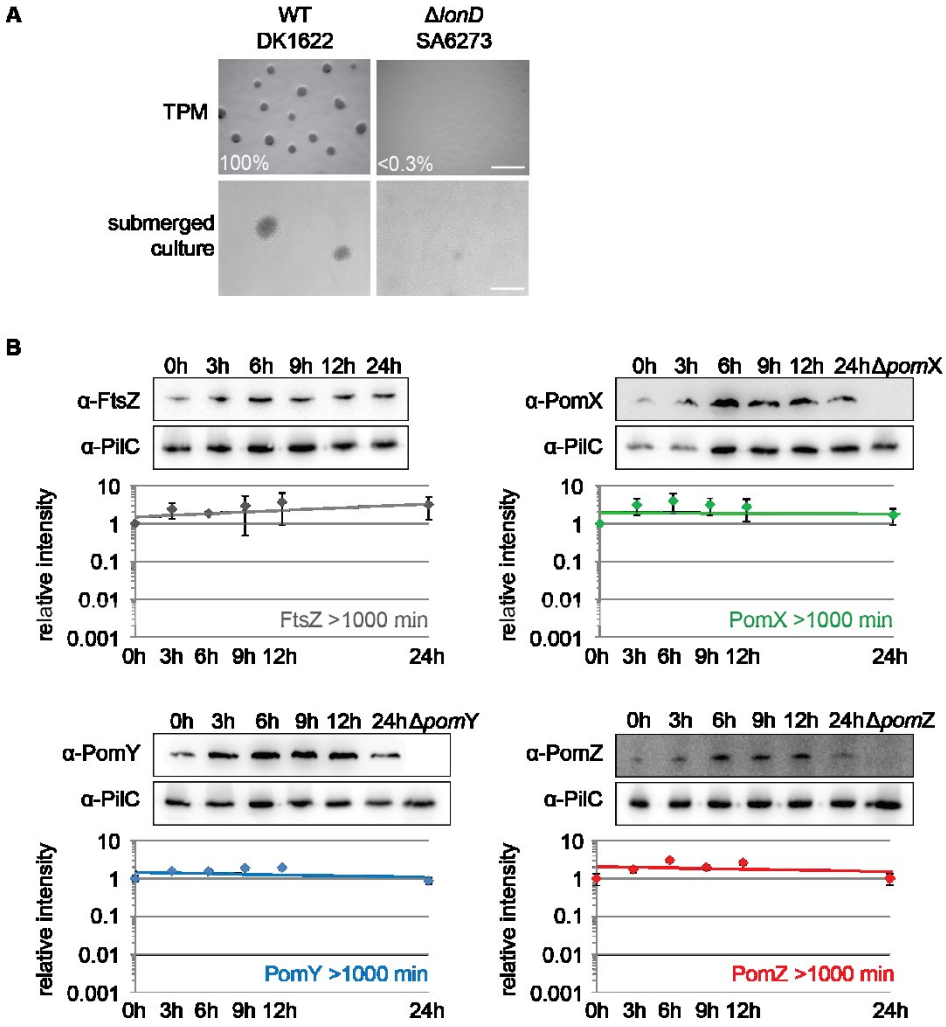


**Figure 27: LonD is involved in regulating FtsZ, PomX, PomY and PomZ protein levels during development**

**(A)** Development phenotype of Δ*lonD* in-frame deletion mutant. Cells of indicated strains were starved in submerged culture using MC7 buffer or on TPM agar for 120 h. Numbers indicate sporulation frequency relative to WT determined from spores formed on TPM. Scale bar 500 µm (TPM) and 100 µm (submerged culture). **(B)** Immunoblot analysis of FtsZ (44.7 kDa), PomX (43.9 kDa), PomY (70.1 kDa) and PomZ (44.7 kDa) during development in the absence of LonD. Cells were starved in submerged culture using MC7 buffer. Samples were taken at indicated time points. Blots were probed with specific α-FtsZ (grey), α-PomX (green), α-PomY (blue), α-PomZ (red) (Treuner-Lange *et al.*, 2013, Schumacher *et al.*, 2017) and α-PilC (45.2 kDa) antibodies (Bulyha *et al.*, 2009). Graphs were created by densitometry analysis of immunoblots to calculate the time until the proteins reduce to 50% of initial intensity which is indicated by coloured numbers. Data are presented as mean of two technical replicates relative to α-PilC loading control. Error bars indicate standard deviation.

In the absence of LonD the protein levels of FtsZ, PomX, PomY and PomZ did not decrease during development as observed for WT cells (6.4.1). The time to until PomX, PomY and PomZ levels were decreased to 50% increased to >1000 min, respectively. Furthermore, FtsZ levels slightly increased in Δ*lonD* cells during starvation (Figure 27B). These observations suggest that LonD is involved in regulating the levels of FtsZ, PomX, PomY and PomZ.

### 6.7.3. In the absence of LonD, FtsZ half-life increases during vegetative growth and development

Since the absence of LonD caused a stabilization of FtsZ (and PomX, PomY, PomZ) protein levels during development (Figure 27), we determined FtsZ half-life in Δ*lonD* cells in vegetatively growing and in cells starving in submerged culture using MC7 buffer. Chloramphenicol was added to a final concentration of 25 µg/ml to shut off protein synthesis. Samples were taken every 30 min and cell lysates were subjected to SDS-PAGE and immunoblot analysis with specific α-FtsZ antibodies.

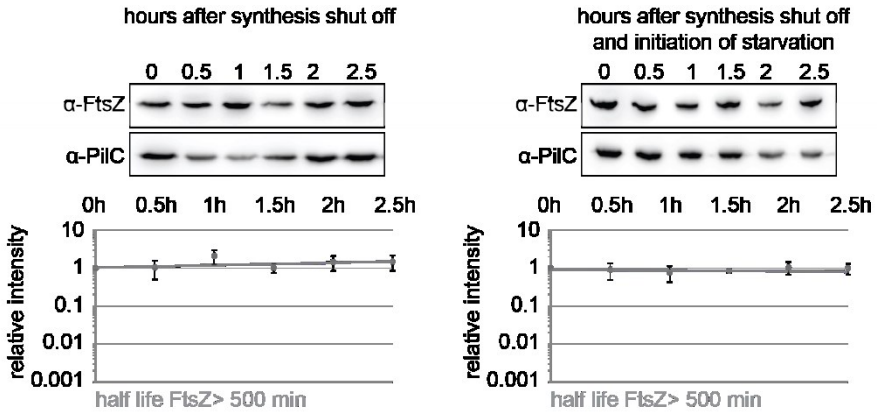


**Figure 28: Half-life of FtsZ increases in the absence of LonD during vegetative growth and development**
*In vivo* determination of FtsZ (44.7 kDa) stability during vegetative growth **(A)** and development **(B)** in the absence of LonD. After addition of 25 µg/ml to vegetatively growing cells or to cells starved in submerged culture using MC7 buffer, samples were taken at indicated time points. Blots were probed with specific α-FtsZ (Treuner-Lange *et al.*, 2013) and α-PilC (45.2 kDa) antibodies (Bulyha *et al.*, 2009). Graphs were created by densitometry analysis of immunoblots to calculate the half-life of FtsZ which is indicated by grey numbers. Data are presented as mean of two independent biological replicates relative to α-PilC loading control. Error bars indicate standard deviation.

The half-life of FtsZ was strongly increased in the absence of LonD during vegetative growth as well as during development. For both conditions, we determined a half-life of more than 500 minutes (Figure 28), whereas the half-life of FtsZ was 25 min in vegetatively growing and 29 min in developing WT cells (6.5.2). These results indicated, that LonD is involved in degrading FtsZ during vegetative growth and during development. However, if LonD is directly or indirectly involved in controlling FtsZ levels remains unclear.

### 6.7.4. LonD does not degrade FtsZ *in vitro*

In the absence of LonD, protein levels of FtsZ, PomX, PomY and PomZ are stabilized during development and the half-life of FtsZ increased during vegetative growth and starvation conditions. To analyze if LonD is the protease directly degrading FtsZ, we checked this possibility in an *in vitro* degradation assay. The purified proteins LonD-$His_6$ (1.2 µM) and FtsZ (0.5 µM) (purified by M. Polatynska and A. Harms) were incubated in the presence of 1.5 mM

ATP. Creatine kinase (43 kDa/75 µg/ml) and creatine phosphate (15 mM) function as ATP regeneration system and were added to avoid the accumulation of AMP. As a control, we checked the degradation of PopD-StrepII (4.0 µM) in parallel, since this protein was shown to be a substrate of the LonD protease (personal communication M. Polatynska). At several time points, samples were taken, mixed with 1x SDS loading dye, heated for 10 min at 95°C and separated by SDS-PAGE.

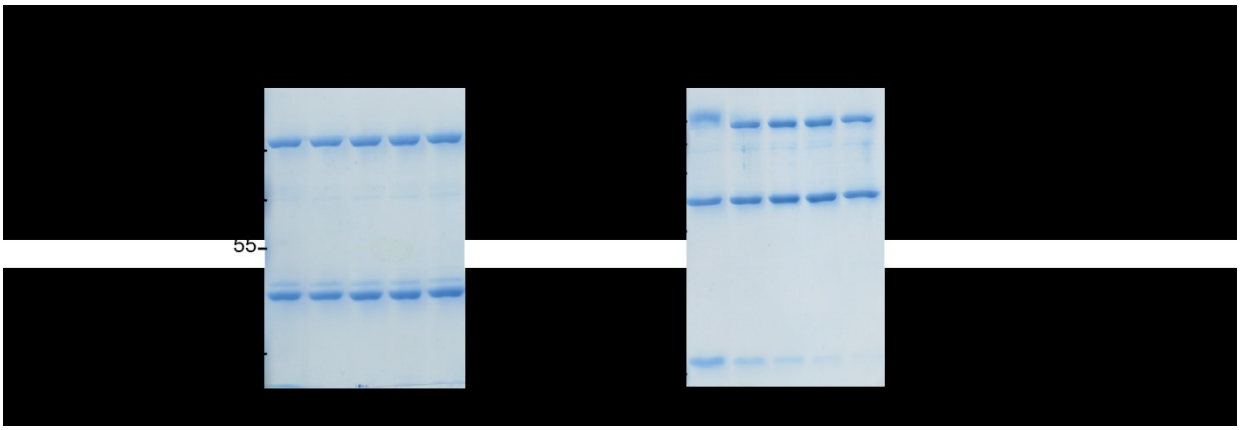


**Figure 29: LonD does not degrade FtsZ *in vitro***
LonD-$His_6$ (92.0 kDa/1.2 µM) was incubated with FtsZ (44.7 kDa/0.5 µM) or PopD-StrepII (16.5 kDa/4.0 µM) in the presence of 1.5 mM ATP, creatine kinase (43 kDa/75 µg/ml) and creatine phosphate (15 mM) at 32°C and samples were taken at indicated time points. Creatine kinase and creatine phosphate are part of the ATP regeneration system.

We could not observe any degradation of FtsZ in the presence of LonD-$His_6$ *in vitro* under the tested conditions. Up to 4 h, the level of FtsZ did not change. As a control, we checked for the degradation of PopD-StrepII, which is a protein involved in C-signaling in *M. xanthus*. Over time, we observed degradation of PopD-StrepII, indicating that LonD-$His_6$ is active (Figure 29). Since it has been shown, that the addition of poly phosphate can stimulate LonD protease activity in other organisms (Kuroda *et al.*, 2006), we also checked if the addition of this compound led to FtsZ degradation in our assay. Additionally, we added ppGpp to investigate if this second messenger that is essential to initiate the stringent response in *M. xanthus* (Manoil & Kaiser, 1980b) has an influence on LonD activity. However, we were not able to observe any degradation of FtsZ by LonD-$His_6$ by the addition of polyphosphate or ppGpp (data not shown). Thus, LonD might not directly degrade FtsZ. Nonetheless presence of LonD is essential to regulate FtsZ levels during vegetative growth and starvation.

### 6.7.5. LonD is not involved in transcriptional control of *ftsZ* or *pomXYZ*

Based on our *in vitro* data (Figure 29) we suggest that LonD is not the protease directly degrading FtsZ. However, the absence of LonD led to a stabilization of FtsZ, PomX, PomY and PomZ levels during development (Figure 27). Furthermore, LonD absence led to an increase in FtsZ half-life during vegetative growth and development (6.7.3). Already in 1987 it

was suggested, that LonD is involved in controlling the expression of developmentally regulated genes (Kroos & Kaiser, 1987). We observed that *ftsZ, pomX, pomY* and *pomZ* are transcriptionally downregulated upon starvation (Figure 20), causing decreasing levels of corresponding proteins (Figure 16). One possibility could be that LonD is involved in regulating the expression of those genes. To address this hypothesis, we determined *ftsZ, pomX, pomY* and *pomZ* transcript levels upon starvation in the absence of LonD via qRT-PCR. Δ*lonD* cells were starved in submerged culture using MC7 buffer and RNA samples were prepared. 1 µg RNA was used to generate cDNA and qRT-PCRs were performed.

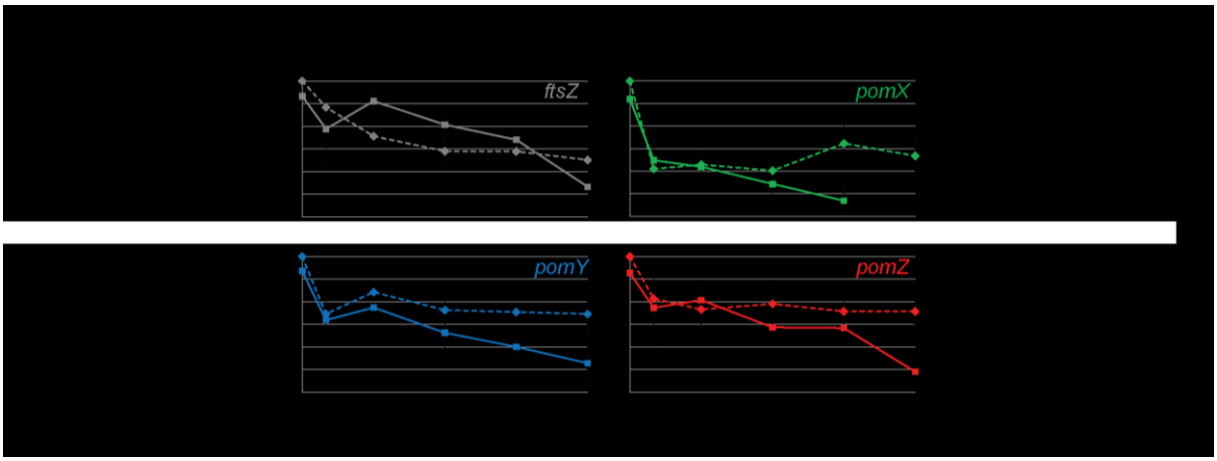


**Figure 30: LonD is not involved in transcriptional regulation of *ftsZ, pomX, pomY* and *pomZ***
qRT-PCR analysis of *ftsZ*, *pomX*, *pomY* and *pomZ* expression during starvation in the absence of LonD (solid line) and in WT cells (dashed line). Cells were starved in submerged culture using MC7 buffer. At indicated time points RNA samples were prepared and cDNA synthesized. Please note, that WT data are presented as in Figure 20. Values at each time point represent the log2 change in total cells compared to time point 0 of WT cells. Values are the average of two independent

biological replicates. Error bars indicate standard deviation.

Starvation results in an immediate decrease of *ftsZ, pomX, pomY* and *pomZ* mRNA levels in WT cells (Figure 20/Figure 30). In the absence of LonD we also observed a decrease of mRNA levels, which is comparable to the WT situation for the four genes tested. Although the drop of *ftsZ* mRNA levels was not visible early during starvation, the number of transcripts decreased 16-fold after 24 h. *pomX* mRNA levels dropped 6-fold after 2 h of starvation and are decreased approximately 32-fold after 18 h. *pomY* and *pomZ* mRNA levels dropped approximately 4-fold after starving for 2 h and dropped 8-fold and 16-fold until 24 h, respectively (Figure 30). We conclude, that the ATP-dependent protease LonD is not involved in transcriptional regulation of genes important for cell division tested in this experiment.

## 6.8. Spore morphology depends on chromosome content

Interestingly, we noticed that cells expressing *ftsZ* in the presence of 10 µM vanillate and subsequently spotted on TPM agar without vanillate formed spores increased in chromosome content (Figure 24). We also noticed an increased number of ParB-eYFP signals in spores

formed while *ftsZ* was expressed in a vanillate-dependent manner that were increased in cell length and number of ParB-eYFP clusters during vegetative growth despite the presence of high vanillate concentrations (Figure 23D/Figure 25B). We investigated if higher chromosome content influences spore morphology. We used spores formed while *ftsZ* is expressed in a vanillate-dependent manner and spores formed in the absence of one of the Pom proteins.

### 6.8.1. Vanillate-dependent *ftsZ* expression and spore morphology

To check morphology of spores formed while *ftsZ* is expressed in a vanillate-dependent manner, we used the strain described before (6.4.4). In this strain, we express *ftsZ* via the vanillate inducible promoter as the only *ftsZ* copy in the cell (SA6755). The cells were grown to exponential growth phase in the presence of indicated vanillate concentrations for at least eight generations to induce the expression of *ftsZ* and subsequently spotted on TPM agar plates supplemented with the corresponding vanillate concentrations to induce starvation. To shut off *ftsZ* transcription during starvation, cells grown with 10 µM vanillate were applied to starvation media supplemented with no vanillate. Under the described conditions, cells were able to aggregate into fruiting bodies and to sporulate, although sporulation frequency was reduced when spores were formed in the absence of vanillate (Figure 24). Furthermore, we observed, that constitutive *ftsZ* expression resulted in a stabilization of FtsZ levels during development (Figure 22).

Besides of spores formed under varying FtsZ levels, we examined spores which have been formed in the absence of FtsZ. To do so, we incubated cells in the presence of 25 µM vanillate followed by incubation without vanillate for 9 h. This results in FtsZ depletion as shown via immunoblot analysis and in an increase in average cell length (Figure 19A/B). Cells depleted for FtsZ were spotted on TPM agar plates without vanillate to induce starvation. The absence of FtsZ did not interfere with the ability to aggregate into fruiting bodies and to sporulate as shown in a previous experiment (Figure 19C). After 120 h spores were harvested and imaged on 1% agarose buffered with TPM at 32°C to analyze their morphology. Additionally, also exponentially cells, grown under the described conditions, were imaged.

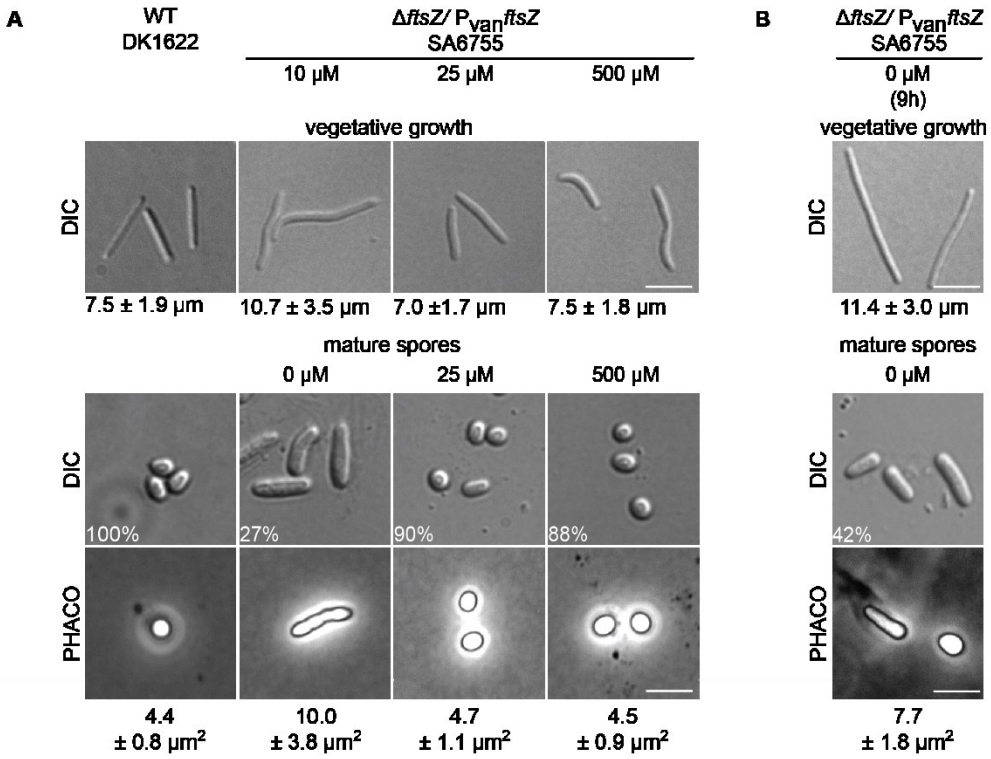


**Figure 31: Vanillate-dependent *ftsZ* expression and spore morphology**
**(A)** Exponentially growing WT cells and cells expressing *ftsZ* in a vanillate dependent manner were grown in the presence of indicated vanillate concentrations for at least eight generations and imaged on 1% agarose buffered with TPM. Cell length is indicated by numbers (same data as presented in Figure 23A). Same cells were transferred to TPM agar including the indicated vanillate concentrations and spores were harvested after 120 h to be imaged on 1% agarose buffered with TPM. Sporulation frequency and average spore size is indicated by numbers. Scale bar: 5 µm. **(B)** Cells expressing *ftsZ* in a vanillate dependent manner were incubated in the presence of 25 µM vanillate for at least eight generations and subsequently depleted for FtsZ by incubating them in the absence of vanillate for 9 h (see also Figure 19) Cells were imaged and transferred to TPM agar without vanillate as described in (A). After 120 h spores were imaged as described in (A). Sporulation frequency and average spore size is indicated by numbers. Scale bar: 5 µm.

During vegetative growth, WT cells had an average cell length of 7.5 ± 1.9 µm. After 120 h of starvation on agar plates WT cells formed heat and sonication resistant spores that had an average size of 4.4 ± 0.8 µm$^2$. WT spores appeared to be phase bright in phase contrast microscopy. *ftsZ* induction in the presence of 25 µM and 500 µM vanillate led to WT like cell morphology during vegetative growth as described in 6.6.1. Spores formed while *ftsZ* expression is induced in the presence of 25 µM or 500 µM vanillate had an average size of 4.7 ± 1.1 µm$^2$ and 4.5 ± 0.9 µm$^2$, respectively and appeared to be phase bright in phase contrast microscopy. Their size, their spherical shape and the sporulation frequency are comparable to WT spores. Incubation in the presence of 10 µM vanillate led to elongated cells during vegetative growth (6.6.1/Figure 23B). Spotting these cells on starvation medium without vanillate led to a drop in sporulation frequency to 27% (Figure 24A). The spores which were formed were phase bright and had an increased average size of 10.0 ± 3.8 µm$^2$.

Cells which were incubated in the absence of vanillate for 9 h, which resulted in complete FtsZ depletion (Figure 19A), had an average cell length of 11.4 ± 3.0 µm$^2$. These cells were able to

sporulate, but the sporulation frequency was reduced to 42% in comparison to WT cells. The spores which were formed had an average size of 7.7 ± 1.8 µm$^2$ and appeared to be elongated and phase bright in phase contrast microscopy.

In addition, we investigated spores formed while *ftsZ* was expressed in a vanillate-dependent manner and in parallel *parB-eYFP* or *tetR-eYFP* were expressed under control of the cupper inducible promoter. Vanillate-dependent *ftsZ* expression in concert with expression of *parB-eYFP* caused an increased average cell length in comparison to WT cells during vegetative growth. The expression of *tetR-eYFP* in the same background led to WT cell length in the presence of higher vanillate concentrations as described in 6.6.1. Cells were incubated in the presence of different vanillate concentrations to induce *ftsZ* expression for at least eight generations before the cells were spotted on TPM medium including the corresponding vanillate concentrations. To shut off *ftsZ* transcription during starvation, cells grown with 10 µM vanillate were applied to starvation media supplemented with no vanillate. Spotting these cells on starvation medium without vanillate led to a drop in sporulation frequency to 58% (SA6152) and 29% (SA6158). In the presence of 25 µM or 500 µM vanillate cells were able to aggregate into fruiting bodies and to sporulate at WT level as described in 6.6.2. After 120 h spores were harvested and imaged on 1% agarose buffered with TPM at 32°C to analyze their morphology. In addition, vegetatively growing cells were imaged as described in 6.6.1.

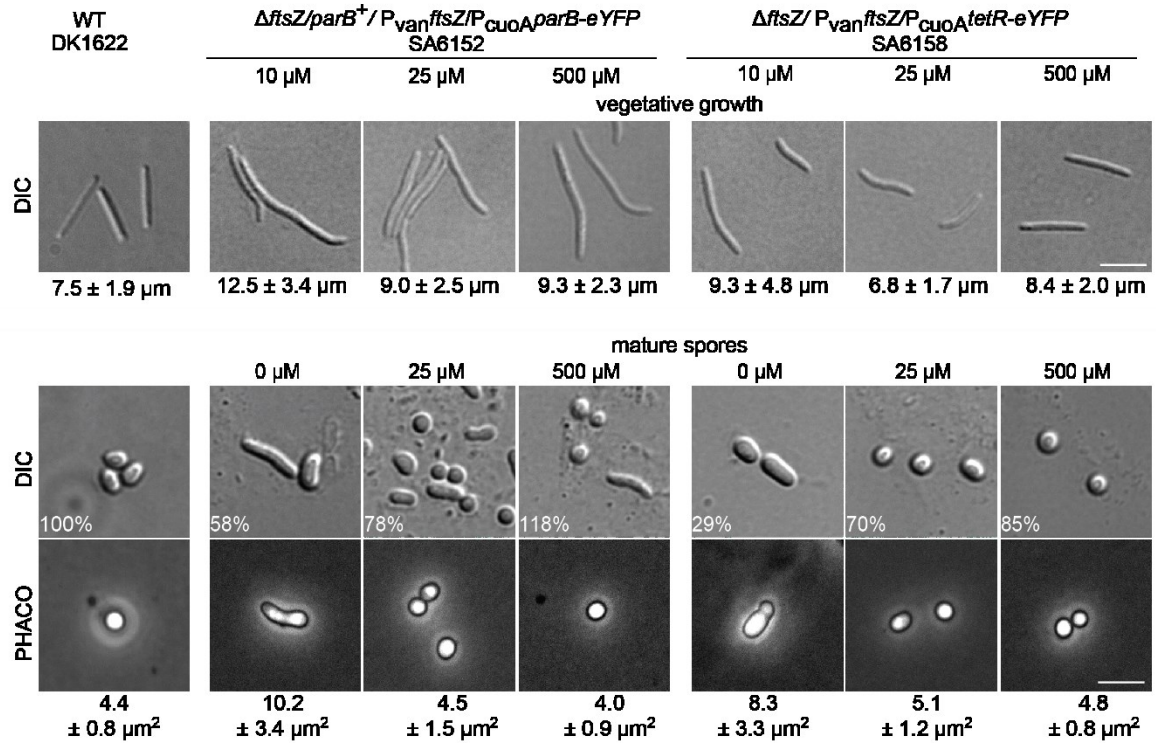


**Figure 32: Spore morphology of spores formed during vanillate-dependent *ftsZ* expression and copper-dependent *parB-eYFP* or *tetR-eYFP* expression**
Exponentially growing WT cells and cells expressing *ftsZ* in a vanillate dependent manner in concert with *parB-eYFP* (SA6152) or *tetR-eYFP* (SA6158) under control of the copper inducible promoter were grown in the presence of indicated vanillate concentrations for at least eight

generations and imaged on 1% agarose buffered with TPM. Cell length is indicated by numbers (same data as presented in Figure 23D). Same cells were transferred to TPM agar including the indicated vanillate concentrations and spores were harvested after 120 h to be imaged on 1% agarose buffered with TPM. Sporulation frequency and average spore size is indicated by numbers. Scale bar: 5 µm.

The spores formed by cells of the strain expressing *parB*-e*YFP* together with *ftsZ* in the presence of 25 µM vanillate had a size of 4.5 ± 1.5 µm$^2$. Starvation in the presence of 500 µM led to a spore size of 4.0 ± 0.9 µm$^2$. These values were comparable to WT cells, since these spores had a size of 4.4 ± 0.8 µm$^2$.Shut off of *ftsZ* transcription in the absence of vanillate led to an increase in spore size to 10.2 ± 3.4 µm$^2$. All spores appeared to be phase bright in phase contrast microscopy (Figure 32).

For cells expressing *tetR-eYFP* in concert with varying *ftsZ* expression we observed a similar situation. Spore formation in the absence of vanillate resulted in a spore size of 8.3 ± 3.3 µm$^2$. The presence of 25 µM vanillate led to formation of WT like spores with an average size of 5.1 ± 1.2 µm$^2$. 500 µM vanillate led to spores similar to WT spores as well. They had a size of 4.8 ± 0.8 µm$^2$. Also this strain formed spores that were phase bright in phase contrast microscopy under all conditions (Figure 32).

Taken together we showed, that constitutive expression of *ftsZ* resulting in WT cell length during vegetative growth did not result in aberrant spore morphology or a decrease in sporulation frequency. However, if cells were elongated during vegetative growth due to low FtsZ levels they formed spores which were increased in average size and the sporulation frequency dropped to approximately 30-50%. Furthermore, we showed that spores increased in size were increased in chromosome content (Figure 24C). We conclude that cell morphology and chromosome content higher than WT during vegetative growth determines spore morphology and leads to the formation of spores containing more than two chromosomes.

### 6.8.2. Absence of PomX PomY or PomZ leads to increased spore size and chromosome content

The presence of the cell division regulators PomX, PomY or PomZ. During vegetative growth, deletion of one of them causes a cell division defect and as a consequence an increase in cell length. Since neither chromosome replication nor segregation are affected, these cells tend to contain more than two chromosomes (Schumacher *et al.*, 2017, Treuner-Lange *et al.*, 2013). None of these proteins is required for *M. xanthus* cells to form spores. However, the sporulation frequencies are decreased to 29 – 62% (Figure 18).

We investigated spore morphology and chromosome content by expressing *parB-eYFP* via the vanillate inducible promoter in Δ*pomY* cells (SA6177). The cells were grown to exponential growth phase in the presence of 100 µM vanillate to induce the expression of the fluorescent fusion protein and subsequently spotted on TPM agar plates including 100 µM vanillate to

induce starvation. Also Δ*pomX,* Δ*pomY* and Δ*pomZ* cells were grown to exponential growth phase und spotted on TPM starvation medium. After 120h spores were harvested and imaged on 1% agarose buffered with TPM at 32°C. To not miss any fluorescent signals in the spherical spore, we performed Z-stacks with 0.15 µm intervals through the spores and analyzed the maximal projection of these pictures. Furthermore, exponentially growing cells were imaged on 1% agarose buffered with TPM.

We performed flow cytometry in addition to single cell analysis via microscopy to analyze the average chromosome content in the cell population. Exponentially growing WT (DK1622) cells were used as a standard as described before (6.1). Exponentially growing Δ*pomY* cells were grown to exponentially growth phase and stained with 10 µM Vybrant® DyeCycle™ Orange for 40 min before the DNA content was quantified by flow cytometry. To investigate chromosome content of Δ*pomY* cells which differentiated into peripheral rods and spores, these cells were grown to exponentially growth phase and spotted on TPM agar plates to induce starvation. After 120h cells were harvested, resuspended in TPM buffer and their chromosome was stained with 10 µM Vybrant® DyeCycle™ Orange for 40 min. The fluorescent intensity which is proportional to DNA content was subsequently quantified by flow cytometry.

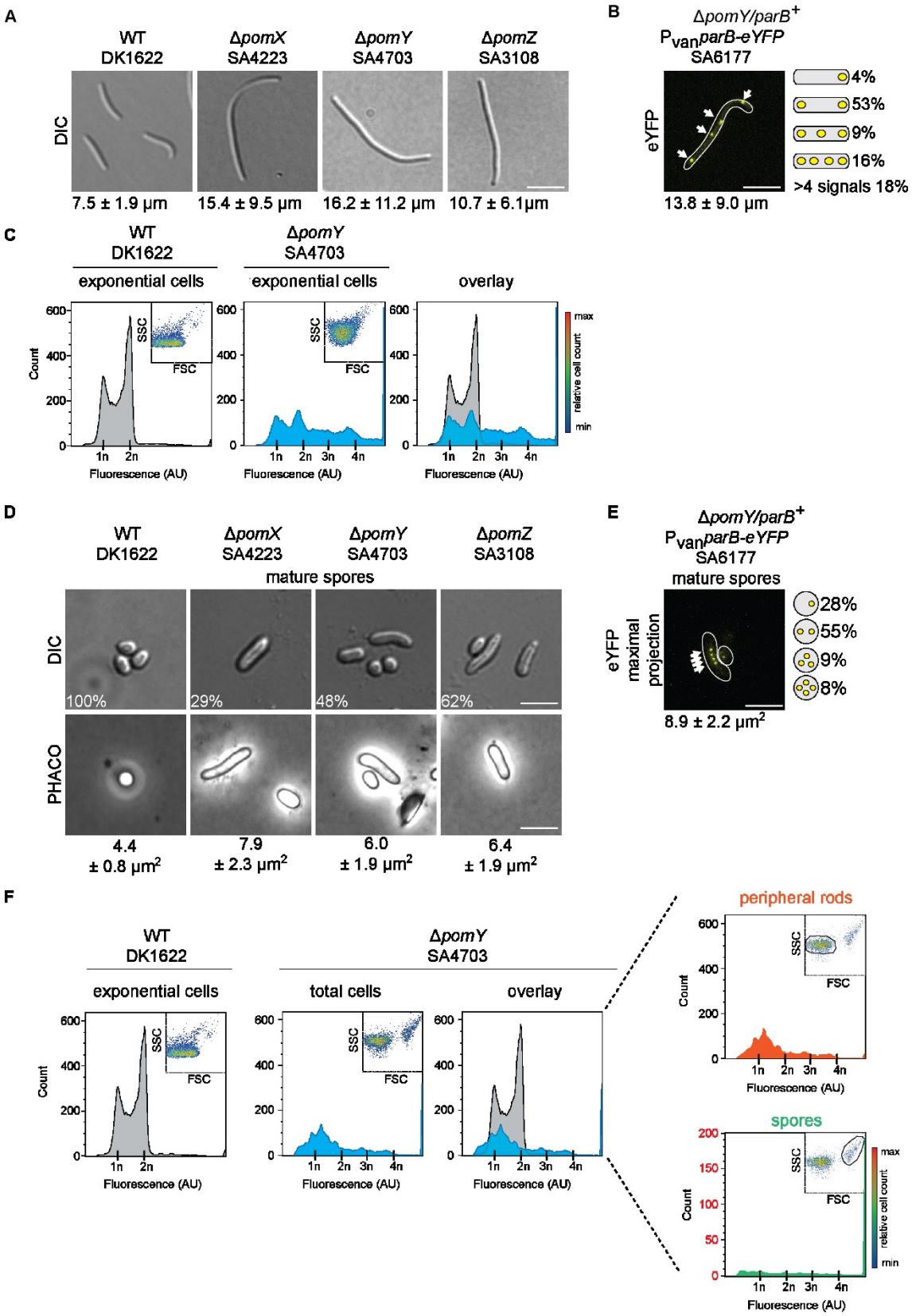


**Figure 33: Absence of PomX, PomY or PomZ leads to aberrant spore morphology and spores containing more than two chromosomes**

**(A)** Exponentially growing cells of indicated strains were imaged on 1% agarose buffered with TPM at 32 °C. Average cell length is indicated by numbers (Schumacher *et al.*, 2017, Treuner-Lange *et al.*, 2013). Scale bar: 5 µm. **(B)** Exponentially growing Δ*pomY* cells expressing *parB-eYFP* (SA6177) in the presence of 100 µM vanillate were imaged as described in A. Average cell length as well as abundance of localization patterns is indicated (n>100). Scale bar: 5 µm. **(C)**

Flow cytometry profile of exponentially growing WT (DK1622) and Δ*pomY* (SA4703) cells. Cells were stained with Vybrant® DyeCycle™ Orange. The x-axis represents arbitrary fluorescence intensity and the y-axis represents cell count, whereby each experimental run consisted of analysis of 10.000 individual cells. Tick marks represent the expected positions of fluorescent intensities corresponding to one and two copies of the chromosome based on the fluorescence of exponentially growing WT cells. Correlated measurements of side-scattered (SSC) and forward-scattered light (FSC) are presented in a scatter plot. The color scale shows relative cell count from lowest (blue) to highest (red). **(D)** Spores of indicated strains were harvested from TPM medium after 120 h of starvation and were imaged on 1% agarose buffered with TPM at 32 °C via DIC and PHACO. Sporulation frequencies (same data as in Figure 18) and average size are indicated by numbers. Scale bar 5 µm. **(E)** Δ*pomY* spores expressing *parB-eYFP* (SA6177) were harvested from TPM including 100 µM vanillate to induce expression of fluorescent fusion protein, were imaged as described in (D). Z-stacks with 0.15 µm intervals were performed. Maximal projection of representative spores is shown. Outline was obtained from DIC pictures. Cartoons indicate occurrence of given localization patterns and average size is presented (n>100) Scale bar 5 µm. **(F)** Flow cytometry profile of exponentially growing WT (DK1622) and Δ*pomY* (SA4703) cells starved on TPM for 120 h. Cells were stained and data are presented as described in (C). Based on correlated SSC and FSC measurements, cell populations were analyzed separately.

During vegetative growth, WT cells have an average cell length of 7.5 ± 1.9 µm. In the absence of one of the *pom* genes the cell length during vegetative growth is increased to 15.4 ± 9.5 µm (Δ*pomX*), 16.2 ± 11.2 µm (Δ*pomY*) and 10.7 ± 6.1 µm (Δ*pomZ*) (Schumacher *et al.*, 2017, Treuner-Lange *et al.*, 2013) (Figure 33A). In addition to 4% and 53% of cells which showed one and two ParB-eYFP clusters respectively, we observed three signals in 9% of Δ*pomY* cells expressing *parB-eYFP* as marker for the origin of replication. 16% of cells showed four signals and in 18% of cells we counted more than 4 foci (Figure 33B). This indicated the presence of three to four origins of replication in a fraction of cells. This observation is coincident with the known cell length phenotype of Δ*pomY* cells and the collected flow cytometry data. Comparison of the flow cytometric profile of Δ*pomY* with WT cells revealed, that Δ*pomY* cells have more than one or two chromosomes. In addition to the 1n and 2n peak no clear peak was visible. However, the measurement showed the presence of cells having a higher fluorescent intensity suggesting the presence of cells having three, four or more chromosomes. Correlated measurements of SSC and FSC revealed one cell population which appeared to be more diverse in cell size and complexity than the WT, since the scatter plot showed a more heterogenous distribution (Figure 33C, insets).

The analysis of cells which were starved for 120 h on TPM agar plates revealed that the WT had formed heat and sonication resistant spores which have an average size of 4.4 ± 0.8 µm$^2$. For spores which differentiated in the absence of PomX, PomY or PomZ we observed an increased average size of 7.9 ± 2.3 µm$^2$, 6.0 ± 1.9 µm$^2$ and 6.4 ± 1.9 µm$^2$, respectively. On top of that, these spores appeared to have a different shape in comparison to WT spores. Whereas WT spores were usually spherical, several Δ*pom* spores were elongated. Nonetheless, the absence of one of the Pom proteins seemed to not result in a general spore formation defect. The spores appeared phase bright in phase contrast microscopy which indicates a functional spore coat as observed for WT spores (Figure 33D).

In 28% of spores, formed in the absence of PomY, we found one ParB-eYFP focus and in 55% of spores two ParB-eYFP signals. Additionally we observed in 9% and 8% of spores three and four ParB-eYFP signals, respectively (Figure 33E). This indicated the presence of three to four origins of replication, so more than two chromosomes in mature spores. Thus, spores increased in average size seem to be increased in average chromosome content.

Flow cytometric analysis of Δ*pomY* cells starved for 120 h did not show a clear peak corresponding to 1n or 2n as observed for vegetatively growing WT cells. In fact, we observed one peak which would correspond to one to two chromosomes. Nevertheless, we also observed cells having a higher fluorescent intensity suggesting the presence of more than two chromosomes. Based on SSC and FSC measurements, we observed a cell population which appears to have the same properties as vegetative Δ*pomY* cells which are the peripheral rods. Additionally, a second cell population arised, which is increased in both, SSC and FSC values, presumably displaying the spores. Inspection of both cell populations revealed a different flow cytometric profile. Whereas cells coincident with properties of vegetative cells, the peripheral rods, displayed one peak corresponding to the presence of one to two chromosomes we also observed cells having a higher fluorescent intensity suggesting the presence of more than two chromosomes. The second cell population, the spores, displayed no distinct peak. In fact, we observed a distribution of cells having a fluorescence intensity corresponding to the presence of less than one to four chromosomes (Figure 33F).

These data suggested, that cells which lack one of the Pom proteins and have more than two chromosomes during vegetative growth are able to differentiate into spores. However, spore frequency is decreased. Spores that were formed appeared to be increased in average size. Furthermore, some spores contained more than two chromosomes.

Thus, spore formation does not depend on chromosome content, which means that also spores which are having more than two chromosomes can be formed. Indeed, cell morphology during vegetative growth seems to determine spore morphology. Longer cells having more than two chromosomes will differentiate into bigger spores increased in chromosome content. We conclude, that cell morphology and chromosome content higher than WT during vegetative growth determines spore morphology and leads to the formation of spores containing more than two chromosomes. This is in line with the results we obtained for spores formed while *ftsZ* is expressed at different levels (6.8.1).

## 6.9. Decreasing FtsZ levels leading to inhibition of cell division are specific to starvation

Our results suggested that decreasing FtsZ levels lead to inhibition of cell division during development ensuring the formation of spores containing two fully duplicated genomes. The developmental program is a complex process, which depends on a variety of intercellular signaling pathways, regulation of gene expression and the production of second messengers. The question arises if the inhibition of cell division is a phenomenon that is specific to development or a response to poor growth conditions. Furthermore, it would be interesting to unveil if the decrease in FtsZ protein levels depends on signals or second messengers known to be important for development. In the next chapters, experiments to test the influence of some of these signaling molecules will be described.

### 6.9.1. FtsZ decrease is specific to development

Development of *M. xanthus* is a response to poor growth conditions, such as carbon, nitrogen or phosphate deprivation (Dworkin, 1962). However, during stationary growth phase, cells are exposed to unfavorable conditions as well. Depletion of essential nutrients leads to a situation in which growth rate and death rate are equal. To examine, if the decrease in FtsZ levels is a phenomenon specific to development, we analyzed FtsZ accumulation during stationary growth phase. Samples were taken at different time points during exponential and stationary growth phase (Figure 34A) and cell lysates were subjected to SDS-page and immunoblotting with specific α-FtsZ and α-PilC antibodies.

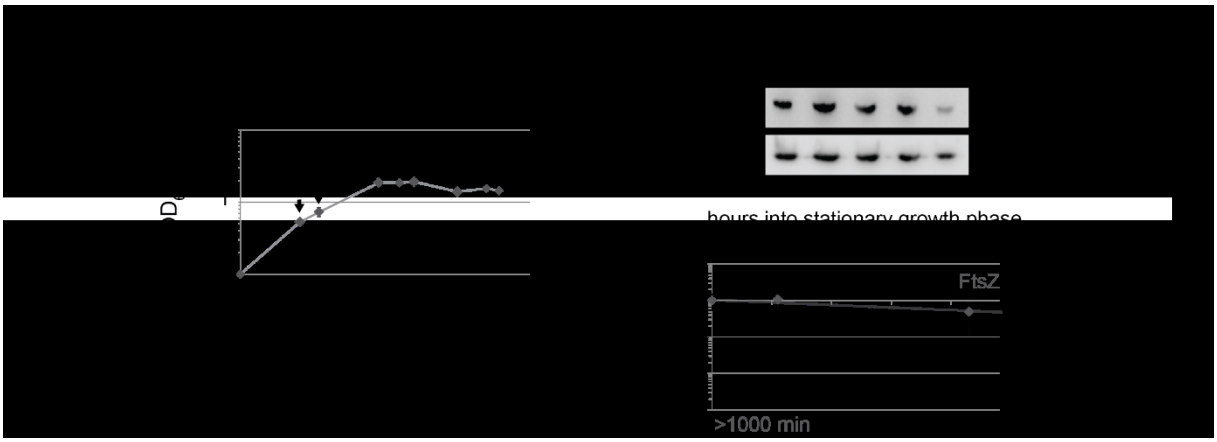


**Figure 34: Decreasing FtsZ levels are specific to development**
**(A)** Growth curve of WT DK1622 cells. Values are presented as mean of two independent biological replicates. Numbers indicate time points when samples for immunoblots were taken. **(B)** Immunoblot analysis of FtsZ (44.7 kDa) during exponential and stationary growth phase. Samples were taken as indicated in (A). Cell lysates were probed with specific α-FtsZ (Treuner-Lange *et al.*, 2013) and α-PilC (45.2 kDa) antibodies (Bulyha *et al.*, 2009). Representative blot of two independent biological replicates is shown. Graph were created by densitometry analysis of immunoblots calculate the time to reduce to 50% of initial intensity at the beginning of stationary phase. Data are presented as mean of two independent biological replicates relative to α-PilC loading control. Error bars indicate standard deviation.

During vegetative growth, cells FtsZ accumulates (Figure 34B, samples 1 and 2). At the onset of stationary phase (0 h) and at early stationary growth phase (6 h), FtsZ is detectable in comparable amounts to the ones detected during exponential phase. The protein level dropped not before late stationary phase (22 h) (Figure 34B). By analyzing the relative intensities, we were able to calculate the time to reduce to 50% of initial intensity at the beginning of stationary phase, which was >1000 min. Since we calculated a reduction to 50% in 227 min upon initiation of starvation (6.4.1), FtsZ levels were clearly more stable when cells entered the stationary growth phase. These data indicated that the reduction of FtsZ protein levels is a phenomenon specific to development, but is not a response to poor growth conditions such as stationary growth phase.

### 6.9.2. Upon starvation, FtsZ decreases independently of RelA

We observed that the reduction of FtsZ levels is specific to development (6.9.1). Initiation of the developmental program of *M. xanthus* requires the stringent response, which is initiated by accumulation of the second messenger (p)ppGpp produced by the the (p)ppGpp synthase RelA (Singer & Kaiser, 1995, Harris *et al.*, 1998). Δ*relA* cells show an early development defect and important events specific to development rely on RelA function, e.g. A-signaling (Harris *et al.*, 1998) or PopC secretion to generate the C-signal (Konovalova *et al.*, 2012).To figure out if the decrease in FtsZ level and number of *ftsZ* transcripts depends on the presence of RelA and the accumulation of (p)ppGpp, we used the Δ*relA* mutant (MS1000). It is important to note that this mutant was constructed in the DK101 WT background. Therefore, DK101 cells were used as a control. Cells were starved in MC7 buffer, incubated with shaking at 32°C. Samples were taken at different time points and cell lysates were subjected to SDS-page and immunoblotting with specific α-FtsZ and α-PilC antibodies. Cells treated in the same way were also harvested at different time points to prepare RNA samples. 1 µg RNA was used to generate cDNA and qRT-PCRs were performed.

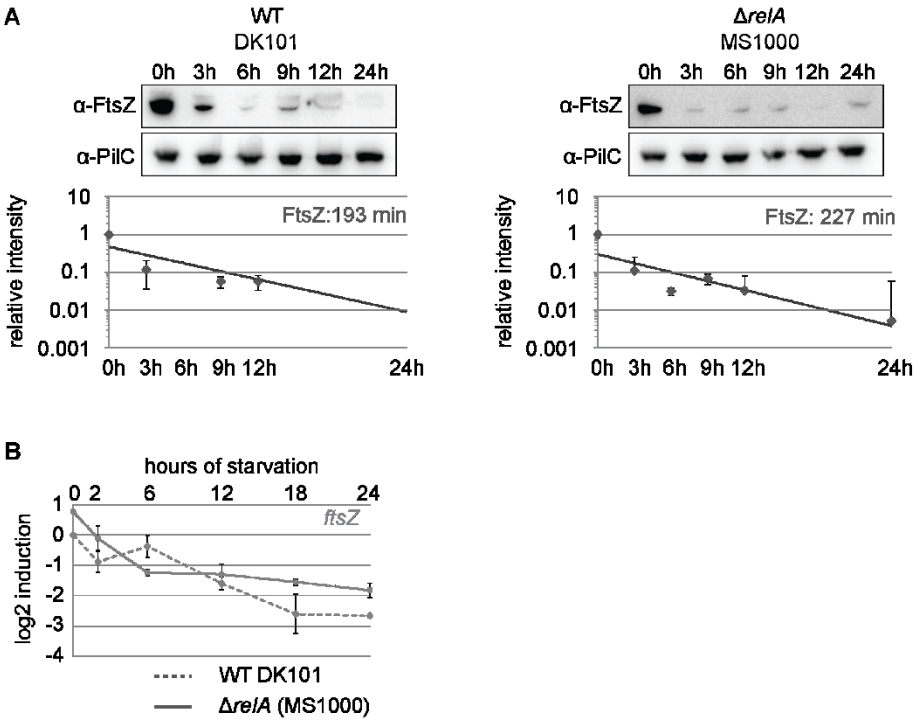


**Figure 35: FtsZ levels and *ftsZ* transcripts decrease independently of RelA**
**(A)** Immunoblot analysis of FtsZ (44.7 kDa) during development. WT (DK101) and Δ*relA* (in DK101 background) cells were starved in MC7 shaking culture. Samples were taken at indicated time points. Cell lysates were probed with specific α-FtsZ (Treuner-Lange *et al.*, 2013) and α-PilC (45.2 kDa) antibodies (Bulyha *et al.*, 2009). Graphs were created by densitometry analysis of immunoblots to calculate the time to reduce to 50% of initial intensity which is indicated by numbers. Data are presented as mean of two technical replicates relative to α-PilC loading control. **(B)** Quantitative PCR analysis of *ftsZ* expression during starvation in WT DK101 and Δ*relA* (in DK101 background). Cells were starved as described in A. At indicated time points RNA samples were prepared and cDNA synthesized. Values at each time point represent the log2 change in total cells compared to time point 0. Values are an average of two independent biological replicates, each three technical replicates. Error bars indicate standard deviation.

In DK101 WT cells, FtsZ levels decreased upon starvation. In 193 min, the initial amount was reduced to 50% (Figure 35A) which is comparable to the WT DK1622. (227 min/Figure 16). In the absence of RelA, FtsZ decreased upon starvation as well. In 227 min it was reduced to 50% (Figure 35A). Starvation did also result in an almost 8-fold decrease in the number of *ftsZ* transcripts in cells of the DK101 WT until 24 h. In cells of the WT DK1622, *ftsZ* transcripts decreased 6-fold until 24 h (6.5.1). Also in the Δ*relA* mutant *ftsZ* mRNA levels decreased approximately 8-fold until 24 h. In both strains tested in this experiment, mRNA levels decreased continuously over the time course (Figure 35B).

Taken together, the results indicated, that the decrease in FtsZ accumulation and *ftsZ* transcripts upon starvation occurs in cells of both WT strains, DK101 and DK1622. Second, the decrease of FtsZ levels and *ftsZ* transcripts is independent of the (p)ppGpp synthase RelA and the stringent response.

### 6.9.3. FtsZ protein level and *ftsZ* transcripts decrease independently of the diguanylate cyclase DmxB

The second messenger bis-(3´5´)-cyclic dimeric GMP (c-di-GMP) has been shown to be an essential regulator of multicellular development in *M. xanthus*. The level of c-di-GMP increases during development. Responsible for the increased c-di-GMP accumulation is the diguanylate cyclase DmxB. In the absence of DmxB, c-di-GMP levels do not elevate and cell are deficient in fruiting body formation and aggregation (Skotnicka *et al.*, 2016). To check if an increasing level of c-di-GMP is important for *M. xanthus* to regulate FtsZ levels during development, we checked FtsZ levels and *ftsZ* number of transcripts in the absence of DmxB during starvation. Cells were starved in submerged culture using MC7 buffer at 32°C. Samples were taken at different time points and cell lysates were subjected to SDS-page and immunoblotting with specific α-FtsZ antibodies. Cells treated in the same way were also harvested at different time points to prepare RNA samples. 1 µg RNA was used to generate cDNA and qRT-PCRs were performed.

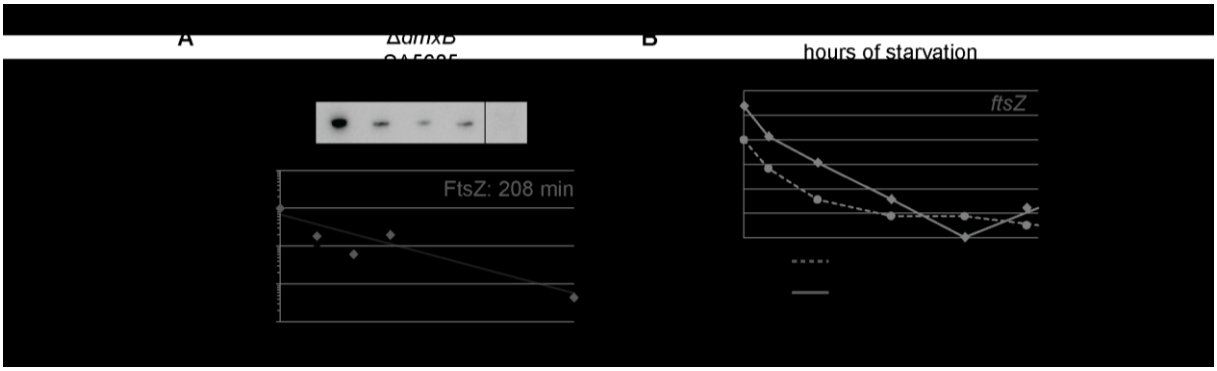


**Figure 36: FtsZ levels and *ftsZ* transcript numbers decrease independently of the diguanylate cyclase DmxB**
**(A)** Immunoblot analysis of FtsZ (44.7 kDa) during development in the absence of DmxB. Cells were starved in MC7 submerged culture. Samples were taken at indicated time points. Cell lysates were probed with specific α-FtsZ antibodies (Treuner-Lange *et al.*, 2013). Graphs were created by densitometry analysis of immunoblots to calculate the time to reduce to 50% of initial intensity which is indicated by numbers. Data are presented as mean of two technical replicates. **(B)** Quantitative PCR analysis of *ftsZ* expression during starvation in Δ*dmxB* cells. Cells were starved as described in A. At indicated time points RNA samples were prepared and cDNA synthesized. Values at each time point represent the log2 change in total cells compared to time point 0. Values are an average of two independent biological replicates, each three technical replicates. Please note that WT data are the same as presented in Figure 20. Error bars indicate standard deviation.

In the absence of the diguanylate cyclase DmxB, FtsZ levels decreased during development. The time to reduce to 50% of the initial intensity was 207 min. This was comparable to the decrease observed in WT cells, since in this strain, FtsZ levels were reduced to 50% in 227 min (Figure 16). On top of that, also *ftsZ* transcript numbers decreased in the absence of DmxB as observed in WT in which we observed a 6-fold decrease until 24 h (6.5.1). In the absence

of DmxB, *ftsZ* mRNA levels were decreased continuously over the time course to approximately 8-fold until 24 h of starvation.

These results indicated, that FtsZ protein levels decrease independently of DmxB and as a consequence thereof independently of the global pool of c-di-GMP, which accumulates in *M. xanthus* cells upon starvation. Hence, c-di-GMP seems not to be involved in FtsZ regulation during development.

# 7. Discussion

Several bacteria have evolved mechanisms to survive unfavorable environmentally conditions by differentiation into dormant spores. Although the spores which are formed do share a round or oval shape and are covered with a spore coat, the sporulation process itself is organized very differently (Flärdh & Buttner, 2009, Piggot & Hilbert, 2004, Kroos, 2017). However, sporulation processes have in common, that the important cell cycle events replication, segregation and cell division are modified and tightly coordinated. The organisms *S. coelicolor* and *B. subtilis* form haploid spores due to an essential cell division event. In contrast, *M. xanthus*, forms diploid spores independent of a septation event.

In this study we addressed replication and cell division during starvation induced cell differentiation in *M. xanthus*. Our results suggest, that all cells replicate during earlier stages of development. At later stages, peripheral rods synthesize DNA and contain one to two chromosomes. Mature spores are diploid and do not replicate. By analyzing synthesis, accumulation and degradation of proteins known to be important to regulate and perform cell division we investigated cell division during development. Our results indicate that proteolysis of FtsZ outperforms FtsZ synthesis during development resulting in elimination of FtsZ. This elimination is sufficient to guarantee the formation of diploid myxospores. Moreover, our results suggest that average spore size increases when spores contain more than two chromosomes.

## 7.1. Mature spores contain two fully duplicated genomes and peripheral rods are diverse in their chromosomal content

Based on flow cytometry and FISH (fluorescent *in situ* hybridization) it was concluded that myxospores contain two fully duplicated genomes and peripheral rods contain one chromosome (Tzeng & Singer, 2005). Furthermore, replication during aggregation phase is essential for *M. xanthus* to form diploid myxospores and to complete the developmental program (Tzeng *et al.*, 2006). Up to now, it was not clear if replication is restricted to cells dedicated to become spores or all cells undergo replication during development.

Recent work on the chromosome organization throughout the cell cycle during vegetative growth conditions revealed, that after replication in parallel to chromosome segregation, cell division takes place (Harms *et al.*, 2013). During starvation cells undergo replication (Rosario & Singer, 2007, Rosario & Singer, 2010). Early work showed that when chemically induced by the addition of 0.5 M glycerol, spore differentiation does not require a cell dvision event (Dworkin & Gibson, 1964). These facts lead to the idea that cell division is inhibited in cells destined to become myxospores.

In order to support previous findings we performed flow cytometry as it was done before. Furthermore, we investigated the chromosome on a single cell level. On one hand, this allows to confirm existing data and to analyze the chromosome content of cells early during development. On the other hand, single cell analysis is a possibility to address if replication is restricted to one cell fate during fruiting body formation and if synthesis of DNA is happening exclusively during the first 12 h of starvation. We took advantage of tools established to investigate vegetatively growing cells: FROS gives the possibility to visualize different chromosomal loci in order to examine chromosome organization. ParB-eYFP functions as a marker for the origin of replication and Ssb-eYFP clusters visualize single stranded DNA at the replication forks (Harms *et al.*, 2013). Additionally, EdU labeling in *M. xanthus* cells was established to visualize active DNA synthesis.

Different cell types formed during development are distinguishable already after 2-3 h after initiation of starvation (O'Connor & Zusman, 1991b). The distinct accumulation of ProteinC, a 31 kDa fragment of the extracellular protease FibA which is exclusively produced in aggregating cells (Lee *et al.*, 2011), confirmed this finding. We observed a difference in protein accumulation specific to cell fate already after 3 h (Figure 10). Thus, cell fate determination is an early event during the developmental program. Previous work suggests, that replication is essential for fruiting body formation and sporulation and occurs before 12 h after the onset of starvation conditions (Tzeng *et al.*, 2006). More specifically upregulation of *dnaA* transcription between 4-5 h of starvation leads to the assumption that replication is initiated at this point in time (Rosario & Singer, 2010). This is also supported by incorporation of radiolabeled thymidine, which peaks at around 4-5 h after initiation of starvation (Tzeng *et al.*, 2006). Replication is thought to be required for the formation of diploid spores. In contrast, peripheral rods are suggested to contain one chromosome (Tzeng & Singer, 2005).

We observed in most of the cells of both fractions starving for 24 h two origins of replication and one terminus (Figure 11). Exploration of replication did also not show any differences between aggregating and non-aggregating cells. Ssb-eYFP clusters were found in 40% of both cell fractions and active DNA replication visualized by EdU labeling was observed in around 35% of all cells (Figure 12). Although the number of Ssb-eYFP clusters is reduced in comparison to vegetative growth, the number of cells actively synthesizing DNA is comparable to vegetative growth conditions.

Of note, the application of EdU labeling proved, that the presence of a Ssb-eYFP foci does not confirm ongoing DNA replication, since we found Ssb-eYFP signals in cells blocked in elongation but not initiation of replication by hydroxy urea treatment (Figure 12). Additionally, even though we detected Ssb-eYFP signals in 76% of vegetatively growing cells, we detected active DNA synthesis in 41% of cells, when exposed to EdU labeling for 30 min. Thus, Ssb-

eYFP clusters are a proxy for the presence of single stranded DNA at the replication forks (Harms *et al.*, 2013), but are not necessarily a guarantor for active DNA synthesis (at least during a time period of 30 min). Nevertheless, we showed that Ssb-eYFP colocalizes with the place of active DNA replication since in cells which show a signal for both (36%), the signals are overlapping (Figure 12).

Considering the data we collected for aggregating and non-aggregating cells which were starving for 24 h, we think that cells of both cell types are in the replication process, which leads to EdU incorporation similar to vegetative growth. Conclusively, replication is not restricted to one cell fate, but all cells undergo replication upon starvation. Of note, the number of cells actively replicating after 24 h of development (~35%) is slightly reduced in comparison to vegetatively growing cells (41%). This generates the idea that replication speed is reduced. During vegetative growth, chromosome replication takes about 70% of cell cycle which is approximately 210 min (Harms *et al.*, 2013). This time period could be elongated due to starving conditions. Anyway, to explore the timing of replication leading to a difference in chromosome content in both cell types formed during development in more detail, the cells need to be examined at more time points. Furthermore after 24 h of starvation we observed two termini in 38% of aggregating cells, whereas 23% of non-aggregating cells showed to termini regions which is both increased in comparison to vegetative growth (6%). This might give a hint how the chromosome content will evolve in mature spores and peripheral rods.

Although analysis of cell fractions after 24 h of starvation did not reveal differences in replication or chromosome content, the investigation of mature spores and peripheral rods after 120 h revealed the different chromosome content in both cell fates. Fluorescence microscopy showed two ParB-eYFP and two termini regions in the majority of myxospores. Furthermore two origins of replication and two termini could be visualized in one spore. In contrast, peripheral rods are diverse in their chromosomal content. Fluorescence microscopy visualized two origins of replication and one terminus region in most cells (Figure 14) which was supported by flow cytometry (Figure 9) suggesting that peripheral rods are a population of cells in various stages of the cell cycle. This is supported by the fact, that we demonstrated active DNA synthesis in 10% of peripheral rods although no Ssb-eYFP signals could be observed in mature spores or peripheral rods (Figure 15).

One very interesting finding was the chromosome content of peripheral rods after 120 h of starvation. The biology of peripheral rods was investigated in several studies. This subpopulation located between and surround mature fruiting bodies is suggested to allow *M. xanthus* the exploration of low amounts or transient influxes of nutrients without the investment of energy in spore germination. They are thought to have similarities to persister like cells (Balaban, 2011) which do not undergo cell division (O'Connor & Zusman, 1991a). Furthermore

they were suggested to be clearly distinguishable from vegetatively growing cells since they express proteins specific to peripheral rods (O'Connor & Zusman, 1991a, O'Connor & Zusman, 1991b). Due to our results, peripheral rods are comparable to vegetatively growing cells when it comes to chromosome content. They actively synthesize DNA. However, we observe a reduction of cells actively replicating their genome to 10%, which could be a hint that replication speed is reduced due to poor growth conditions these cells are exposed to for 120 h. Nevertheless, peripheral rods could be slowed down, but still be capable to perform all processes to complete the cell cycle as vegetatively growing cells. Although peripheral rods are distinguishable from vegetatively growing cells in a different nutritional state (O'Connor & Zusman, 1991a), they are not in a dormant state.

In this context, there is still the important question why *M. xanthus* does form spores containing two chromosomes while other spore formers such as *B. subtilis* and *S. coelicolor* do not? It was proposed earlier (Tzeng & Singer, 2005), that a copy of the chromosome could enhance spore survival in response to DNA damage, since this second chromosome provides a higher probability for recombination-mediated DNA repair. This model has been proven correct in the organisms *Bacillus megaterium*, *Bacillus cereus* and *Bacillus thuringiensis*, since their spores contain two chromosomes and have been shown to be more resistant to DNA damage than its close relative *B. subtilis* which spores contain one chromosome (Hauser & Karamata, 1992, Woese, 1958). Another idea would be, that the presence of two chromosomes prior to germination provides an advantage. When the conditions improve, the cells do not need to spend energy and time on the replication process before they can perform their first cell division. One round of cell division after germination doubles the population size and would enhance the probability of species survival.

## 7.2. Control of FtsZ protein level by a combination of constitutive degradation and transcriptional downregulation during development

In order to address the hypothesis of inhibition of cell division in sporulating cells, we analyzed proteins which are known to be involved and required for cell division in *M. xanthus*. The central component of the cell division machinery in bacterial cells is FtsZ. The tubulin homologue polymerizes into a ring like structure in a GTPase-dependent manner at the incipient cell division site and functions as a scaffold to recruit and coordinate the assembly of proteins involved in cytokinesis. Together they build the divisome (Adams & Errington, 2009). In order to inhibit cell division, FtsZ is a promising target (Hurley *et al.*, 2016). Regulators that influence its GTPase activity (Thanbichler & Shapiro, 2006) in concert with its ability to form polymers (Cabre *et al.*, 2015) or its self-interaction (Beaufay *et al.*, 2015) have been shown to alter Z-ring assembly and prevent cell division. FtsZ regulation is necessary to position the Z-ring to the future cell division site (Thanbichler & Shapiro, 2006, Wu & Errington, 2012) and to couple

FtsZ assembly to nutrient availability and growth rate (Weart *et al.*, 2007, Hill *et al.*, 2013). In addition to control of Z-ring assembly also FtsZ stability has been shown to be an important factor to regulate cell division. ClpX, which possesses ATP-dependent protein remodeling activities interacts with its proteolytic partner ClpP to form the ATP-dependent protease ClpXP (Kirstein *et al.*, 2009) and has been shown to degrade FtsZ to regulate Z-ring dynamics in a proteolysis dependent manner (Viola *et al.*, 2017) in a variety of organisms (Camberg *et al.*, 2009, Feng *et al.*, 2013, Williams *et al.*, 2014).

*M. xanthus* lacks a known homolog of FtsZ inhibitors like the MinCD core components of the two Min systems, MipZ of the MipZ/ParB system or nucleoid occlusion proteins like Noc or SlmA (Schumacher *et al.*, 2017, Treuner-Lange *et al.*, 2013). In addition to inhibit FtsZ itself, the proteins which are involved in positioning FtsZ to the incipient cell division site in *M. xanthus* could be targets to alter cell division as well. Recently, major progress has been made to understand the interplay of the Pom system. The ParA ATPase PomZ is responsible to tether a complex which consists out of the three proteins PomX, PomY and PomZ to the nucleoid. The PomXYZ complex transclocates on the nucleoid to the mid-nucleoid which coincides with midcell and the incipient cell division site. The movement depends on PomZ ATPase activity. At the incipient constriction site the complex promotes cell division probably by recruiting FtsZ. The absence of one of them leads to severe cell division defects (Schumacher *et al.*, 2017, Treuner-Lange *et al.*, 2013). To address inhibition of cell division during starvation, we analyzed synthesis, accumulation and degradation of these proteins, but particularly we focused on FtsZ.

Our experiments revealed, that the protein levels of FtsZ, PomX, PomY and PomZ decrease upon starvation, which indicated that the accumulation of these proteins is regulated during development (Figure 16). In line with these observations we found, that neither the presence of FtsZ nor the presence of PomX, PomY or PomZ is essential for fruiting body formation or sporulation. Although the sporulation frequencies of cells lacking one of these proteins were decreased in comparison to WT cells, the general sporulation process was not affected (Figure 18/Figure 19). In this context, the elongated cell morphology of these cells (Figure 19/Figure 33) should be considered, that might cause a motility defect which in turn might lead to a disadvantage in aggregation. Accordantly, *pomZ* (originally known as *agmE)* was initially identified as a gene involved in motility (Youderian *et al.*, 2003).

To get an insight into possible mechanisms regulating cell division, we determined the transcription rate of *ftsZ*, *pomX*, *pomY* and *pomZ* by qRT-PCR. The mRNA levels of these four genes decreased upon starvation (Figure 20). Thus, proteins important for cell division are regulated on the transcriptional level during development. Indeed, decrease of a specific protein might be due to degradation as well. We determined the half-life of FtsZ by analyzing

its stability when protein synthesis is shut off during vegetative growth and during development. During both conditions we calculated an FtsZ half-life of 25 and 29 minutes, respectively.

In *E. coli* an FtsZ half-life of 115 min was determined. The ATP-dependent protease ClpXP was shown to be responsible for FtsZ degradation, whereas FtsZ polymers are degraded more rapidly than monomers (Camberg *et al.*, 2009). ClpXP-dependent FtsZ degradation was shown to be important for Z-ring dynamics at the division site (Viola *et al.*, 2017). In *C. crescentus* FtsZ degradation is catalyzed by the chaperones ClpX and ClpA in conjunction with the ClpP protease and is differently regulated in both cell fates. In the non-replicative swarmer cells FtsZ is rapidly degraded with a half-life of 26 minutes whereas no degradation could be observed in stalked cells. The observed half-life of 25 and 29 minutes in *M. xanthus* cells led to the assumption, that a protease is responsible for FtsZ turnover during both conditions. Often, ATP-dependent proteases are involved in regulated proteolysis in order to control key proteins (Konovalova *et al.*, 2014). In the *M. xanthus* genome seven ATP-dependent proteases are encoded: three Clp proteases (two ClpP (*mxan_2014* and *mxan_6438*) and one ClpQ (*mxan3012*)) two FtsH proteases (*mxan4333* and *mxan4359*) and two Lon proteases (*mxan2017* and *mxan3993*)) (Konovalova, 2010). Whereas attempts to insert mutations in one of the three *clp* genes failed suggesting that these genes are essential (Konovalova, 2010), the deletion of *ftsH*$^{D}$ did not result in a developmental defect (M. Polatynska, personal communication/Figure 26). LonV was shown to be essential for growth (Tojo *et al.*, 1993a) and LonD (also known as BsgA) to be important for development (Tojo *et al.*, 1993b). Decreasing FtsZ levels during development in the absence of FtsH$^{D}$ indicated that this protease is not involved in FtsZ degradation (Figure 26). Interestingly, the absence of LonD led to a stabilization of FtsZ, PomX, PomY and PomZ levels during starvation (Figure 27). Furthermore, we could show, that in the absence of LonD FtsZ half-life increases remarkably under vegetative and starving conditions to more than 500 minutes (Figure 28). Although we could not observe a direct degradation *in vitro* (Figure 29), these results suggested that LonD is involved in FtsZ turnover during vegetative growth and development.

*M. xanthus* accumulates polyphosphate early during development and a mutation in the gene encoding polyphosphate kinase-1, which synthesizes polyphosphate reversibly from ATP, causes a developmental defect (Zhang *et al.*, 2005). Lon proteases were shown to be stimulated by polyphosphate (Kuroda *et al.*, 2006) but the addition of this compound did not lead to FtsZ degradation by LonD. Furthermore, we could not observe any FtsZ degradation by LonD in the presence of the starvation signal ppGpp which is essential for the stringent response and fruiting body formation (Manoil & Kaiser, 1980b). Although we could not show a direct degradation of FtsZ by LonD *in vitro*, there are a variety of possibilities how LonD could be involved in FtsZ degradation. One idea would be that an unknown adaptor protein needs to target FtsZ to LonD. Such an adaptor protein for LonD was identified recently in *B. subtilis*

(Mukherjee *et al.*, 2015). One more idea would be, that LonD could be a regulator of Z-ring dynamics during vegetative growth, as shown for the ClpXP protease in *E. coli* (Viola *et al.*, 2017). Furthermore, LonD was shown to be involved in regulating the transcription of genes important for development earlier (Kroos & Kaiser, 1987). However, the absence of *lonD* did not change the transcriptional downregulation of *ftsZ*, *pomX*, *pomY* or *pomZ* during starvation (Figure 30), leading to the conclusion that this protease is not involved in the transcriptional control of these genes. Furthermore it is important to keep in mind that mutations in *lonD* lead to an early developmental defect, since these mutants are affected in aggregation phase and are not able to sporulate (Tojo *et al.*, 1993b). Due to the impaired developmental program, the signals which lead to decrease of FtsZ and PomX, PomY and PomZ might be impaired as well. So, the absence of *lonD* might lead to a number of downstream effects which subsequently influence the accumulation of the proteins important for cell division.

Taken together, FtsZ (and PomX, PomY and PomZ) is constitutively degraded during vegetative growth and during development. Upon starvation, the protein is additionally controlled by transcriptional downregulation leading to decreasing protein levels. We cannot exclude, that regulation also occurs on the level of translation. However, since we observed decreasing mRNA levels, we assume that this is the main factor regulating protein synthesis. Although we did not determine the half-lives of one of the Pom proteins reliably, preliminary results suggest that the decrease of the protein levels is regulated similar to FtsZ levels. We predicted that transcriptional downregulation is the event leading to decreasing FtsZ levels. To test this prediction we bypassed the transcriptional downregulation by constitutively expressing *ftsZ*. This resulted in a stabilization of FtsZ levels during starvation (Figure 22) and confirmed our prediction.

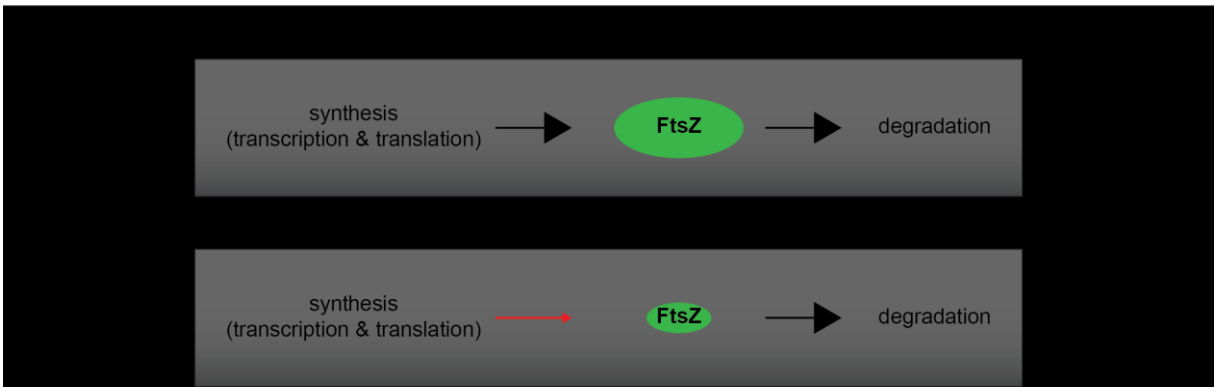


**Figure 37: FtsZ degradation outperforms FtsZ synthesis during development**
Proposed mechanism which leads to decreasing FtsZ protein levels during development. FtsZ is constitutively degraded during vegetative growth and development. Upon starvation, *ftsZ* transcription is downregulated (represented by small, red arrow) leading to elimination of FtsZ in developing cells.

Transcriptional control of *ftsZ* particularly during sporulation was reported earlier. Endosporulation of *B. subtilis* and also sporulation of *S. coelicolor* depend on a cell division event accompanied by an increase of FtsZ levels (Carniol *et al.*, 2005, Schwedock *et al.*, 1997). In both organisms, *ftsZ* transcription is controlled by three individual promoters, whereas one of them is specifically upregulated during sporulation (Flärdh *et al.*, 2000, Gonzy-Treboul *et al.*, 1992). However, the need for FtsZ presence is opposite to *M. xanthus* sporulation, since myxospores are formed independent of a septation event (Munoz-Dorado *et al.*, 2016). Generally, *ftsZ* transcription is very complex and driven by multiple promoters and regulators in various organisms (Francis *et al.*, 2000, Flärdh *et al.*, 1997, Dewar & Dorazi, 2000, Letek *et al.*, 2007, Roy & Ajitkumar, 2005). The analysis of the *ftsZ* promoter, e.g. by reporter gene fusions or mutational analysis might supply more insights into the transcriptional control of this gene during development. However, our attempts to identify the transcriptional start site of *ftsZ* in *M. xanthus* were not successful.

The combination of regulated transcription and constitutive proteolysis is a known mechanism used also by *B. subtilis* to ensure coupling between the cell cycle and initiation of sporulation by the protein Sda. Sda binds and inhibits the histidine protein kinase KinA (Burkholder *et al.*, 2001) which in turn phosphorylates the master regulator of sporulation, the response regulator Spo0A. Accumulation of Sda results in reduced levels of phosphorylated Spo0A which leads to a block in sporulation initiation. The *sda* gene is transcribed in a cell cycle dependent manner and activated by DnaA at the onset of replication (Veening *et al.*, 2009). Furthermore Sda is constantly degraded by the ATP-dependent protease ClpXP (Ruvolo *et al.*, 2006). Thus regulated transcription together with constitutive proteolysis ensures coupling between chromosome status and initiation of sporulation. One more example showing that degradation of a key protein coordinating the cell cycle outpaces synthesis was reported in *C. crescentus*. However, not transcriptional regulation but post-transcriptional control was shown to determine protein levels. The rate of DnaA degradation is not significantly altered by changes in nutrient availability but *dnaA* translation is downregulated which leads to a decrease in protein level. The 5´untranslated leader region of the *dnaA* transcript was reported to be important for the downregulation (Leslie *et al.*, 2015).

## 7.3. Cell cycle modification during *M. xanthus* development: Inhibition of cell division guarantees formation of spores containing two chromosomes

FtsZ is the main cell division protein and is responsible to initiate the assembly of the remaining divisome components (Adams & Errington, 2009, Goehring & Beckwith, 2005). The absence of FtsZ leads to cell division defects. Rod-shaped bacteria produce long, filamentous cells due to continuous growth of cells that are no longer dividing (Dai & Lutkenhaus, 1991, Treuner-Lange *et al.*, 2013). In conclusion, the absence of FtsZ leads to a defect in cell division.

Our results indicate that FtsZ levels are decreasing in cells dedicated to become spores due to a combination of transcriptional downregulation and constitutive proteolysis. Constitutive *ftsZ* expression led to stabilization of FtsZ levels during development (Figure 22). Interestingly, the stabilization of FtsZ did not interfere with the sporulation process itself, but with the chromosome content of mature myxospores. This led to the conclusion that cell division inhibition caused by decreasing FtsZ levels is sufficient to guarantee the formation of diploid spores but is not essential for the developmental program itself.

In well studied sporulating organisms, the chromosome number in spores is strictly organized due to modifications of the cell cycle. In *B. subtilis* this is regulated by at least three proteins: SirA, Sda and SpoOA~P. They coordinate sporulation and replication to ensure the presence of two chromosomes at the onset of sporulation (Rahn-Lee *et al.*, 2011, Boonstra *et al.*, 2013). RacA is the protein which anchors the two chromosomes to the cell poles, responsible for the correct organization of the nucleoid before sporulation (Ben-Yehuda *et al.*, 2003, Wu & Errington, 2003). In *S. coelicolor* a high level of chromosome replication leads to a multigenomic aerial hyphae (Ruban-Osmialowska *et al.*, 2006). The chromosomes are segregated by ParA and ParB (Kim *et al.*, 2000, Jakimowicz *et al.*, 2007). In both organisms, an essential cell division event follows, which leads to the formation of haploid spores. Interfering with one of these processes leads to sporulation defects (Piggot & Hilbert, 2004, Flärdh & Buttner, 2009). Hence, coordination of replication, segregation and cell division and the correct chromosome number are essential for spore formation.

In comparison, for the *M. xanthus* sporulation process replication was shown to be essential as well (Tzeng *et al.*, 2006). A checkpoint was proposed which couples DNA replication to continuation of the developmental program which goes along with the idea that cells do not have to have two chromosomes at the onset of development (Rosario & Singer, 2007). How this checkpoint would ensure coordination of DNA replication and progression of development is very speculative. One might think of a transcriptional regulation of downstream development genes by DnaA, since *dnaA* mRNA levels were shown to peak upon starvation (Rosario & Singer, 2010). DnaA does not just bind to DnaA - boxes at the origin of replication to initiate chromosome duplication (Messer, 2002) but is also an important transcription factor as shown for *E. coli* (Messer & Weigel, 1997).

In case of chromosome organization during myxospore formation no conclusive data are available. It was proposed that the origin of replication and the terminus region are associated with the peripheral regions of the myxospore and apparently in close proximity (Tzeng & Singer, 2005). However, our microscopy data did not conclusively support these observations, since the clusters representing the origin or terminus regions are not always found in the peripheral regions (see Figure 13B/C). Presumably, the chromosomes do not need a certain

organization during the rearrangement of the cell envelope but are “squeezed” in the shrinking spore. However, during germination the organization of the nucleoid might have an important role, which would need further investigation.

Moreover, our results indicated that inhibition of cell division is not essential for *M. xanthu*s to continue the developmental program. Even if inhibition of cell division was overrode by stabilization of FtsZ levels, sporulation was not affected. The only observed difference, while FtsZ levels were stabilized was a changed chromosome content in spores. Thus, sporulation is independent of the chromosome content. Accordingly, even if there is a checkpoint which couples one round of replication to sporulation (Rosario & Singer, 2007), there seems to be no checkpoint which ensures chromosome integrity.

Stabilization of FtsZ levels could lead to the following scenario: Upon starvation, cells undergo replication leading to two chromosomes in cells dedicated to become spores. When replication is finished FtsZ is still available in future spores, which gives the chance to initiate cell division and results in two cells having each one chromosome. These cells will differentiate into spores, although no two fully duplicated genomes are present. Thus, spores containing one chromosome are formed. This scenario would not include spores that are having one to two chromosomes whose formation cannot be excluded based on our analysis (Figure 24/Figure 25). One might speculate that cells in all stages of the cell cycle enter the developmental program. This might lead to the production of spores containing one to two chromosomes, but only if after “artificially induced” cell division replication is newly initiated. In order to clarify this, we need to improve our data regarding replication and chromosome content early during development to investigate the timing of replication upon starvation in more detail as discussed before. Furthermore, it would be interesting to investigate germination of spores formed while FtsZ levels are stabilized. Do haploid myxospores have a disadvantage during germination? What happens if they are treated for example with UV-light to induce DNA damage? These are interesting questions which will need further investigation to be answered and might give ideas about the advantages of diploid spores.

## 7.4. Cell fate determines cell cycle control

Our results indicated a control of FtsZ (and PomX, PomY, PomZ) levels by constant degradation in concert with transcriptional downregulation upon starvation. If cell division is specifically inhibited in cells dedicated to become spores, we hypothesize that the key players of cell division are actively regulated due to distinct cell fate. In line with this, we observed decreasing protein levels of FtsZ, PomX, PomY and PomZ specifically in future myxospores (Figure 17), which suggests a distinct control of cell cycle events in both cell populations. This is also supported by the different chromosome content and replication occurrence in mature spores and peripheral rods.

This principle is well known in the asymmetric dividing organism *C. crescentus*. Whereas the replicative stalked cell is able to enter the division cycle right away, the swarmer cell has to differentiate into a stalked cell before. The master regulator CtrA is responsible for cell fate determination. CtrA accumulates in swarmer cells, where it binds to the origin of replication to silence replication initiation (Radhakrishnan *et al.*, 2008) and controls, among others, genes involved in chromosome replication and cell division (Laub *et al.*, 2002). One example is *ftsZ* which is repressed in swarmer cells leading to the specific accumulation in stalked cells (Kelly *et al.*, 1998). DnaA, the replication initiator protein and important transcription factor is preferentially degraded in swarmer and stabilized in stalked cells (Grünenfelder *et al.*, 2001). Also divisome components including FtsZ are degraded due to cell fate by regulated protease activity (Williams *et al.*, 2014). In turn, CtrA demonstrates dimorphic synthesis and proteolysis as well (Domian *et al.*, 1997). In *B. subtilis* sporulation is coordinated by a number of σ factors which regulate gene expression specifically due to cell fate in the mother cell and prespore (Piggot & Hilbert, 2004).

In case of *M. xanthus*, we hypothesize that the transcriptional downregulation that we observe for *ftsZ*, *pomX*, *pomY* and *pomZ* is restricted to future spores leading to decreasing protein levels specifically in those cells. This idea would also include the possibility of a transcriptional regulator which coordinates *ftsZ* (*pomX*, *pomY*, *pomZ*) expression specifically in sporulating cells. Indeed, it was shown before, that peripheral rods and sporulating cells display different gene expression profiles (Julien *et al.*, 2000). There are a number of transcriptional regulators as well as σ factors known which are important for the developmental program of *M. xanthus* (Kroos, 2007, Kroos, 2017). The transcriptional regulators FruA and MrpC were shown to accumulate specifically in sporulating cells (Lee *et al.*, 2012) and are able to bind cooperatively to regulate gene expression. (Mittal & Kroos, 2009). However, a recent publication identifying potential MrpC binding sites could not identify target sites in the promoter regions of *pomXY* or *ftsZ*. For *pomZ* a putative binding site was found (Robinson *et al.*, 2014). Up to now, we do not have any experimental data which would support the idea of cell fate specific transcriptional regulation of *ftsZ*, *pomX*, *pomY* and *pomZ*. In order to test this possibility, we will need to determine the number of transcripts specifically in future spores and future peripheral rods in a future experiment. As discussed before, the determination of the transcriptional start site of *ftsZ* would help to unveil the transcriptional regulation. Attempts to identify this site were not successful.

In concert with cell division, replication is a cell cycle process which underlies a cell fate specific control. It was shown that replication is essential for sporulation (Rosario & Singer, 2007). Although we could not detect any differences in replication in future spores and peripheral rods after 24 h of starvation (6.3.2), the different chromosome content in mature spores and peripheral rods suggests a cell fate specific control which might occur later during

development. Maybe, the expression peak which was observed for *dnaA* (Rosario & Singer, 2010) is restricted to future spores, causing an initiation of replication, whereas replication is not specifically initiated in peripheral rods. This would ensure, in combination with inhibition of cell division, the formation of diploid myxospores. One more possibility would be that *dnaA* expression peaks in both cell fates, accompanied by initiation of replication and the distinct cell cycle control occurs later on the level of cell division. Whereas the cell cycle "stops" in future spores after chromosome duplication, the cell cycle might progress in peripheral rods. Chromosome duplication and segregation might be unaffected and be followed by a cell division event, indicated by FtsZ accumulation in peripheral rods (Figure 17). This would lead to a population of cells in all stages of the cell cycle (Figure 38). However, if peripheral rods indeed undergo cell division is not clear. Although the timing remains unclear, a distinct regulation is very likely. This is supported by the fact, that we visualized ongoing replication in peripheral rods, whereas no active replication was visible in mature spores (Figure 15).

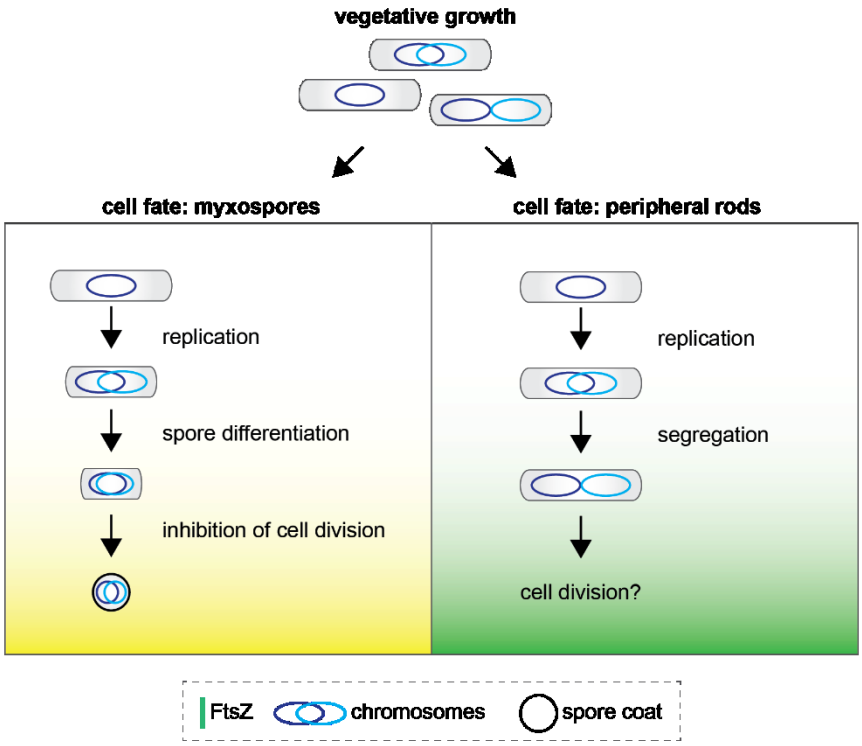


**Figure 38: Distinct cell cycle regulation in future spores and future peripheral rods**
Model of distinct cell cycle progression in cells dedicated to become myxospores or peripheral rods. Upon starvation, cells in all stages of the cell cycle will enter the developmental program. After replication, which ensures the presence of two chromosomes, cell division is inhibited in cells dedicated to become spores. This results in the formation of diploid myxospores. Future peripheral rods undergo replication, probably followed by segregation. If peripheral rods undergo cell division is not clear.

However, to explore timing of replication in different cell fates formed during starvation in more detail, more experiments need to be performed. Nonetheless, the distinct control of the cell

cycle seems to be a mechanism which is part of cell fate determination during the developmental program of *M. xanthus*.

## 7.5. Number of chromosomes correlates with spore morphology

Stabilization of FtsZ protein levels led to the formation of an increased number of spores containing less than two chromosomes. These spores appeared to have a size and morphology comparable to WT spores (Figure 32). Interestingly we noticed that cells which were elongated during vegetative growth due to the absence of one of the Pom proteins (Figure 33), low FtsZ levels or complete FtsZ depletion (Figure 32) formed spores that were increased in average spore size. This was accompanied by increased chromosome content (Figure 33/Figure 23). Together with spores formed while FtsZ protein levels were stabilized, this was a hint, that sporulation is independent of chromosome content and suggests once more the absence of a checkpoint ensuring chromosome integrity as discussed in 7.3.

Cells which are increased in chromosome content during vegetative growth are accompanied by an increased cell length (Figure 23/Figure 33). Sporulation in *M. xanthus* happens by rearrangement of the rod-shaped cell into an spherical spore while cells simultaneously widen as they shorten and the surface area of the cell continuously decreases, which excludes rod-to-sphere morphogenesis to be simply a matter of degradation of the rod-shaped determining peptidoglycan sacculus (Higgs, 2014). The cell cytoskeletal protein MreB is involved in this process (Müller *et al.*, 2012), maybe by guiding penicillin binding proteins or lytic enzymes (Higgs, 2014). Thus, elongated cells might be limited in their ability to shrink into a spherical spore, due to physical reasons. The increased chromosome content probably contributes to this phenomenon. One might imagine that four chromosomes need more space than two chromosomes, resulting in an increased spore size. The correlation between size and chromosome organization or number in spores was reported earlier.

In *S. coelicolor*, SepG is involved in maintaining spore shape. The localization of SsgB, the protein recruiting FtsZ to cell division sites, depends on SepG. The protein itself localizes in a ring at the periphery of the spores thereby surrounding the nucleoids in WT cells. In the absence of SepG, large doughnut-shaped nucleoids are formed accompanied by thinner spore walls which are reduced in heat-resistance. It was proposed that the expanded nucleoids enforce the formation of larger spores (Zhang *et al.*, 2016). In *B. subtilis*, the absence of Sda leads to cells that overreplicate accompanied by polyploidy, leading to two or more chromosomes in the forespore compartment. Spores formed under this conditions are heterogenous in shape and coat morphology. However, time-lapse microscopy revealed, that spores unable to germinate were significantly larger than successful germinating spores. It was suggested, that spores containing more than one chromosome are larger and reduced in spore viability (Veening *et al.*, 2009).

Neither chromosome replication nor segregation is affected in the absence of one of the Pom proteins (Schumacher *et al.*, 2017, Treuner-Lange *et al.*, 2013). Also depletion of FtsZ seems to not affect chromosome replication or segregation, suggested by chromosome arrangement in DAPI stained cells (Schumacher, 2016). This implies that Δ*pom* or cells depleted for FtsZ could be able to pass the "replication checkpoint", which was discussed in 7.3, and proceed the developmental program. However, we noticed a reduced sporulation frequency of Δ*pom* or FtsZ depleted cells (Figure 18/Figure 19), suggesting that sporulation efficiency is affected or that the spores are impaired in heat and sonication resistance. Moreover, we do not know how spore morphology or increased chromosome content affects germination as also discussed for spores decreased in chromosome content (7.3). This will be interesting to be investigated in future studies.

## 7.6. The signal which leads to inhibition of cell division upon development remains unknown

The developmental program of *M. xanthus* depends on the (p)ppGpp synthase RelA which is essential to initiate the stringent response. In the absence of RelA, cells are blocked in development prior to aggregation (Harris *et al.*, 1998). RelA produces (p)ppGpp as a response to of uncharged tRNAs in the A-site of the ribosomes (Potrykus & Cashel, 2008). Important events during development which depend on RelA are for example A - signaling (Harris *et al.*, 1998) the expression peak of *dnaA* after 4 – 6 hours of starvation (Rosario & Singer, 2010) or PopC secretion in order to generate the C-signal (Konovalova *et al.*, 2012). Surprisingly, our data suggest that the decrease of FtsZ protein levels and *ftsZ* transcripts during starvation does not depend on RelA (Figure 35). One more signaling molecule which was shown to be important for *M. xanthus* development (Skotnicka *et al.*, 2016) and cell cycle control in various organisms (Collier, 2016, Pesavento & Hengge, 2009) is c-di-GMP. However, in the absence of the diguanylate cyclase DmxB which is responsible for the elevated global pool of c-di-GMP during starvation (Skotnicka *et al.*, 2016) FtsZ protein levels as well as number of *ftsZ* transcripts decreased (Figure 36). This suggests, that the elevated global pool of c-di-GMP is not responsible for inhibition of cell division during development. However, we showed that FtsZ decrease is specific to starvation and not an answer to poor growth conditions (Figure 34). This implies a development specific signal which leads to cell cycle modification. Since we observed decreasing FtsZ levels already after 3 h after initiation of starvation (Figure 16/Figure 17) this signal operates probably quite early during development. Candidates to be tested could be known developmental regulators or signaling pathways. Examples would be FruA, MrpC or A-signaling. However, until now, the signal inducing decrease of FtsZ protein levels and inhibition of cell division remains unknown.

# 8. Conclusion and future perspectives

This work focused on elucidating replication and cell division during development of *M. xanthus*. By investigating accumulation, synthesis and degradation of the cell division protein FtsZ (and its regulators PomX, PomY and PomZ) we concluded that FtsZ degradation outperforms FtsZ synthesis during starvation leading to elimination of FtsZ and inhibition of cell division which guarantees the formation of diploid myxospores. Interestingly, sporulation did not depend on chromosome content, but cell morphology and chromosome content during vegetative growth led to formation of spores increased in average size and chromosome content.

Although the mechanism leading to inhibition of cell division was identified during this study, there are still interesting questions which remain unanswered. Whereas mature spores were shown to contain two chromosomes, peripheral rods are a population of cells in all stages of the cell cycle that are able to actively replicate their genome. The distinct control of the cell cycle might be a feature which determines cell fate. However, the timing of the distinct control remains unclear. Analyzing the number of *ftsZ* transcripts or analysis of replication control in both cell populations might give more insights. Moreover it would be interesting to check if peripheral rods are indeed able to undergo complete rounds of the cell cycle, for example by following localization of FtsZ over time in these cells. Are they able to mark the incipient constriction site and to divide? Following FtsZ localization at earlier time points during starvation would give insights into the distinct control of cell division in both cell fates. Since transcriptional downregulation was shown to be the main factor leading to decreasing FtsZ levels it would be interesting to map the promoter region and identify possible transcriptional regulators which ensure this regulation. LonD is most likely indirectly involved in FtsZ degradation. How LonD is connected to FtsZ is still unclear. Maybe, an adaptor protein that targets FtsZ to LonD is involved. Since FtsZ half-life increases not just during development but also during vegetative growth in the absence of LonD, the protease might be involved in regulating Z-ring dynamics as well. Preliminary results suggest that the protein levels of the cell division regulators PomX, PomY and PomZ are regulated in the same way as FtsZ level. However, more reliable experiments need to be performed to show this. One more interesting and still unanswered question is: What is the advantage of diploid spores? Analysis of germination or the resistance to harsh environmental conditions of spores altered in number of chromosomes could give insights into this topic. Last but not least, the signal which leads to decreasing FtsZ protein levels is still unknown and would need more investigation to be identified. Good candidates could be players which are involved in early development regulation or signaling.

# 9. Material and Methods

## 9.1. Chemicals, equipment and software

All reagents, enzymes, kits and antibiotics (Table 1), equipment (Table 2) and software (Table 3) used in this study including their suppliers or manufacturers are listed.

**Table 1: Reagents, enzyme, kits and antibiotics used in this study**

| Reagent | Supplier |
|---|---|
| Chemicals | Carl Roth GmbH u. Co KG (Karlsruhe)<br>Millipore Merck Chemicals GmbH (Schwalbach)<br>Sigma-Aldrich (Taufkirchen)<br>Roche (Mannheim)<br>TriLink Biotechnology (San Diego, USA) |
| Media components, agar | Carl Roth GmbH u. Co KG (Karlsruhe)<br>Millipore Merck Chemicals GmbH (Schwalbach)<br>BD Difco (Heidelberg)<br>Invitrogen™ life technologies (Karlsruhe) |
| Oligonucleotides | Eurofins MWG Operon (Ebersberg)<br>Invitrogen™ life technologies (Karlsruhe) |
| 2-log DNA ladder | New England Biolabs (Frankfurt a. M.) |
| Rabbit antisera | Eurogentec (Seraing, Belgium) |
| Goat anti-rabbit IgG | Pierce™ Thermo Scientific™ (Darmstadt) |
| Luminata Western HRP substrate | Merck Millipore (Darmstadt) |
| Page Ruler Plus Prestained Protein Ladder | Pierce™ Thermo Scientific™ (Darmstadt) |
| Restore™ Western Blot Stripping Buffer | Pierce™ Thermo Scientific™ (Darmstadt) |
| **Enzymes** | |
| Phusion High Fidelity DNA Polymerase | Pierce™ Thermo Scientific™ (Darmstadt) |
| Antarctic Phosphatase | New England Biolabs (Frankfurt a. M.) |
| T4 DNA Ligase | New England Biolabs (Frankfurt a. M.) |
| Restriction endonucleases | New England Biolabs (Frankfurt a. M.) |
| 5´PRIME Mastermix | 5 PRIME GmbH Hamburg |
| *Taq* 2X Master Mix | New England Biolabs (Frankfurt a. M.) |
| Quick-Load® *Taq* 2X Master Mix | New England Biolabs (Frankfurt a. M.) |
| Power SYBR™ Green Master Mix | Applied Biosystems (Darmstadt) |
| Turbo™ Dnase | Ambion™ Thermo Scientific™ (Darmstadt) |

| **Kits** | |
|---|---|
| MasterPure DNA purification kit | Epicentre Biotechnologies (Wisconsin, USA) |
| NucleoSpin® Gel and PCR Clean-up kit | Macherey & Nagel (Düren) |
| NucleoSpin® Plasmid kit | Macherey & Nagel (Düren) |
| HighCapacity cDNA Reverse Transcription Kit | Applied Biosystems (Darmstadt) |
| NucleoSpin® RNA Plus | Macherey & Nagel (Düren) |
| Click-iT® EdU Alexa Fluor® 594 Imaging Kit | Molecular Probes™ Thermo Scientific™ (Darmstadt) |
| Vybrant® DyeCycle™ Orange Stain | Molecular Probes™ (Darmstadt) |
| **Antibiotics** | |
| Kanamycin sulfate<br>Oxytetracyclin dehydrate<br>Tetracyclin hydrocloride<br>Chloramphenicol<br>Streptomycin sulfate<br>Gentamycin sulfate | Carl Roth GmbH u. Co KG (Karlsruhe) |

**Table 2: Equipment used in this study**

| **Device** | **Application** | **Manufacturer** |
|---|---|---|
| Branson sonifier | Cell disruption | Heinemann (Schwäbisch Gmünd) |
| Master Cycler personal<br>Master Cycler epigradient | Polymerase Chain Reaction | Eppendorf (Hamburg) |
| Thermomixer Compact<br>Thermomixer Comfort | Incubation of small reaction volumes | Eppendorf (Hamburg) |
| GenePulser Xcell | Electroporation of bacterial cells | Bio-Rad (München) |
| Mini-PROTEAN® 3 cell<br>Mini-PROTEAN® TetraCell | Protein gel electrophoresis | Bio-Rad (München) |
| Fuji Photo Film FPM 100A<br>Luminescent image analyser LAS-400 | Chemiluminescent detection | Fujifilm (Düsselforf) |
| Ultrospec 2100 pro<br>Spectrophotometer | Determination of optical densities | GE Healthcare Europe GmbH (Freiburg) |
| Nanodrop ND-1000 UV-Vis spectrophotometer | Nucleic acid quantification | Nanodrop (Wilmington) |

| | | |
|---|---|---|
| TransBlot® TurboTM Transfer System | Western blotting | Bio-Rad (München) |
| Eppendorf Centrifuge 5424<br>Eppendorf Centrifuge 5424 R | Centrifugation of small reaction volumes | Eppendorf (Hamburg) |
| Thermo Scientific Heraeus Multifuge | Centrifugation 15 ml and 50 ml Falcon tubes | Pierce™ Thermo Scientific™ (Darmstadt) |
| E-BOX VX2 imaging system | Illumination of DNA in agarose gels | PeqLab (Erlangen) |
| DMI6000B microscope with adaptive focus control (AFC), temperature control and Hamamatsu Flash 4.0 camera | Fluorescence microscopy | Leica (Wetzlar) |
| MZ8 stereomicroscope with DFC320 camera | Following and documentation of development phenotypes on solid media | Leica (Wetzlar) |
| DMIRE2 microscope with DFC280 CCD camera | Following and documentation of development phenotypes in submerged culture | Leica (Wetzlar) |
| 7500 Real Time PCR system | qRT PCR | Applied Biosystems (Darmstadt) |
| BD LSR Fortessa | Flow cytometry | Becton Dickinson GmbH (Heidelberg) |
| FastPrep-24 | Dispersal of cell aggregates | MP Biomedicals (Eschwege) |

**Table 3: Software used in this study**

| **Software** | **Application** | **Supplier** |
|---|---|---|
| Vector NTI advance software, suite 11 | Checking of DNA and protein sequences, *in silico* cloning of plasmids, sequence alignments | Invitrogen™ life technologies (Karlsruhe) |
| DNASTAR | Checking of DNA and protein sequences, *in silico* cloning of plasmids, sequence alignments | DNASTAR (Madison, Wisconsin, USA) |

| | | |
|---|---|---|
| Metamorph® v 7.5 | Data analysis of microscopy pictures | Molecular Devices (Union City, CA) |
| Leica MM AF | Image Acquisition and data analysis of microscopy pictures | Leica (Wetzlar) |
| ImageJ | Quantification of Western Blots | National Institutes of Health (Bethesda, Maryland, USA) |
| 7500 Software v2.3 | Acquisition and analysis of qRT PCR data | Applied Biosystems (Darmstadt) |
| BD FACSDiv Software | Flow cytometry Data aquisition | Becton Dickinson GmbH (Heidelberg) |
| FlowJo | Flow cytometry data analysis | FlowJo, LLC (Ashland, USA) |

## 9.2. Media

*E. coli* cells were cultivated in Luria-Bertani (LB) liquid medium or on LB agar plates including 1.5% agar. *M. xanthus* cells were cultivated in 1% CTT media or on 1% CTT agar plates including 1.5% agar. Media compositions are described in Table 4. Appropriate antibiotics or additives were added to cultures when needed and are listed in Table 5.

**Table 4: Media used to cultivate *E. coli* and *M. xanthus***

| **Media** | **Composition** |
|---|---|
| ***E. coli*** | |
| LB (Luria-Bertani) medium | 1% (w/v) tryptone<br>0.5% (w/v) yeast extract<br>1% (w/v) NaCl |
| LB agar plates | LB medium<br>1.5% (w/v) agar |
| ***M. xanthus*** | |
| 1% CTT | 1% (w/v) Bacto TM casitone<br>10 mM Tris-HCl pH 8.0<br>1 mM $KH_2PO_4$ pH 7.6<br>8 mM $MgSO_4$ |
| 1% CTT agar plates | 1% CTT medium<br>1.5% (w/v) agar |

**Table 5: Media additives and their concentrations**

| Additive | dissolved in | final concentration |
|---|---|---|
| ***E. coli*** | | |
| Kanamycin sulfate | $H_2O$ | 50 µg/ml |
| Tetracyclin hydrochloride | 99.99% EtOH | 15 µg/ml |
| ***M. xanthus*** | | |
| Kanamycin sulfate | $H_2O$ | 50 µg/ml |
| Oxytetracycline dehydrate | 100mM HCl | 10 µg/ml |
| Chloramphenicol | 99.99% EtOH | 25 µg/ml |
| Gentamycin sulfate | $H_2O$ | 10 µg/ml |
| Streptomycin sulfate | $H_2O$ | 20 µg/ml |
| $CuSO^4$ | $H_2O$ | 150 µM |
| Vanillate | $H_2O$, pH 7.6 (adjusted with KOH) | 10-500 µM |
| Galactose | $H_2O$ | 2-3% (w/v) |

To starve *M. xanthus* strains in development assays, TPM agar plates and MC7 buffer were used. Media compositions are listed in Table 6.

**Table 6: Media used for development assays**

| Media | Composition |
|---|---|
| TPM buffer | 10 mM Tris-HCl pH=7.6<br>1 mM $KH_2PO_4$ pH 7.6<br>8 mM $MgSO_4$ |
| TPM plates | TPM buffer<br>1.5% (w/v) agar |
| MC7 buffer | 10 mM MOPS pH 7.0<br>1 mM $CaCl_2$ |

## 9.3. Microbiological methods

### 9.3.1. *E. coli* strains used in this study

**Table 7: *E coli* strains used in this study**

| Strain | Genotype | Reference |
|---|---|---|
| TOP10 | F- *mcr*A Δ(*mrr-hsdRMS-mcrBC*) Φ80*lacZ*ΔM15 Δ*lac*X74 *rec*A1 *ara*D139 Δ(*ara leu*) 7697 *gal*U *gal*K *rps*L (Str$^R$) *end*A1 *nup*G | Invitrogen$^{TM}$ life technologies (Karlsruhe) |
| NEB Turbo | F- *proA+B+ lacIq ΔlacZM15 / fhuA2 Δ(lac-proAB) glnV galK16 galE15 R(zgb-210::Tn10)*TetS *endA1 thi-1 Δ(hsdS-mcrB)5* | New England Biolabs (Frankfurt a. M.) |

### 9.3.2. *M. xanthus* strains used in this study

All *M. xanthus* strains used in this study are listed in Table 1. Km$^R$, Tc$^R$ and Strep$^R$ indicate kanamycin, tetracycline and streptomycin resistance, respectively. Δ indicates that a strain contains an in-frame deletion of the corresponding gene. How gene deletions are obtained is described in 9.4.3. Fusions integrated in the native or *attB* site or in the *mxan0018-0019* intergenic region are expressed from the native promoter ($P_{nat}$) or the vanillate-dependent promoter ($P_{van}$). Plasmids containing fusions expressed via the *cuoA* promoter ($P_{cuoA}$) were integrated into the $P_{cuoA}$. A "+" indicates that a strain contains a native copy of the corresponding gene.

**Table 8: *M. xanthus* strains used in this study**

| Strain | Genotype | Reference |
|---|---|---|
| DK1622 | Wild type | (Kaiser, 1979) |
| DK11063 | *fruA*::Tn5 lacΩ7540; Km$^R$ | (Sogaard-Andersen *et al.*, 1996) |
| SA4223 | Δ*pomX* | (Schumacher *et al.*, 2017) |
| SA4703 | Δ*pomY* | (Schumacher *et al.*, 2017) |
| SA3108 | Δ*pomZ* | (Treuner-Lange *et al.*, 2013) |
| SA6343 | Δ*ftsH$^D$* | M. Polatynska (MPI Marburg) |
| SA6273 | Δ*lonD* | M. Polatynska (MPI Marburg) |
| SA5605 | Δ*dmxB* | (Skotnicka *et al.*, 2015) |
| SA5831 | *ssb$^+$*/ $P_{nat}$ *ssB::*$P_{nat}$ *ssb-eYFP*, Km$^R$ | A. Harms (MPI Marburg) |

| | | |
|---|---|---|
| SA4194 | *mxan4000::tetO*-array/ *mxan18-19::*$P_{van}$ *tetR-eYFP*, $Km^R$, $Tc^R$ | A. Treuner-Lange (MPI-Marburg |
| SA6755 | Δ*ftsZ/ mxan18-19::*$P_{van}$ *ftsZ,* $Tc^R$ | A. Treuner-Lange (MPI-Marburg |
| SA6143 | *mxan 0733::tetO*-array/ *mxan18-19*::$P_{van}$ *tetR-eYFP* , $Km^R$, $Tc^R$ | This study |
| SA6144 | *mxan18-19::*$P_{van}$ *parB-eYFP*, $Tc^R$ | This study |
| SA6166 | *mxan18-19*::$P_{van}$ *eYFP*, $Tc^R$ | This study |
| SA6182 | *mxan4000::tetO*-array/ *mxan18-19*::$P_{van}$ *tetR-eYFP*, $P_{cuoA}$::$P_{cuoA}$ *parB-mCerulean*, $Km^R$, $Tc^R$, $Strep^R$ | This study |
| SA6152 | Δ*ftsZ/ mxan18-19::*$P_{van}$ *ftsZ*/ $P_{cuoA}$::$P_{cuoA}$ *parB-eYFP*, $Tc^R$, $Km^R$ | This study |
| SA6158 | Δ*ftsZ/ mxan18-19::*$P_{van}$ *ftsZ*/ *mxan4000::tetO*-array/ $P_{cuoA}$::$P_{cuoA}$ *tetR-eYFP*, $Tc^R$, $Km^R$, $Strep^R$ | This study |
| SA6177 | Δ*pomY/ mxan18-19::*$P_{van}$ *parB-eYFP*, $Tc^R$ | This study |
| DK101 | Wild type | (Hodgkin & Kaiser, 1977) |
| MS1000 | Δ*relA* (in DK101 background) | (Diodati *et al.*, 2006) |

### 9.3.3. Cultivation of bacterial strains

All used media and solutions were autoclaved at 121°C for 20 min and 1 bar over pressure. Antibiotics and additives were filter sterilized by using 0.22µm pore-size filters (Millipore Merck, Schwalbach) and added to the pre-cooled media at around 55°C.

*E. coli* strains were used for cloning and for generating plasmids. *E. coli* cells were cultivated on LB agar plates at 37°C. Liquid cultures were inoculated from one single colony and incubated at 37°C and 230rpm horizontal shaking. Corresponding antibiotics were added. When necessary, growth was followed by monitoring the optical density at 600nm ($OD_{600}$). *M. xanthus* cells were cultivated on 1% CTT agar plates at 32°C in the dark. Liquid cultures were inoculated by harvesting the cells from plate, resuspending them in 1ml of 1% CTT and subsequently transferred to a bigger volume of media. Liquid cultures were grown in Erlenmeyer flasks in 1/10 of the total flask volume and incubated at 32°C with horizontal shaking at 230rpm. Optical density was monitored at 550nm ($OD_{550}$). Media used for cultivating *M. xanthus* contained 10µg/mL gentamycin to prohibit contamination and additional supplements were added when necessary.

### 9.3.4. Short- and long-term storage of bacterial strains

*E. coli* and *M. xanthus* cells on solid media were stored up to four weeks at 4°C and 18°C, respectively. For long-term storage, glycerol stocks were prepared. *E. coli* liquid cultures were grown overnight and 1mL was mixed with glycerol to a final concentration of 10% in cryo-tubes. *M. xanthus* cells were grown to an $OD_{550}$ 0.8-1.0 and mixed with glycerol to a final concentration of 10% in cryo-tubes. Cells were frozen in liquid nitrogen and stored at -80°C.

### 9.3.5. Development assay and spore assay for *M. xanthus*

*M. xanthus* ability to form fruiting bodies and to sporulate was examined by using two different methods: TPM starvation agar and submerged culture in MC7 buffer. The strains to be tested were grown to $OD_{550}$ 0.5 - 0.9 while keeping the cells constantly in exponential growth phase by diluting them regularly. The cells were harvested and resuspended in TPM or MC7 buffer to $OD_{550}$ 7. Cells resuspended in TPM buffer were spotted in 20 µl aliquots on TPM agar plates. For development phenotype in submerged culture, 50 µl of in MC7 buffer concentrated cells were diluted in 350 µl MC7 in 15 mm well in a microtiter dish. Cells were incubated at 32 °C in the dark and aggregation was followed for 120h using MZ8 stereomicroscope with DFC320 camera or DMIRE2 microscope with DFC280 CCD camera (Leica, Wetzlar).If total cells were planned to be analyzed subsequently by immunoblot analysis, the volume of the submerged culture was increased to a total volume of 16 ml in a petri dish with a diameter of 9 cm. In case lysates of aggregating and non-aggregating cells were analyzed separately, the total volume was increased to 34 ml in a petri dish with a diameter of 14 cm.

Sporulation frequency was determined by counting heat and sonication resistant spores which have been formed after 120h of starvation on TPM agar plates. Five 20 µl spots were scratched from plate, resuspended in 400 µl of TPM, incubated for 2h at 55°C and sonicated 2x, 30%, output 3 to disperse fruiting bodies and disrupt cells. Spores were counted in a counting chamber (Hawksley, depth 0.02 mm) and presented relatively to wild type spore frequency.

### 9.3.6. Separation between aggregating and non-aggregating cells during *M. xanthus* development

To separate distinct cell populations, we used a previously validated method (Lee *et al.*, 2011). Cells starved on TPM medium or in submerged culture with MC7 buffer were harvested at indicated time points. Subsequently samples were centrifuged for 5 min at 50 x g resulting in separation of cells in aggregates to the pellet and non-aggregating cells in the supernatant. The supernatant was removed carefully to not swirl up the pellet and separated cells were centrifuged with higher speed to concentrate cells in appropriate volumes. Depending on the following approach, samples were processed differently. In case of preparing cell lysates to

analyze the samples via immunoblotting, cells were resuspended in 1x SDS buffer and boiled for 10 min at 95 °C. Total protein amounts were determined (9.6.1) and samples were applied to immunoblot analysis (9.6.3). To investigate cells via fluorescence microscopy, aggregating and non-aggregating cells were dispersed by bead beating for 40 sec and 5 m/s before they were spotted on 1 % agarose pads buffered with TPM to image them at 32°C. In case of samples taken after 120h of starvation, the spore containing sample was sonicated 2 x, 30%, output 3, to make sure we imaged mature spores.

## 9.4. Molecular biology methods

### 9.4.1. Oligonucleotides and plasmids

All primers used in this study including their sequence are listed in Table 9. Forward (fwd) or reverse (rev) sequences are indicated. Blue sequences refer to recognition sites for restriction endonucleases, whereas red sequences indicate start and stop codons. Green sequences highlight additional nucleotides used as linker sequences.

**Table 9: List of primers used in this study**

| Name | description | Sequence: 5´-3´ |
|---|---|---|
| **Primers to clone pMAT112, expressing $P_{van}$ *tetR-eYFP*, Strep$^R$** | | |
| pIJ778 SacI down | | |
| pIJ778BglII PstI up | | |
| **Primers to clone pSH62, expressing $P_{van}$ *parB-eYFP*** | | |
| SH59 fwd | fwd, EcoRI | GCGGAATTCTCACTTGTACAGCTCGTC |
| SH60 rev | rev, NdeI | GCGCATATGGTGGTGAAAGCAGACATGC |
| **Primers to clone pSH65, expressing $P_{cuoA}$ *tetR-eYFP*, Strep$^R$** | | |
| SH74 | fwd, ClaI | GCGATCGATTTATTTGCCGACTACCTTGG |
| SH75 | rev, HindIII | GCGAAGCTTTGCAGTTCGAAGTTCCTATTC |
| **Primers to clone pSH66, expressing $P_{van}$ *eYFP*** | | |
| SH59 | fwd, EcoRI | GCGGAATTCTCACTTGTACAGCTCGTC |
| SH81 | rev, NdeI | CGCCATATGATGGTGAGCAAGGGCGAG |

| | | |
|---|---|---|
| **Primers to clone pSH74, expressing $P_{cuoA}$ *parB*-mCerulean** | | |
| Amplification of *parB* | | |
| SH134 | fwd, XbaI | GCGTCTAGAGTGGTGAAAGCAGACATGC |
| SH135 | rev, BamHI, linker | GCGGGATCCGCCGGCGCCCTCCTTCCTGAGAAGCTTC |
| Ampflication of mCerulean | | |
| SH136 | fwd, BamHI, linker | GCGGGATCCGCCGGCGCCGCGATGGTGAGCAAGGGCGAG |
| SH137 | stop codon, HindIII | GCGAAGCTTTCACTTGTACAGCTCGTCCATGCC |
| **Primers to check for Mx8 *attB* integration of plasmids** | | |
| attB left | | CGGCACACTGAGGCCACATC |
| attB right | | GGAATGATCGGACCAGCTGAA |
| attP left | | GGGAAGCTCTGGGTGACGAA |
| attP right | | GCTTTCGCGACATGGAGGA |
| **Primers to check for *mxan0018-0019* site integration of plasmids** | | |
| int18-19 C | fwd | CCCACGGAGAGCTGCGTGAC |
| int18-19 C | rev | GAGAAGGGTGCCGTCACGTC |
| int18-19 P | fwd | GGCAAGGCGACAAGGTGCTG |
| int18-19 P | rev | CCCTGGCCGCCATTCGTAAC |
| **Primers used for qRT-PCRs** | | |
| SH45 *ftsZ* | fwd | GTCACCAAGCCCTTCCTCT |
| SH46 *ftsZ* | rev | GCTTGAAGGTCTCCAGCAG |
| SH57 *pomX* | fwd | GAGAAGGCCACGGAAGAG |
| SH58 *pomX* | rev | GTCTCCTGGAGCGACAGC |
| SH47 *pomY* | fwd | GAGATGGAGCACCTCAAGC |
| SH48 *pomY* | rev | CAGCAGCTTGTCCATCATCT |
| SH49 *pomZ* | fwd | ACTATCCGGAGTTCCTGCTG |
| SH50 *pomZ* | rev | CAATCATGGCCTGGATGTC |
| **Primers to check for insertion of pNV3** | | |
| rodK up | fwd | AGGTCCGGGTCGTCGTCC |
| rodK down | rev | CAACTGGCGGAAACGCTG |
| M13 | fwd | CGCCAGGGTTTTCCCAGTCACGAC |
| M13 | rev | TAGCTCACTCATTAGGCACCCCAG |
| **Sequencing primers** | | |

| | | |
|---|---|---|
| KA231 | fwd, sequencing primer pSWU30 | GGATGTGCTGCAAGGCGATTAAGTTGG |
| KA232 | rev, sequencing primer pSWU30 | GCTTTACACTTTATGCTTCCGGCTCG |
| YFP fwd | fwd (binds inside *eYFP)* | GCAAAGACCCCAACGAGAAGCGCG |
| YFP rev | rev (binds inside *eYFP)* | GGACTTGAAGAAGTCGTGCTGCTT |
| pMR3691 rev | rev, sequencing primer pMR3691 | CGACGGCCAGTGAATGGC |
| $P_{van}$ fwd | fwd (binds inside $P_{van}$) | TGGACTCTAGCCGACCGACTGAGACGC |
| pSH65 rev | rev, sequencing primer pSH65 | GGAATCAATAAAGCCCTGCGCAGC |
| AHA couA fwd | fwd (binds inside $P_{cuoA}$) | ACGGAAATCGTCATGGCC |
| AH19 | fwd (binds inside *parB*) | GTCCTCAAGCTCCCCATC |

**Table 10: List of plasmids used in this study**

| Plasmid | Description | Reference |
|---|---|---|
| pSWU30 | Vector containing *Mx8 attP* fragment for integration into genomic *Mx8* attB site, $Tc^R$ | (Wu *et al.*, 1997) |
| pBJ114 | Vector containing $Km^R$ and *galK* gene, used for in-frame deletion of genes and native site integration of plasmid DNA | (Julien *et al.*, 2000) |
| pMR3691 | Vector for expression of genes under regulation of a vanillate-inducible promoter for integration into the *mxan0018-0019* intergenic region. $Tc^R$ | (Iniesta *et al.*, 2012) |
| mCerulean C1 (Addgene plasmid # 27796) | Plasmid used as a template to amplify mCerulean | (Koushik *et al.*, 2006) |
| pAH7 | Plasmid used as a template to amplify *parB-eYFP* | (Treuner-Lange *et al.*, 2013) |
| pAH73 | $P_{cuoA}$ *parB-eYFP*, integrates into *cuoA* locus, $Km^R$ | (Harms *et al.*, 2013) |
| pIJ778 | Plasmid used as a template to amplify the streptomycine resistance gene *aadA* | (Gust *et al.*, 2003) |

| | | |
|---|---|---|
| pMAT3 | pSWU30, $P_{cuoA}$, integration into genomic *Mx8* attB site, $Tc^R$ | (Gomez-Santos *et al.*, 2012) |
| pMAT6 | pMAT3, $P_{cuoA}$ *tetR-eYFP*, integration into genomic *Mx8* attB site, $Tc^R$ | (Harms *et al.*, 2013) |
| pMAT13 | pBJ114, *tetO*-array + fragment of *mxan4000* region (192°), integrates into endogenous region, $Km^R$ | (Harms *et al.*, 2013) |
| pMAT56 | pMR3691 with altered multiple cloning site, integrates into *mxan0018-0019* intergenic region, $Tc^R$ | (Schumacher *et al.*, 2017) |
| pMAT76 | pMAT56, $P_{van}$ *tetR-eYFP*, integrates into *mxan0018-0019* intergenic region, $Tc^R$ | (Schumacher *et al.*, 2017) |
| pMAT112 | pMAT76, $P_{van}$ *tetR-eYFP*, integrates into *mxan0018-0019* intergenic region, $Strep^R$ | (Schumacher *et al.*, 2017) |
| pNV3 | pBJ114, *tetO*-array + fragment of *mxan0733* region (33°), integrates into endogenous region, $Km^R$ | (Harms *et al.*, 2013) |
| pSH62 | pMR3691, $P_{van}$ *parB-eYFP*, integrates into *mxan0018-0019* intergenic region, $Tc^R$ | This study |
| pSH65 | pMAT6, $P_{cuoA}$ *tetR-eYFP*, integration into genomic *Mx8* attB site, $Strep^R$ | This study |
| pSH66 | pMR3691, $P_{van}$ *eYFP*, integrates into *mxan0018-0019* intergenic region, $Tc^R$ | This study |
| pSH73 | pMAT3, $P_{cuoA}$ *mCerulean*, integration into genomic *Mx8* attB site, $Tc^R$ | This study |
| pSH74 | pSH74, $P_{cuoA}$ *parB-mCerulean*, integration into genomic *Mx8* attB site, $Tc^R$ | This study |

### 9.4.2. Plasmid construction

To amplify genes or genomic regions of interest, either purified *M. xanthus* genomic DNA or plasmids were used as a template. Cloning steps were done by using *E. coli* Top10 or NEB Turbo strains. Sequencing was performed by Eurofins MWG Operon (Ebersberg) using custom made primers. Analysis of sequencing data was done with the help of either

ContigExprerss of Vector NTI advance suite 11 (Invitrogen TM life technologies, Karlsruhe) or MegAlign of DNASTAR (Madison, Wisconsin, USA).

**pSH62: vanillate-dependent expression of *parB-eYFP* for fluorescence microscopy**

To clone the plasmid pSH62, *parB-eYFP* was amplified using pAH7 as a template (Treuner-Lange *et al.*, 2013) with the help of the primers SH59 and SH60. Subsequently the amplified fragment was digested using the restriction endonucleases EcoRI and NdeI and ligated into pMR3691 digested with the same restriction enzymes.

**pSH65: copper-dependent expression of *tetR-eYFP* for fluorescence microscopy, replacing $Tc^R$ with $Strep^R$**

In order to select clones expressing *tetR-eYFP* in a copper-dependent matter using streptomycin as selection marker, we replaced the kanamycin resistance cassette of pMAT6 with a streptomycin resistance cassette. pIJ778 (Gust *et al.*, 2003) was used as a template to amplify the streptomycin resistance gene *aadA* using primers SH74 and SH75. The PCR product was digested using ClaI and HindIII. In parallel, the kanamycin resistance cassette was excised from pMAT6 by digestion with the same enzymes. Subsequently pMAT6 and the digested PCR fragment containing the *aadA* gene were ligated giving rise to pSH65.

**pSH66: vanillate-dependent expression of *eYFP* for fluorescence microscopy**

To clone the plasmid pSH66, *eYFP* was amplified using pAH7 as a template (Treuner-Lange *et al.*, 2013) with the help of the primers SH59 and SH81. Subsequently the amplified fragment was digested using the restriction endonucleases EcoRI and NdeI and ligated into pMR3691 digested with the same restriction enzymes.

**pSH74: copper-dependent expression of *parB-mCerulean* for fluorescence microscopy**

To be able to express *parB-mCerulean* in a copper-dependent manner, the plasmid pSH74 was created in two steps. First, mCerulean was amplified using mCerulean C1 (Addgene plasmid # 27796) (Koushik *et al.*, 2006) as a template by performing a PCR with the primers SH136 and SH137. The fragment as well as the plasmid pMAT3 were digested with the restriction enzymes BamHI and HindIII and were ligated giving rise to pSH73. Subsequently *parB* was amplified with primers SH134 and SH135 using genomic *M.xanthus* DNA as template. pSH73 and the amplified *parB* DNA fragment were digested with XbaI and BamHI and ligated.

### 9.4.3. Construction of *M. xanthus* in-frame deletion mutants

Particularly for this study, no in-frame deletion mutant was constructed. Nevertheless, strains were used in which corresponding genes were deleted. In the following, the general principle to construct in-frame deletions in *M. xanthus* will be described.

In-frame deletion mutants are obtained by performing a method described before with small modifications (Shi *et al.*, 2008). In brief, two DNA fragments with a length of approximately 500 bp are amplified by PCR. Primer AB and CD are used to amplify a DNA sequence upstream and downstream of the region to be deleted, respectively. For in-frame deletions of genes upstream- and downstream fragments contain usually 30 bp of the beginning and the end of the gene. In a first step, the upstream-fragment is cloned into pBJ114 ($Km^R$) followed by cloning the downstream fragment in the originated plasmid. Plasmids are checked via sequencing to prove they are correct and used for transformation of the corresponding *M. xanthus* strain. The plasmid pBJ114 cannot replicate autonomously but encodes a kanamycin resistance which is integrated into the genome by homologous recombination along the up- or downstream-fragment. Transformants can be selected via their kanamycin resistance on 1 % CTT plates supplemented with 50 µg/ml kanamycin. Single transformants are picked and integration of the plasmid is mapped by PCR using M13 fwd/E and M13 rev/F (primers E (fwd) and F (rev) are designed to bind upstream and downstream of the gene to be deleted). If possible, clones with an upstream and a downstream integration are used for further steps. In order to obtain a marker-less in-frame deletion, a second homologous recombination has to take place to excise the plasmid including its kanamycin resistance and the corresponding gene region. This counter-selection is based on the selection marker *galK* (gene encoding for galactokinase from *E. coli*) which is encoded on pBJ114 as well. The gene product GalK converts galactose into glactose-1-phosphate, which accumulates up to toxic levels when the cells grow on galactose containing media, since *M. xanthus* is not able to metabolize this compound. Therefore only cells undergoing a second homologous recombination are not affected in growth and can grow under this conditions. If the gene region to be deleted is not essential for viability, excision of the plasmid will result in 50% of cells being deleted for the corresponding gene region. The other 50% of cells will restore the original genomic situation. To induce the second homologous recombination, cells containing an up- or downstream integration of the plasmid are grown in liquid to exponential growth phase in the absence of kanamycin and subsequently plated in dilution series on 1% CTT plates containing 10 µg/ml gentamycin and 2.5 % galactose. Grown colonies are picked and transferred in parallel on 1% CTT plates containing kanamycin and 1% CTT plates containing galactose. Colonies growing on 1% CTT including galactose but not on 1% CTT containing kanamycin are used to check the in-frame deletion by PCR using primer

combinations E/F and G/H (primers G (fwd) and H (rev) are designed to bind inside of the gene to be deleted).

### 9.4.4. DNA isolation from *E. coli* and *M. xanthus*

Plasmid DNA was amplified in and extracted from *E. coli* Top10 or NEB Turbo cells. Either QIAprep Spin Miniprep Kit (Quiagen, Hilden) or NucleoSpin® Plasmid Kit (Macherey-Nagel, Düren) was used to extract plasmid DNA. The extraction of genomic *M. xanthus* DNA was performed with the MasterPure DNA preparation Kit (Epicentre® Biozym, Oldendorf) according to the manufacturers instructions. To determine quality and concentration of isolated DNA, the Nanodrop ND-1000 spectrophotometer (Nanodrop, Wilmington) was used. Crude genomic DNA extracts were obtained by boiling cells in 20 µl $H_2O$ for 10 min at 95°C. To sediment cell debris, samples were centrifuged for 2 min at 13.000 rpm before DNA extracts were used.

### 9.4.5. Amplifying DNA fragments: Polymerase chain reaction (PCR)

To amplify specific DNA fragments by polymerase chain reaction, Phusion High-Fidelity DNA Polymerase (Thermo Scientific™, Darmstadt) was used in a total reaction volume of 20 µl as described in Table 11.

**Table 11: General PCR reaction mix to amplify DNA fragments with Phusion High Fidelity Polymerase**

| Component | Volume | final conentration |
|---|---|---|
| Genomic or plasmid DNA | 1 µl | 50-100 ng |
| Primer A (10 µM) | 0.5 µl | 0.25 µM |
| Primer A (10 µM) | 0.5 µl | 0.25 µM |
| dNTP mix (10 µM) | 0.4 µl | 0.2 mM |
| 5 x Phusion GC buffer | 4 µl | 1 x |
| 5 x enhancer | 4 µl | 1 x |
| Phusion DNA Polymerase | 0.2 µl | 1 unit/50 µl volume |
| HPLC $H_2O$ | 9.4 µl | |

For polymerase chain reactions performed using Phusion High-Fidelity DNA Polymerase, the the PCR program described in Table 12 was used. Modifications were applied depending on GC content of the primers and length of the DNA fragment to be amplified.

**Table 12: PCR program for PCR´s using Phusion Polymerase**

| Step | Temperature | Time | |
|---|---|---|---|
| Initial denaturation | 95 °C | 3 min | |
| Denaturation | 95 °C | 30 sec | 35 x |
| Annealing | 5 °C below predicted melting temperature (mostly 55 -62 °C) | 30 sec | |
| Elongation | 72 °C | 30 sec/1000 bp | |
| Final elongation | 72 °C | 10 min | |
| hold | 4 °C | ∞ | |

Amplified PCR products were separated by agarose gel electrophoresis to check for correct size by comparing to a DNA size standard. DNA fragments were either purified directly by using the NucleoSpin® Gel and PCR Clean-up kit (Macherey & Nagel, Düren) or isolated from the agarose gel by excision of the gel piece containing the corresponding fragment and purified with the NucleoSpin® Gel and PCR (Macherey & Nagel, Düren) Clean-up kit. To elute the fragments, either 30 µl of elution buffer or $H_2O$ was used.

### 9.4.6. Checking for in-frame deletions or plasmid integrations via PCR

To test clones for plasmid integration in the *M. xanthus* genome or to test for gene deletions, check PCR´s were performed. In order to prepare crude DNA extracts, cells were scratched from agar plates and resuspended in 20 µl HPLC $H_20$, followed by incubation at 95°C for 10 min. Cell debris were pelleted by centrifugation for 2 min at 13.000 rpm and the supernatant was used as DNA extract. The PCR´s were performed using the 5´PRIME Master Mix (5 PRIME GmbH Hamburg) or the *Taq* 2X Master Mix New England Biolabs (Frankfurt a. M.) in a total reaction volume of 25 µl and 20 µl as described in Table 13 and Table 14.

**Table 13: General PCR reaction mix to amplify DNA fragments using 5´PRIME Master Mix**

| Component | Volume | final concentration |
|---|---|---|
| 5`PRIME Master Mix | 10 µl | 1 x |
| DMSO | 2 µl | 10 % (v/v) |
| Primer A (10 µM) | 0.5 µl | 0.25 µM |
| Primer B (10 µM) | 0.5 µl | 0.25 µM |
| Crude genomic DNA | 2 µl | |
| HPLC $H_2O$ | 10 µl | |

**Table 14: General PCR reaction mix to amplify DNA fragments using Taq 2x Master Mix**

| Component | Volume | final concentration |
|---|---|---|
| Taq 2 x Master Mix | 10 µl | 1 x |
| DMSO | 2 µl | 10 % (v/v) |
| Primer A (10 µM) | 1 µl | 0.5 µM |
| Primer B (10 µM) | 1 µl | 0.5 µM |
| Crude genomic DNA | 2 µl | |
| HPLC $H_2O$ | 4 µl | |

For polymerase chain reactions performed using the 5´PRIME Master Mix (5 PRIME GmbH Hamburg) or the *Taq* 2X Master Mix New England Biolabs (Frankfurt a. M.) the PCR program described in Table 15 was used. Modifications were applied depending on GC content of the primers and length of the DNA fragment to be amplified.

**Table 15: PCR program for PCR´s using 5`PRIME Master Mix or Taq 2x Master Mix**

| Step | Temperature | Time | |
|---|---|---|---|
| Initial denaturation | 96 °C | 5 min | |
| Denaturation | 96 °C | 30 sec | 35 x |
| Annealing | 5 °C below predicted melting temperature (mostly 60 – 62 °C) | 30 sec | |
| Elongation | 72 °C | 1 min/1000 bp | |
| Final elongation | 72 °C | 5 min | |
| hold | 4° C | ∞ | |

### 9.4.7. RNA preparation from *M. xanthus*

Total RNA was isolated from cell pellets by using a hot-phenol extraction method as used before for *M. xanthus* (Overgaard *et al.*, 2006). Either 5 ml of exponentially growing cells or cells starved in submerged culture in a total volume of 16 ml were used for RNA extraction. Starving cells were harvested, pelleted by centrifugation and resuspended in 5 ml of MC7 buffer. Samples were transferred to a tube containing 5 ml of ice-cold stop solution and centrifuged for 10 min at 4700 rpm and 4 °C. The pellet was resuspended in 2.5 ml ice cold solution 1 and transferred into tubes containing 2.5 ml hot (65 °C) solution 2. RNA was extracted by treating the samples twice with 5 ml hot (65 °C) phenol. Each time, samples were incubated at 65°C for 5 min in hot phenol and inverted every 60 sec during incubation. Subsequently samples were chilled in liquid nitrogen and centrifuged for 5 min at 4700 rpm and 4 °C. The aqueous layer was transferred to a fresh tube containing hot phenol to repeat

this step. After phenol extraction, the aqueous layer was transferred to a fresh tube containing 5 ml chilled phenol-chloroform-isoamyl alcohol (25:24:1). Samples were mixed gently by inversion and centrifuged for 5 min at 4700 rpm and 4 °C and the RNA containing layer was transferred to a fresh tube containing 5 ml chloroform-isoamyl alcohol (24:1). Again, samples were mixed and centrifuged for 5 min at 4700 rpm and 4 °C. In the last step, the RNA was precipitated from the aqueous phase by transferring the aqueous layer to a fresh tube containing 400 µl of 3 M sodium acetate solution and 9 ml 96 % ethanol and incubating it over night at -20 °C. To pellet the RNA, samples were centrifuged for 25 min at 4700 rpm and 4°C and the pellet was washed twice with 2 ml 75 % ice cold ethanol. After removal of the supernatant, the pellet was dried briefly at room temperature and resuspended in 100 µl RNase-free $H_2O$ to be stored at -80 °C.

**Table 16: Solutions used to extract total RNA from *M. xanthus***

| solution | Composition |
|---|---|
| Stop-solution | 5 % saturated acid phenol (pH < 6.0) in 96% ethanol |
| Solution 1 | 0.3 M sucrose<br>0.01 M NaAC,<br>pH 4.5 (adjusted with acetic acid) |
| Solution 2 | 2 % SDS<br>0.01 M NaAc<br>pH 4.5 (adjusted with acetic acid) |
| Sodium acetate | 3 M, dissolved in sterile water |

### 9.4.8. RNA purification and cDNA synthesis

The purified total RNA was treated with 20 U RNase-free Turbo™ Dnase (Ambion™ Thermo Scientific™, Darmstadt) for 3 h at 37 °C. Every 15 min during the incubation time, samples were gently mixed and spun down. RNA was purified using NucleoSpin® RNA Plus Kit (Macherey & Nagel, Düren) according to the manufacturers protocol. The removal of DNA was checked by PCR reaction and Dnase treatment was repeated in case of DNA contamination. Integrity of the RNA sample was verified by separation of 23S and 16S rRNA via agarose gel electrophoresis. RNA was considered to be intact if both bands were observed as clear and sharp on a 1% agarose gel. 1 µg DNA-free, intact total RNA was used to synthesize cDNA with the help of the HighCapacity cDNA Reverse Transcription Kit (Applied Biosystems, Darmstadt) according to the manufacturers protocol summarized in Table 17 and Table 18.

**Table 17: Reaction mix to synthesize cDNA from total *M. xanthus* RNA (HighCapacity cDNA Reverse Transcription Kit)**

| Component | Volume | final concentration |
|---|---|---|
| 10 x reverse transcription buffer | 2.5 µl | 1 x |
| 25 x dNTPs | 1 µl | 1 x |
| 10 x random primers | 2.5 µl | 1 x |
| RNA | xx µl | 1 µg |
| MultiScribe™ reverse transcriptase (50 U/µl) | 1.25 µl | 62.5 U / 25 µl volume |
| Nuclease-free H2O | to 20 µl | |

**Table 18: Thermal cycler conditions for cDNA synthesis**

| Step | Temperature | Time |
|---|---|---|
| 1 | 25 °C | 10 min |
| 2 | 37 °C | 120 min |
| 3 | 85 °C | 85 min |
| hold | 4 °C | ∞ |

### 9.4.9. qRT-PCR

To perform qRT-PCR reactions the Power SYBR™ Green Master Mix (Applied Biosystems, Darmstadt) was used in a total volume of 20 µl as summarized in Table 19 and Table 20. cDNA samples were diluted 1:10 before they were applied to this reaction. The primer efficiency of the used oligonucleotides was determined prior to the experiment by using defined concentrations of genomic DNA as template. The 7500 Real Time PCR system was used to perform the reactions and to detect the signals. Analysis of the data was done with the help of the 7500 Software v2.3 (Applied Biosystems, Darmstadt). Experiments were performed in two biological replicates, each of them in technical triplicates. To calculate the relative gene expression, the comparative Ct (cycle threshold) method was used.

**Table 19: Reaction mix to perform qRT-PCR**

| Component | Volume | final conentration |
|---|---|---|
| SYBR Green Master Mix | 12.5 µl | 1 x |
| Primer A (10 µM) | 0.25 µl | 0.1 µM |
| Primer A (10 µM) | 0.25 µl | 0.1 µM |
| cDNA | 1 µl | |
| Nuclease-free H2O | 11 µl | |

**Table 20: qRT-PCR program**

| Step | Temperature | Time | |
|---|---|---|---|
| 1 | 50 °C | 2 min | |
| 2 | 95 °C | 10 min | |
| 3 | 95 °C | 15 sec | 40 x |
| 4 | 60 °C | 1 min | |
| 5 | 95 °C | 15 sec | |
| 6 | 60 °C | 30 sec | |
| 7 | 95 °C | 15 sec | |

### 9.4.10. Agarose gel electrophoresis

PCR reactions, digested plasmids and RNA samples were visualized by performing agarose gel electrophoresis. Samples were mixed with 10 x DNA loading buffer (New England Biolabs, Frankfurt a. M.) and separated on 1 % agarose gels supplemented with 0.01 % (v/v) ethidium bromide in 1 x TBE buffer (Life Technologies GmbH, Karlsruhe). As size standard 2-log DNA ladder (New England Biolabs, Frankfurt a. M.) was used. Gels were documented using the E-BOX VX2 imaging system (PeqLab, Erlangen).

### 9.4.11. Restriction and ligation of DNA fragments

In order to clone plasmids, PCR products and vector backbones were digested with the help of endonucleases (New England Biolabs, Frankfurt a. M.) to make them applicable to ligation. 2–3 µg of plasmid DNA was digested according to the manufacturer´s protocol for 3 h at 37 °C in a total volume of 50 µl. Subsequently, 6 µl of 10 x Antarctic phosphatase buffer, 3 µl of HPLC H2O and 1 µl Antarctic Phosphatase (New England Biolabs, Frankfurt a. M.) were added to the reaction and incubated another 1 h at 37 °C to perform dephosphorylation reaction. After that, the digest was applied to agarose gel electrophoresis and DNA fragments of correct size were excised from the gel and purified with the NucleoSpin® Gel and PCR Clean-up kit (Macherey & Nagel, Düren) according to manufacturer´s protocol. Purified PCR fragments were digested with endonucleases (New England Biolabs, Frankfurt a. M.) according to manufacturer´s protocol for 3 h at 37 °C in a total volume of 50 µl. Afterwards, the digested DNA fragments were purified using NucleoSpin® Gel and PCR Clean-up kit (Macherey & Nagel, Düren).

DNA fragments and plasmids were ligated with the help of the T4 DNA Ligase (New England Biolabs, Frankfurt a. M.) in a reaction volume of 20 µl according to manufacturer´s instructions. The reaction was incubated over night at room temperature or for 1 h at 37 °C. Ligation of PCR fragments into vectors was performed in the presence of 3- to 5-fold excess of insert DNA.

### 9.4.12. Preparation and transformation of chemically competent *E. coli* cells

To prepare chemically competent *E. coli* NEB Turbo or TOP10 cells, an overnight culture was used to inoculate 100 ml of fresh LB medium. Cell were incubated shaking at 37 °C and growth was followed by determining the optical density. At $OD_{600}$ of 0.5-0.8 cells were harvested by centrifugation for 15 min at 4700 rpm and 4 °C. The pellets were resuspended in 20 ml TFB1 (Table 21) and incubated on ice for 10 min. Cells were centrifuged again for 15 min at 4700 rpm and 4°C to resuspend the pellet in 2 ml TFB2 (Table 21). Cells were incubated on ice for 1 h and 50 µl aliquots were snap frozen in liquid nitrogen to store them at -80°C.

**Table 21: Buffers used to prepare chemically competent *E. coli* cells**

| Buffer | Composition |
|---|---|
| TFB1 | 30 mM potassium acetate<br>10 mM $CaCl_2$<br>50 mM $MnCl_2$<br>100 mM RbCl<br>15% glycerol (v/v)<br>pH 5.8 (adjusted with 1M acetic acid) |
| TFB2 | 10 mM MOPS pH 6.5 (adjusted with KOH)<br>75 mM $CaCl_2$<br>10 mM RbCl<br>15% glycerol (v/v) |

For transformation 50 µl of cells were thawed on ice and mixed gently with 10 µl of ligation reaction or 1 µl plasmid DNA. The mixture was incubated on ice for 30 min. Cells were heat-shocked for 1 min at 42 °C in a water bath, chilled on ice for 2 min, mixed with 1 ml fresh LB medium and incubated for 45 min shaking at 37°C. Subsequently, cells were pelleted for 2 min at 13.000 rpm at room temperature, resuspended in 50-100 µl LB medium and spread on LB agar plates supplemented with corresponding antibiotics. Plates were incubated at 37 °C over night. Grown colonies were checked for the presence of the correct plasmid by restriction digestion followed by sequencing.

### 9.4.13. Preparation and transformation of electrocompetent *M. xanthus* cells

*M. xanthus* cells were inoculated from a single colony in a total volume of 10 ml 1% CTT and incubated over night at 32°C and 230 rpm. Exponentially growing cells ($OD_{600}$ 0.4 – 0.7) were harvested in falcon tubes at 4700 rpm for 10 min at room temperature. The pellet was

resuspended in sterile dd$H_2O$ to the original volume. The pelleting and washing step was repeated twice. Subsequently, pelleted cells were resuspended in 80 – 400 µl dd$H_2O$. 80 µl of cells was transferred into a sterile 0.1 cm electroporation cuvette (Bio-Rad, München) and mixed with 5 – 10 µl of plasmid DNA, which corresponded to a total amount of 1 – 2 µg DNA. The cells mixed with DNA were pulsed with 0.65 kV, 25 µF and 400 Ω. Afterwards, 1 ml 1% CTT was added to the mixture and the electroporated cells were transferred to a 25 ml Erlen-Meyer flask containing 1.5 ml 1% CTT, which results in a total volume of 2.5 ml. Cells were incubated at 32°C and 230 rpm for 6 – 8 h or over night. After recovery, cells were pelleted at 8000 rpm for 5 min. The supernatant was discarded and the cells were resuspended in 100 µl 1% CTT to spread them on 1% CTT agar plates supplemented with the corresponding antibiotics in dilution series. The agar plates were incubated at 32°C for several days. Grown colonies were transferred to fresh 1% CTT agar plates including antibiotics and checked via PCR for plasmid insertion.

## 9.5. Analytical cell biology methods

### 9.5.1. Live cell imaging by fluorescence microscopy

To perform fluorescence microscopy with vegetative *M. xanthus* cells, strains were inoculated in 10 ml 1% CTT medium supplemented with corresponding antibiotics and inducer at indicated concentrations. Cells were grown for at least 48 h at 32°C shaking while they were constantly diluted to keep them in exponential growth phase. At $OD_{550}$ 0.3 – 0.6 10 µl of cells were spotted on 1% agarose slides buffered with TPM. Cells were incubated for 5 min in the dark to let them attach to the surface and subsequently covered with a 0.17 mm coverslip before microscopy. To perform fluorescence microscopy with cells during development cells were starved on TPM agar as described in 9.3.5. For microscopy 25 spots (each 20 µl concentrated cells) were harvested at indicated time points and cell aggregates were dispersed using the FastPrep-24 for 40 sec at 5 m/s (MP Biomedicals, Eschwege). In case cell aggregates were still visible, this step was repeated. If aggregating and non-aggregating cells were analysed individually, cell fractions were separated prior to dispersal as described in 9.3.6. Afterwards, cells were spotted on 1% agarose slides buffered with TPM (Table 6), incubated for 5 min in the dark and covered with a 0.17 mm coverslip. Cells were imaged using with a DMI 6000 B microscope (Leica, Wetzlar) at 32°C the dark using a Hamamatsu Flash 4.0 sCMOS camera. Z-stacks were performed in order to record images at different focal planes with a step size of 0.15 µm. Images were acquired with Leica MM AF (Leica, Wetzlar) and processed with Metamorph® v 7.5 (Molecular Devices).

### 9.5.2. EdU labeling

EdU labeling was performed in order to visualize newly replicated DNA using the commercially available Click-iT® EdU Alexa Fluor® 594 Imaging Kit (Molecular Probes™ Thermo Scientific™, Darmstadt). The nucleoside analog of thymidine EdU (5-ethynyl-2´-deoxyuridine) is incorporated into the DNA during active DNA synthesis and can be detected by a click reaction using AlexaFluor594. A method developed for *E. coli* (Ferullo *et al.*, 2009) was slightly modulated for *M. xanthus*. Either exponentially growing or developing cells, treated as described in 9.5.1, were applied to EdU labeling in a total volume of 2 ml. If aggregating and non-aggregating cells were analyzed individually, cell fractions were separated prior to EdU staining as described in 9.3.6. To the 2 ml cell aliquots, 15 µl EdU was added, giving a final concentration of 18.75 µg/ml and incubated shaking for 30 min at 32 °C. Cells were pelleted by centrifugation (5 min, 8000 x g at room temperature) and washed using 2 ml of 1 x PBS (137 mM NaCl, 2.7 mM KCl, 10 mM $Na_2HPO_4$, 2 mM $KH_2PO_4$, pH 7.4). The pelleting step was repeated and the cells were resuspended in 2 ml 1 x PBS. To fix the cells 54 µl of 37 % formaldehyde was added, giving a final concentration of 1% and the samples were incubated shaking for 30 min at room temperature in the dark. Afterwards, 100 µl of 1 M Tris-HCl, pH 7.6 was added resulting in a final concentration of 50 mM and incubated for 5 min at room temperature in the dark. Samples were pelleted and washed with 2 ml 1 x PBS as described above. Subsequently, cells were pelleted again and resuspended in 0.5 % of TritonX-100 in 1 x PBS to permeabilize their membranes. After 5 min of incubation in the dark at room temperature, cells were washed again with 2 ml 1 x PBS, pelleted and resuspended in 200 µl Click-iT reaction cocktail per ml cell culture as described in the manufacturers protocol. Cells were incubated for 30 min at room temperature in the dark, washed once more with 2 ml 1 x PBS, pelleted and resuspended in 300 µl 1 x PBS. Afterwards, cells were spotted on 1% agarose pads buffered with TPM and imaged as described in 9.5.2.

### 9.5.3. Fluorophores and filter sets for fluorescence microscopy

Fluorophores, dyes and filter systems used in this study to activate and follow the localization of fluorescently tagged proteins are listed in Table 22 and Table 23.

**Table 22: Fluorophores and dyes used for fluorescence microscopy in this study**

| Fluorophore | specification |
|---|---|
| eYFP | Excitation maximum: 514 nm<br>Emission maximum: 527 nm |
| mCerulean | Monomeric fluorophore, derivative of ECFP<br>Excitation maximum: 433 nm<br>Emission maximum: 475 nm |
| Alexa Fluor 594 | Excitation maximum: 590 nm<br>Emission maximum: 617 nm |

**Table 23: Filter sets used for the DMI 6000 B microscope (Leica)**

| Fluorophore | Excitations | Emissions |
|---|---|---|
| YFP | 500/20 | 535/30 |
| CFP | 436/20 | 480/40 |
| TX2 (Alexa Fluor 594) | 560/40 | 645/75 |

numbers of excitation and emission wavelength are given in nm

### 9.5.4. Flow cytometry

Flow cytometry provides a snapshot of the distribution of the numbers of cells that contain a distinct amount of DNA which reflects several stages in the cell cycle. Exponentially growing or cells in the stationary growth phase were diluted to $OD_{550}$ 0.1 with 1 x CTT in a total volume of 100 µl. 25 spots of concentrated cells which developed on TPM medium (9.3.5) were harvested and resuspended in 500 µl TPM buffer. Cell aggregates were dispersed using the FastPrep-24 for 40 sec at 5 m/s (MP Biomedicals, Eschwege). In case cell aggregates were still visible, this step was repeated. The chromosome was stained with 10 µM Vybrant® DyeCycle™ Orange for 40 min at 32°C shaking in the dark. Cells were diluted 1:10 in sterile filtered tethering buffer (Table 24) and incubated for 10 min before samples were transferred to the BD LSR Fortessa (Becton Dickinson GmbH, Heidelberg) and the fluorescence intensity which is proportional to the DNA content was subsequently quantified by flow cytometry. Each experimental run consisted on an analysis of 10.000 individual events corresponding to cells. The position the two fluorescent intensity peaks of stained wild type cells was used as a standard for the experiments which was previously confirmed by comparison with stationary cells (Tzeng & Singer, 2005). Correlated measurement of SSC (side-scattered light) and FSC (forward-scattered light) can allow the differentiation of cell types in a heterogeneous cell population by their size. Side-scattered light is proportional to internal cell complexity, whereas forward-scattered light is proportional to cell-surface area or size. Based on these parameters

distinct cell populations were analyzed separately. Obtained data were analyzed using FlowJo software (FlowJo, LLC, Ashland, USA).

**Table 24: Buffer used to dilute flow cytometry samples**

| Buffer | Composition |
|---|---|
| Tethering buffer | 10 mM $K_2HPO_4$<br>10 mM $KH_2PO_4$<br>0.1 mM EDTA<br>0.1 M L-Methionin<br>10 mM Lactic acid<br>pH 7.0 (adjusted with 40% NaoH) |

## 9.6. Biochemical methods

### 9.6.1. Determination of protein concentrations by Bradford assay

To determine the total amount of protein in samples used for immunoblot analysis, the Bio-Rad protein assay kit was used according to the manufacturer´s recommendations. Briefly, 980 µl of 1:5 diluted Bradford reagent was mixed with 20 µl protein sample and incubated 5 min at room temperature in the dark. In the same way a standard curve was created using known concentrations of BSA (bovine serum albumin) showing protein concentration versus measured absorbance. Absorbance was measured using an Ultrospec 2100 pro spectrophotometer (GE Healthcare Europe GmbH, Freiburg) at 495 nm. Protein concentrations were determined based on the linear slope of the standard curve.

### 9.6.2. SDS polyacrylamide gel electrophoresis (SDS-PAGE)

To separate proteins under denaturing conditions SDS polyacrylamide gel electrophoresis was performed (Laemmli, 1970). SDS gels containing 10% of Acrylamide were used (Table 25). To denature proteins, they were mixed with 1 x SDS sample buffer (Table 27) and incubated at 95 °C for 10 min. Samples were centrifuged for 2 min at room temperature and 13.000 rpm and protein concentrations were determined when necessary (9.6.1). Geld were run in a BioRad MiniPROTEAN 3 Cell or MiniPROTEAN TetraCell at 110 V for 80 to 100 min in 1 x Tris Glycin SDS (TGS) buffer (BioRad, München). As protein standard PageRuler Prestain Protein Ladder (Pierce™ Thermo Scientific™, Darmstadt) was used.

**Table 25: Composition of SDS-gels**

| Reagent | Resolving gel (10%) | Stacking gel |
|---|---|---|
| Resolving gel buffer | 2.5 ml | X |
| Stacking gel buffer | X | 2.5 ml |
| Acrylamide (30%) | 2.35 ml | 1.1 ml |
| ddH2O | 5.15 ml | 6.5 ml |
| TEMED | 0.02 ml | 0.05 ml |
| APS (10%) | 0.05 ml | 0.0.8 ml |

**Table 26: Composition of buffers used to prepare SDS gels**

| Buffer | Composition |
|---|---|
| Resolving gel buffer | 1.5 M Tris-HCl pH 8.8<br>0.4 % (w/v) SDS |
| Stacking gel buffer | 0.5 M Tris-HCl pH 6.8<br>0.4 % (w/v) SDS |

**Table 27: Composition of SDS sample buffer**

| Buffer | Composition |
|---|---|
| 5 x SDS sample buffer | 225 mM Tris-Hcl pH 6.8<br>50% glycerol<br>10 mM EDTA<br>10% (w/v) SDS<br>500 mM DTT<br>1% (w/v) bromphenol blue |

### 9.6.3. Immunoblot analysis

Immunoblots were performed to detect proteins of interest with specific antibodies in cell lysates. As a first step, protein samples were subjected to SDS-page to separate the individual proteins (9.6.2). Usually, 20 µg to 30 µg of total protein was loaded per sample. Subsequently, proteins were transferred from the SDS-gel to a methanol activated 0.2 µm PVDF membrane (GE healthcare Europe GmbH, Freiburg). To do so the semi-dry TransBlot® TurboTM Transfer System (BioRad, München) was used. Transfer was performed applying 1.3 A and 25 V for 30 min with Blot Buffer (Table 28). The blotted membranes were blocked in 5% non-fat milk powder (w/v) in 1 x TBS (Table 28) shaking for 3 to 4 hours. The first antibody was applied in the corresponding concentrations in 1% non-fat milk powder (w/v) in 1 x TBS over night at 4°C shaking. After washing the blots three times with 1 x TBS-T for 10 min at room temperature,

the secondary horseradish peroxidase-coupled goat α-rabbit immunoglobulin G antibody was diluted 1:25.000 in 1% non-fat milk powder (w/v) in 1 x TBS and applied for two hours at room temperature and shaking. The membranes were washed again three times with 1 x TBS-T for 10 min at room temperature. Finally, the blots were developed with the Luminata Western HRP Substrate (Millipore Merck, Schwalbach) and visualized with the luminescent image analyzer LAS-4000 (Fujifilm, Düsseldorf). Protein specific antibodies were produced using rabbits as production host from full length $His_6$- tagged FtsZ, PomX, PomY and PomZ purified from *E. coli* as described before (Schumacher *et al.*, 2017). To analyze immunoblots quantitatively, the software ImageJ (National Institutes of Health, Bethesda, Maryland, USA) was used.

**Table 28: Buffers used for immunoblot analysis**

| Buffer | Composition |
|---|---|
| Blot Buffer | 300 mM glycine<br>300 mM Tris<br>0.0.5 % SDS<br>pH 9-10 |
| 1 x TBS | 50 mM Tris-HCl pH 7.5<br>150 mM NaCl |
| 1 x TBS-T | 1 x TBS<br>0.1 % Tween20 (v/v) |

**Table 29: List of antibodies used in this study**

| Antibody | Dilution | Reference |
|---|---|---|
| α-FtsZ (no. 852) | 1:25.000 | (Treuner-Lange *et al.*, 2013) |
| α-PomX (no. 7099) | 1:15.000 | (Schumacher *et al.*, 2017) |
| α-PomY (no. 7102) | 1:15.000 | (Schumacher *et al.*, 2017) |
| α-PomZ (no. 492) | 1:5000 | (Treuner-Lange *et al.*, 2013) |
| α-PilC (no. 2806) | 1:10.000 | (Bulyha *et al.*, 2009) |
| α-ProteinC | 1:5000 | (Lee *et al.*, 2011) |

### 9.6.4. Membrane stripping

Membrane stripping was performed to remove the primary and secondary antibody from a membrane in order to investigate more than one protein on the same blot. This method was usually used to explore the abundance of proteins of interest and the presence of PilC as a loading control. PilC is an inner membrane protein and part of the pilus machinery in *M. xanthus* (Bulyha *et al.*, 2009). After detection of the protein of interest the membrane was incubated for 15 min in Restore™ Western Blot Stripping Buffer (Pierce™ Thermo Scientific™,

Darmstadt) shaking at room temperature. Subsequently, the membrane was washed three times with 1 x TBS-T and blocked for 2-3 hours in 5% non-fat milk powder (w/v) in 1 x TBS (Table 28) and the first antibody was applied in the corresponding concentrations in 1% non-fat milk powder (w/v) in 1 x TBS over night at 4°C shaking. The protocol was continued as described for immunoblot analysis (9.6.3).

### 9.6.5. Determination of FtsZ protein half-life

To determine the half-life of FtsZ during vegetative growth or development of *M. xanthus*, cells were grown to exponential growth phase or starved in MC7 submerged culture (9.3.5) and chloramphenicol was added to a final concentration of 25 µg/ml to shut off protein synthesis. After addition of the protein synthesis inhibitor 2 ml samples were taken every 30 min. Cells were pelleted by 2 min centrifugation at 13.000 rpm. To denature proteins, cells were mixed with 1 x SDS sample buffer (Table 27) and incubated at 95 °C for 10 min and stored at -20°C. To analyze them via immunoblot, samples were thawed, total protein concentration was determined via Bradford assay (9.6.1) and SDS-page (9.6.2) was performed. For each lane 25 µg of total protein was loaded. Proteins were detected with specific α-FtsZ antibodies via immunoblot analysis (9.6.3). Membranes were stripped (9.6.4) to reprobe them with α-PilC antibodies and relative band intensities in relation to PilC loading control were quantified using ImageJ (National Institutes of Health, Bethesda, Maryland, USA). Data were acquired from two biological and each at least two technical replicates.

### 9.6.6. *In vitro* degradation assay

*In vitro* degradation assays were performed in LonD degradation buffer (Table 30) at 32°C with 75 µg/ml creatine kinase (Roche, Mannheim) and 15 mM creatine phosphate (Sigma-Aldrich, Taufkirchen) and 1.5 mM ATP (Sigma-Aldrich, Taufkirchen) and LonD-$His_6$ (1.2 µM), FtsZ (0.5 µM) or PopD-StrepII (4.0 µM) in a total volume of 100 µl. Proteins were purified by Magdalena Polatynska and Andrea Harms. If needed ppGpp (TriLink Biotechnologies, San Diego, USA) and sodium polyphosphate (Sigma-Aldrich, Taufkirchen) were added at a concentration of 1 mM. Samples were incubated at 32°C and at indicated time points 9 µl of sample were mixed with 3 µl 4xSDS buffer and snap freezed in liquid nitrogen. Samples were heated at 95°C for 10 min and separated by SDS-PAGE. Gels were stained with InstantBlue™ (Expedeon, Cambridgeshire, UK) to detect proteins.

**Table 30: Buffer used for *in vitro* degradation assay with LonD**

| Buffer | Composition |
|---|---|
| LonD degradation buffer | 100 mM KCl<br>10 mM $MgCl_2$<br>1 mM DTT<br>50 mM TRIS<br>pH 8.0 (adjusted with HCl) |

# 10. References


Adams, D.W. & J. Errington, (2009) Bacterial cell division: assembly, maintenance and disassembly of the Z ring. *Nat Rev Microbiol* **7**: 642-653.

Adams, D.W., L.J. Wu & J. Errington, (2015) Nucleoid occlusion protein Noc recruits DNA to the bacterial cell membrane. *EMBO J* **34**: 491-501.

Addinall, S.G. & J. Lutkenhaus, (1996) FtsZ-spirals and -arcs determine the shape of the invaginating septa in some mutants of *Escherichia coli*. *Mol Microbiol* **22**: 231-237.

Anderson, D.E., F.J. Gueiros-Filho & H.P. Erickson, (2004) Assembly dynamics of FtsZ rings in *Bacillus subtilis* and *Escherichia coli* and effects of FtsZ-regulating proteins. *J Bacteriol* **186**: 5775-5781.

Balaban, N.Q., (2011) Persistence: mechanisms for triggering and enhancing phenotypic variability. *Current opinion in genetics & development* **21**: 768-775.

Bath, J., L.J. Wu, J. Errington & J.C. Wang, (2000) Role of *Bacillus subtilis* SpoIIIE in DNA transport across the mother cell-prespore division septum. *Science* **290**: 995-997.

Beaufay, F., J. Coppine, A. Mayard, G. Laloux, X. De Bolle & R. Hallez, (2015) A NAD-dependent glutamate dehydrogenase coordinates metabolism with cell division in *Caulobacter crescentus*. *EMBO J* **34**: 1786-1800.

Ben-Yehuda, S., M. Fujita, X.S. Liu, B. Gorbatyuk, D. Skoko, J. Yan, J.F. Marko, J.S. Liu, P. Eichenberger, D.Z. Rudner & R. Losick, (2005) Defining a centromere-like element in *Bacillus subtilis* by Identifying the binding sites for the chromosome-anchoring protein RacA. *Mol Cell* **17**: 773-782.

Ben-Yehuda, S. & R. Losick, (2002) Asymmetric cell division in *B. subtilis* involves a spiral-like intermediate of the cytokinetic protein FtsZ. *Cell* **109**: 257-266.

Ben-Yehuda, S., D.Z. Rudner & R. Losick, (2003) RacA, a bacterial protein that anchors chromosomes to the cell poles. *Science* **299**: 532-536.

Berkmen, M.B. & A.D. Grossman, (2006) Spatial and temporal organization of the *Bacillus subtilis* replication cycle. *Mol Microbiol* **62**: 57-71.

Berleman, J.E. & J.R. Kirby, (2009) Deciphering the hunting strategy of a bacterial wolfpack. *FEMS microbiology reviews* **33**: 942-957.

Bernhardt, T.G. & P.A. de Boer, (2005) SlmA, a nucleoid-associated, FtsZ binding protein required for blocking septal ring assembly over Chromosomes in *E. coli*. *Mol Cell* **18**: 555-564.

Bhat, N.H., R.H. Vass, P.R. Stoddard, D.K. Shin & P. Chien, (2013) Identification of ClpP substrates in *Caulobacter crescentus* reveals a role for regulated proteolysis in bacterial development. *Mol Microbiol* **88**: 1083-1092.

Bi, E.F. & J. Lutkenhaus, (1991) FtsZ ring structure associated with division in *Escherichia coli*. *Nature* **354**: 161-164.

Bisson-Filho, A.W., Y.P. Hsu, G.R. Squyres, E. Kuru, F. Wu, C. Jukes, Y. Sun, C. Dekker, S. Holden, M.S. VanNieuwenhze, Y.V. Brun & E.C. Garner, (2017) Treadmilling by FtsZ filaments drives peptidoglycan synthesis and bacterial cell division. *Science* **355**: 739-743.

Boonstra, M., I.G. de Jong, G. Scholefield, H. Murray, O.P. Kuipers & J.W. Veening, (2013) Spo0A regulates chromosome copy number during sporulation by directly binding to the origin of replication in *Bacillus subtilis*. *Mol Microbiol* **87**: 925-938.

Boutte, C.C. & S. Crosson, (2013) Bacterial lifestyle shapes stringent response activation. *Trends Microbiol* **21**: 174-180.

Boynton, T.O., J.L. McMurry & L.J. Shimkets, (2013) Characterization of *Myxococcus xanthus* MazF and implications for a new point of regulation. *Mol Microbiol* **87**: 1267-1276.

Bramkamp, M., R. Emmins, L. Weston, C. Donovan, R.A. Daniel & J. Errington, (2008) A novel component of the division-site selection system of Bacillus subtilis and a new mode of action for the division inhibitor MinCD. *Mol Microbiol* **70**: 1556-1569.

Bravo, A., G. Serrano-Heras & M. Salas, (2005) Compartmentalization of prokaryotic DNA replication. *FEMS microbiology reviews* **29**: 25-47.

Bulyha, I., C. Schmidt, P. Lenz, V. Jakovljevic, A. Hone, B. Maier, M. Hoppert & L. Sogaard-Andersen, (2009) Regulation of the type IV pili molecular machine by dynamic localization of two motor proteins. *Mol Microbiol* **74**: 691-706.

Burkholder, W.F., I. Kurtser & A.D. Grossman, (2001) Replication initiation proteins regulate a developmental checkpoint in *Bacillus subtilis*. *Cell* **104**: 269-279.

Bush, M. & R. Dixon, (2012) The role of bacterial enhancer binding proteins as specialized activators of sigma54-dependent transcription. *Microbiol Mol Biol Rev* **76**: 497-529.

Buske, P.J. & P.A. Levin, (2012) Extreme C terminus of bacterial cytoskeletal protein FtsZ plays fundamental role in assembly independent of modulatory proteins. *J Biol Chem* **287**: 10945-10957.

Cabre, E.J., B. Monterroso, C. Alfonso, A. Sanchez-Gorostiaga, B. Reija, M. Jimenez, M. Vicente, S. Zorrilla & G. Rivas, (2015) The Nucleoid Occlusion SlmA Protein Accelerates the Disassembly of the FtsZ Protein Polymers without Affecting Their GTPase Activity. *PLoS One* **10**: e0126434.

Camberg, J.L., J.R. Hoskins & S. Wickner, (2009) ClpXP protease degrades the cytoskeletal protein, FtsZ, and modulates FtsZ polymer dynamics. *Proc Natl Acad Sci U S A* **106**: 10614-10619.

Camberg, J.L., M.G. Viola, L. Rea, J.R. Hoskins & S. Wickner, (2014) Location of dual sites in *E. coli* FtsZ important for degradation by ClpXP; one at the C-terminus and one in the disordered linker. *PLoS One* **9**: e94964.

Carniol, K., S. Ben-Yehuda, N. King & R. Losick, (2005) Genetic dissection of the sporulation protein SpoIIE and its role in asymmetric division in *Bacillus subtilis*. *J Bacteriol* **187**: 3511-3520.

Chater, K.F., (2001) Regulation of sporulation in *Streptomyces coelicolor* A3(2): a checkpoint multiplex? *Curr Opin Microbiol* **4**: 667-673.

Claessen, D., D.E. Rozen, O.P. Kuipers, L. Sogaard-Andersen & G.P. van Wezel, (2014) Bacterial solutions to multicellularity: a tale of biofilms, filaments and fruiting bodies. *Nat Rev Microbiol* **12**: 115-124.

Collier, J., (2016) Cell cycle control in *Alphaproteobacteria*. *Curr Opin Microbiol* **30**: 107-113.

Cordell, S.C., E.J. Robinson & J. Lowe, (2003) Crystal structure of the SOS cell division inhibitor SulA and in complex with FtsZ. *Proc Natl Acad Sci U S A* **100**: 7889-7894.

Crawford, E.W., Jr. & L.J. Shimkets, (2000a) The *Myxococcus xanthus socE* and *csgA* genes are regulated by the stringent response. *Mol Microbiol* **37**: 788-799.

Crawford, E.W., Jr. & L.J. Shimkets, (2000b) The stringent response in *Myxococcus xanthus* is regulated by SocE and the CsgA C-signaling protein. *Genes & development* **14**: 483-492.

Cunningham, K.A. & W.F. Burkholder, (2009) The histidine kinase inhibitor Sda binds near the site of autophosphorylation and may sterically hinder autophosphorylation and phosphotransfer to Spo0F. *Mol Microbiol* **71**: 659-677.

Dai, K. & J. Lutkenhaus, (1991) *ftsZ* is an essential cell division gene in *Escherichia coli*. *J Bacteriol* **173**: 3500-3506.
Dai, K. & J. Lutkenhaus, (1992) The proper ratio of FtsZ to FtsA is required for cell division to occur in *Escherichia coli*. *J Bacteriol* **174**: 6145-6151.
de Boer, P., R. Crossley & L. Rothfield, (1992a) The essential bacterial cell-division protein FtsZ is a GTPase. *Nature* **359**: 254-256.
de Boer, P.A., R.E. Crossley, A.R. Hand & L.I. Rothfield, (1991) The MinD protein is a membrane ATPase required for the correct placement of the Escherichia coli division site. *EMBO J* **10**: 4371-4380.
de Boer, P.A., R.E. Crossley & L.I. Rothfield, (1992b) Roles of MinC and MinD in the site-specific septation block mediated by the MinCDE system of *Escherichia coli*. *J Bacteriol* **174**: 63-70.
Del Sol, R., J.G. Mullins, N. Grantcharova, K. Flardh & P. Dyson, (2006) Influence of CrgA on assembly of the cell division protein FtsZ during development of *Streptomyces coelicolor*. *J Bacteriol* **188**: 1540-1550.
Dewar, S.J., K.J. Begg & W.D. Donachie, (1992) Inhibition of cell division initiation by an imbalance in the ratio of FtsA to FtsZ. *J Bacteriol* **174**: 6314-6316.
Dewar, S.J. & R. Dorazi, (2000) Control of division gene expression in *Escherichia coli*. *FEMS microbiology letters* **187**: 1-7.
Diodati, M.E., F. Ossa, N.B. Caberoy, I.R. Jose, W. Hiraiwa, M.M. Igo, M. Singer & A.G. Garza, (2006) Nla18, a key regulatory protein required for normal growth and development of *Myxococcus xanthus*. *J Bacteriol* **188**: 1733-1743.
Domian, I.J., K.C. Quon & L. Shapiro, (1997) Cell type-specific phosphorylation and proteolysis of a transcriptional regulator controls the G1-to-S transition in a bacterial cell cycle. *Cell* **90**: 415-424.
Donczew, M., P. Mackiewicz, A. Wrobel, K. Flardh, J. Zakrzewska-Czerwinska & D. Jakimowicz, (2016) ParA and ParB coordinate chromosome segregation with cell elongation and division during *Streptomyces* sporulation. *Open biology* **6**: 150263.
Duan, Y., J.D. Huey & J.K. Herman, (2016) The DnaA inhibitor SirA acts in the same pathway as Soj (ParA) to facilitate *oriC* segregation during *Bacillus subtilis* sporulation. *Mol Microbiol* **102**: 530-544.
Duncan, L., S. Alper, F. Arigoni, R. Losick & P. Stragier, (1995) Activation of cell-specific transcription by a serine phosphatase at the site of asymmetric division. *Science* **270**: 641-644.
Dworkin, M., (1962) Nutritional requirements for vegetative growth of *Myxococcus xanthus*. *J Bacteriol* **84**: 250-257.
Dworkin, M. & S.M. Gibson, (1964) A System for Studying Microbial Morphogenesis: Rapid Formation of Microcysts in *Myxococcus xanthus*. *Science* **146**: 243-244.
Dworkin, M. & H. Voelz, (1962) The formation and germination of microcysts in *Myxococcus xanthus*. *J Gen Microbiol* **28**: 81-85.
Edwards, D.H. & J. Errington, (1997) The *Bacillus subtilis* DivIVA protein targets to the division septum and controls the site specificity of cell division. *Mol Microbiol* **24**: 905-915.
Ellehauge, E., M. Norregaard-Madsen & L. Sogaard-Andersen, (1998) The FruA signal transduction protein provides a checkpoint for the temporal co-ordination of intercellular signals in *Myxococcus xanthus* development. *Mol Microbiol* **30**: 807-817.
Erickson, H.P., D.E. Anderson & M. Osawa, (2010) FtsZ in bacterial cytokinesis: cytoskeleton and force generator all in one. *Microbiol Mol Biol Rev* **74**: 504-528.

Erickson, H.P., D.W. Taylor, K.A. Taylor & D. Bramhill, (1996) Bacterial cell division protein FtsZ assembles into protofilament sheets and minirings, structural homologs of tubulin polymers. *Proc Natl Acad Sci U S A* **93**: 519-523.

Errington, J., (1993) *Bacillus subtilis* sporulation: regulation of gene expression and control of morphogenesis. *Microbiological reviews* **57**: 1-33.

Fadda, D., C. Pischedda, F. Caldara, M.B. Whalen, D. Anderluzzi, E. Domenici & O. Massidda, (2003) Characterization of *divIVA* and other genes located in the chromosomal region downstream of the *dcw* cluster in *Streptococcus pneumoniae*. *J Bacteriol* **185**: 6209-6214.

Feng, J., S. Michalik, A.N. Varming, J.H. Andersen, D. Albrecht, L. Jelsbak, S. Krieger, K. Ohlsen, M. Hecker, U. Gerth, H. Ingmer & D. Frees, (2013) Trapping and proteomic identification of cellular substrates of the ClpP protease in *Staphylococcus aureus*. *Journal of proteome research* **12**: 547-558.

Ferullo, D.J., D.L. Cooper, H.R. Moore & S.T. Lovett, (2009) Cell cycle synchronization of *Escherichia coli* using the stringent response, with fluorescence labeling assays for DNA content and replication. *Methods* **48**: 8-13.

Flärdh, K. & M.J. Buttner, (2009) *Streptomyces* morphogenetics: dissecting differentiation in a filamentous bacterium. *Nat Rev Microbiol* **7**: 36-49.

Flärdh, K., T. Garrido & M. Vicente, (1997) Contribution of individual promoters in the *ddlB-ftsZ* region to the transcription of the essential cell-division gene *ftsZ* in *Escherichia coli*. *Mol Microbiol* **24**: 927-936.

Flärdh, K., E. Leibovitz, M.J. Buttner & K.F. Chater, (2000) Generation of a non-sporulating strain of *Streptomyces coelicolor* A3(2) by the manipulation of a developmentally controlled *ftsZ* promoter. *Mol Microbiol* **38**: 737-749.

Fleurie, A., C. Lesterlin, S. Manuse, C. Zhao, C. Cluzel, J.P. Lavergne, M. Franz-Wachtel, B. Macek, C. Combet, E. Kuru, M.S. VanNieuwenhze, Y.V. Brun, D. Sherratt & C. Grangeasse, (2014) MapZ marks the division sites and positions FtsZ rings in *Streptococcus pneumoniae*. *Nature* **516**: 259-262.

Fogel, M.A. & M.K. Waldor, (2006) A dynamic, mitotic-like mechanism for bacterial chromosome segregation. *Genes & development* **20**: 3269-3282.

Francis, F., S. Ramirez-Arcos, H. Salimnia, C. Victor & J.R. Dillon, (2000) Organization and transcription of the division cell wall (*dcw*) cluster in *Neisseria gonorrhoeae*. *Gene* **251**: 141-151.

Garrido, T., M. Sanchez, P. Palacios, M. Aldea & M. Vicente, (1993) Transcription of *ftsZ* oscillates during the cell cycle of *Escherichia coli*. *EMBO J* **12**: 3957-3965.

Garza, A.G., J.S. Pollack, B.Z. Harris, A. Lee, I.M. Keseler, E.F. Licking & M. Singer, (1998) SdeK is required for early fruiting body development in *Myxococcus xanthus*. *J Bacteriol* **180**: 4628-4637.

Giglio, K.M., N. Caberoy, G. Suen, D. Kaiser & A.G. Garza, (2011) A cascade of coregulating enhancer binding proteins initiates and propagates a multicellular developmental program. *Proc Natl Acad Sci U S A* **108**: E431-439.

Giglio, K.M., C. Zhu, C. Klunder, S. Kummer & A.G. Garza, (2015) The enhancer binding protein Nla6 regulates developmental genes that are important for *Myxococcus xanthus* sporulation. *J Bacteriol* **197**: 1276-1287.

Goehring, N.W. & J. Beckwith, (2005) Diverse paths to midcell: assembly of the bacterial cell division machinery. *Current Biology* **15**: R514-526.

Gomez-Santos, N., A. Treuner-Lange, A. Moraleda-Munoz, E. Garcia-Bravo, R. Garcia-Hernandez, M. Martinez-Cayuela, J. Perez, L. Sogaard-Andersen & J. Munoz-Dorado, (2012) Comprehensive set of integrative plasmid vectors for copper-inducible gene expression in *Myxococcus xanthus*. *Appl Environ Microbiol* **78**: 2515-2521.

Gonzalez, D. & J. Collier, (2013) DNA methylation by CcrM activates the transcription of two genes required for the division of *Caulobacter crescentus*. *Mol Microbiol* **88**: 203-218.

Gonzy-Treboul, G., C. Karmazyn-Campelli & P. Stragier, (1992) Developmental regulation of transcription of the *Bacillus subtilis ftsAZ* operon. *J Mol Biol* **224**: 967-979.

Grantcharova, N., U. Lustig & K. Flardh, (2005) Dynamics of FtsZ assembly during sporulation in *Streptomyces coelicolor* A3(2). *J Bacteriol* **187**: 3227-3237.

Gregory, J.A., E.C. Becker & K. Pogliano, (2008) *Bacillus subtilis* MinC destabilizes FtsZ-rings at new cell poles and contributes to the timing of cell division. *Genes & development* **22**: 3475-3488.

Gronewold, T.M. & D. Kaiser, (2001) The act operon controls the level and time of C-signal production for *Myxococcus xanthus* development. *Mol Microbiol* **40**: 744-756.

Grünenfelder, B., G. Rummel, J. Vohradsky, D. Roder, H. Langen & U. Jenal, (2001) Proteomic analysis of the bacterial cell cycle. *Proc Natl Acad Sci U S A* **98**: 4681-4686.

Gust, B., G.L. Challis, K. Fowler, T. Kieser & K.F. Chater, (2003) PCR-targeted *Streptomyces* gene replacement identifies a protein domain needed for biosynthesis of the sesquiterpene soil odor geosmin. *Proc Natl Acad Sci U S A* **100**: 1541-1546.

Haeusser, D.P., R.L. Schwartz, A.M. Smith, M.E. Oates & P.A. Levin, (2004) EzrA prevents aberrant cell division by modulating assembly of the cytoskeletal protein FtsZ. *Mol Microbiol* **52**: 801-814.

Hale, C.A. & P.A. de Boer, (1997) Direct binding of FtsZ to ZipA, an essential component of the septal ring structure that mediates cell division in *E. coli*. *Cell* **88**: 175-185.

Hamoen, L.W., J.C. Meile, W. de Jong, P. Noirot & J. Errington, (2006) SepF, a novel FtsZ-interacting protein required for a late step in cell division. *Mol Microbiol* **59**: 989-999.

Handler, A.A., J.E. Lim & R. Losick, (2008) Peptide inhibitor of cytokinesis during sporulation in *Bacillus subtilis*. *Mol Microbiol* **68**: 588-599.

Haney, S.A., E. Glasfeld, C. Hale, D. Keeney, Z. He & P. de Boer, (2001) Genetic analysis of the *Escherichia coli* FtsZ-ZipA interaction in the yeast two-hybrid system. Characterization of FtsZ residues essential for the interactions with ZipA and with FtsA. *J Biol Chem* **276**: 11980-11987.

Harms, A., A. Treuner-Lange, D. Schumacher & L. Sogaard-Andersen, (2013) Tracking of chromosome and replisome dynamics in *Myxococcus xanthus* reveals a novel chromosome arrangement. *PLoS Genet* **9**: e1003802.

Harris, B.Z., D. Kaiser & M. Singer, (1998) The guanosine nucleotide (p)ppGpp initiates development and A-factor production in *Myxococcus xanthus*. *Genes & development* **12**: 1022-1035.

Hauser, P.M. & D. Karamata, (1992) A method for the determination of bacterial spore DNA content based on isotopic labelling, spore germination and diphenylamine assay; ploidy of spores of several *Bacillu*s species. *Biochimie* **74**: 723-733.

Higgs, P.I., P.L. Hartzell, C. Holkenbrink and E. Hoiczyk, (2014) *Myxococcus xanthus* vegetative and developmental cell heterogeneity. In: Myxobacteria: Genomics, Cellular and Molecular Biology. pp. 51-77.

Higo, A., H. Hara, S. Horinouchi & Y. Ohnishi, (2012) Genome-wide distribution of AdpA, a global regulator for secondary metabolism and morphological differentiation in *Streptomyces*, revealed the extent and complexity of the AdpA

regulatory network. *DNA research : an international journal for rapid publication of reports on genes and genomes* **19**: 259-273.

Hilbert, D.W. & P.J. Piggot, (2004) Compartmentalization of gene expression during *Bacillus subtilis* spore formation. *Microbiol Mol Biol Rev* **68**: 234-262.

Hill, N.S., P.J. Buske, Y. Shi & P.A. Levin, (2013) A moonlighting enzyme links *Escherichia coli* cell size with central metabolism. *PLoS Genet* **9**: e1003663.

Hodgkin, J. & D. Kaiser, (1977) Cell-to-cell stimulation of movement in nonmotile mutants of *Myxococcus*. *Proc Natl Acad Sci U S A* **74**: 2938-2942.

Hoiczyk, E., M.W. Ring, C.A. McHugh, G. Schwar, E. Bode, D. Krug, M.O. Altmeyer, J.Z. Lu & H.B. Bode, (2009) Lipid body formation plays a central role in cell fate determination during developmental differentiation of *Myxococcus xanthus*. *Mol Microbiol* **74**: 497-517.

Holeckova, N., L. Doubravova, O. Massidda, V. Molle, K. Buriankova, O. Benada, O. Kofronova, A. Ulrych & P. Branny, (2014) LocZ is a new cell division protein involved in proper septum placement in *Streptococcus pneumoniae*. *mBio* **6**: e01700-01714.

Hu, Z. & J. Lutkenhaus, (2001) Topological regulation of cell division in E. coli. spatiotemporal oscillation of MinD requires stimulation of its ATPase by MinE and phospholipid. *Mol Cell* **7**: 1337-1343.

Hu, Z., A. Mukherjee, S. Pichoff & J. Lutkenhaus, (1999) The MinC component of the division site selection system in *Escherichia coli* interacts with FtsZ to prevent polymerization. *Proc Natl Acad Sci U S A* **96**: 14819-14824.

Huisman, O., R. D'Ari & S. Gottesman, (1984) Cell-division control in *Escherichia coli*: specific induction of the SOS function SfiA protein is sufficient to block septation. *Proc Natl Acad Sci U S A* **81**: 4490-4494.

Huntley, S., N. Hamann, S. Wegener-Feldbrugge, A. Treuner-Lange, M. Kube, R. Reinhardt, S. Klages, R. Muller, C.M. Ronning, W.C. Nierman & L. Sogaard-Andersen, (2011) Comparative genomic analysis of fruiting body formation in *Myxococcales*. *Molecular biology and evolution* **28**: 1083-1097.

Hurley, K.A., T.M. Santos, G.M. Nepomuceno, V. Huynh, J.T. Shaw & D.B. Weibel, (2016) Targeting the Bacterial Division Protein FtsZ. *Journal of medicinal chemistry* **59**: 6975-6998.

Iniesta, A.A., F. Garcia-Heras, J. Abellon-Ruiz, A. Gallego-Garcia & M. Elias-Arnanz, (2012) Two systems for conditional gene expression in *Myxococcus xanthus* inducible by isopropyl-beta-D-thiogalactopyranoside or vanillate. *J Bacteriol* **194**: 5875-5885.

Inouye, M., S. Inouye & D.R. Zusman, (1979a) Biosynthesis and self-assembly of protein S, a development-specific protein of *Myxococcus xanthus*. *Proc Natl Acad Sci U S A* **76**: 209-213.

Inouye, M., S. Inouye & D.R. Zusman, (1979b) Gene expression during development of *Myxococcus xanthus*: pattern of protein synthesis. *Developmental biology* **68**: 579-591.

Ishikawa, S., Y. Kawai, K. Hiramatsu, M. Kuwano & N. Ogasawara, (2006) A new FtsZ-interacting protein, YlmF, complements the activity of FtsA during progression of cell division in *Bacillus subtilis*. *Mol Microbiol* **60**: 1364-1380.

Jakimowicz, D., K. Chater & J. Zakrzewska-Czerwinska, (2002) The ParB protein of *Streptomyces coelicolor* A3(2) recognizes a cluster of *parS* sequences within the origin-proximal region of the linear chromosome. *Mol Microbiol* **45**: 1365-1377.

Jakimowicz, D., B. Gust, J. Zakrzewska-Czerwinska & K.F. Chater, (2005) Developmental-stage-specific assembly of ParB complexes in *Streptomyces coelicolor* hyphae. *J Bacteriol* **187**: 3572-3580.

Jakimowicz, D., S. Mouz, J. Zakrzewska-Czerwinska & K.F. Chater, (2006) Developmental control of a *parAB* promoter leads to formation of sporulation-associated ParB complexes in *Streptomyces coelicolor*. *J Bacteriol* **188**: 1710-1720.

Jakimowicz, D., P. Zydek, A. Kois, J. Zakrzewska-Czerwinska & K.F. Chater, (2007) Alignment of multiple chromosomes along helical ParA scaffolding in sporulating *Streptomyces* hyphae. *Mol Microbiol* **65**: 625-641.

Jelsbak, L., M. Givskov & D. Kaiser, (2005) Enhancer-binding proteins with a forkhead-associated domain and the sigma54 regulon in *Myxococcus xanthus* fruiting body development. *Proc Natl Acad Sci U S A* **102**: 3010-3015.

Jelsbak, L. & L. Sogaard-Andersen, (2003) Cell behavior and cell-cell communication during fruiting body morphogenesis in *Myxococcus xanthus*. *J Microbiol Meth* **55**: 829-839.

Jensen, R.B. & L. Shapiro, (1999) The *Caulobacter crescentus smc* gene is required for cell cycle progression and chromosome segregation. *Proc Natl Acad Sci U S A* **96**: 10661-10666.

Julien, B., A.D. Kaiser & A. Garza, (2000) Spatial control of cell differentiation in *Myxococcus xanthus*. *Proc Natl Acad Sci U S A* **97**: 9098-9103.

Justice, S.S., J. Garcia-Lara & L.I. Rothfield, (2000) Cell division inhibitors SulA and MinC/MinD block septum formation at different steps in the assembly of the *Escherichia coli* division machinery. *Mol Microbiol* **37**: 410-423.

Kaiser, D., (1979) Social gliding is correlated with the presence of pili in *Myxococcus xanthus*. *Proc Natl Acad Sci U S A* **76**: 5952-5956.

Kaiser, D., (2004) Signaling in myxobacteria. *Annual review of microbiology* **58**: 75-98.

Kawai, Y., S. Moriya & N. Ogasawara, (2003) Identification of a protein, YneA, responsible for cell division suppression during the SOS response in *Bacillus subtilis*. *Mol Microbiol* **47**: 1113-1122.

Kelly, A.J., M.J. Sackett, N. Din, E. Quardokus & Y.V. Brun, (1998) Cell cycle-dependent transcriptional and proteolytic regulation of FtsZ in *Caulobacter*. *Genes & development* **12**: 880-893.

Keseler, I.M. & D. Kaiser, (1995) An early A-signal-dependent gene in *Myxococcus xanthus* has a sigma 54-like promoter. *J Bacteriol* **177**: 4638-4644.

Kiekebusch, D., K.A. Michie, L.O. Essen, J. Lowe & M. Thanbichler, (2012) Localized dimerization and nucleoid binding drive gradient formation by the bacterial cell division inhibitor MipZ. *Mol Cell* **46**: 245-259.

Kim, H.J., M.J. Calcutt, F.J. Schmidt & K.F. Chater, (2000) Partitioning of the linear chromosome during sporulation of *Streptomyces coelicolor* A3(2) involves an *oriC*-linked *parAB* locus. *J Bacteriol* **182**: 1313-1320.

Kirstein, J., N. Moliere, D.A. Dougan & K. Turgay, (2009) Adapting the machine: adaptor proteins for Hsp100/Clp and AAA+ proteases. *Nat Rev Microbiol* **7**: 589-599.

Konovalova, A., (2010) Regulation of secretion of the signalling protease PopC in *Myxococcus xanthus*. *PhD thesis*.

Konovalova, A., S. Lobach & L. Sogaard-Andersen, (2012) A RelA-dependent two-tiered regulated proteolysis cascade controls synthesis of a contact-dependent intercellular signal in *Myxococcus xanthus*. *Mol Microbiol* **84**: 260-275.

Konovalova, A., L. Sogaard-Andersen & L. Kroos, (2014) Regulated proteolysis in bacterial development. *FEMS microbiology reviews* **38**: 493-522.

Kottel, R.H., K. Bacon, D. Clutter & D. White, (1975) Coats from *Myxococcus xanthus*: characterization and synthesis during myxospore differentiation. *J Bacteriol* **124**: 550-557.

Koushik, S.V., H. Chen, C. Thaler, H.L. Puhl, 3rd & S.S. Vogel, (2006) Cerulean, Venus, and VenusY67C FRET reference standards. *Biophysical journal* **91**: L99-L101.

Kroos, L., (2007) The *Bacillus* and *Myxococcus* developmental networks and their transcriptional regulators. *Annual review of genetics* **41**: 13-39.

Kroos, L., (2017) Highly Signal-Responsive Gene Regulatory Network Governing *Myxococcus* Development. *Trends in genetics : TIG* **33**: 3-15.

Kroos, L. & D. Kaiser, (1987) Expression of many developmentally regulated genes in *Myxococcus* depends on a sequence of cell interactions. *Genes & development* **1**: 840-854.

Kuner, J.M. & D. Kaiser, (1982) Fruiting Body Morphogenesis in Submerged Cultures of *Myxococcus xanthus*. *Journal of Bacteriology* **151**: 458-461.

Kuroda, A., K. Nomura, N. Takiguchi, J. Kato & H. Ohtake, (2006) Inorganic polyphosphate stimulates lon-mediated proteolysis of nucleoid proteins in *Escherichia coli*. *Cellular and molecular biology* **52**: 23-29.

Kuspa, A., L. Plamann & D. Kaiser, (1992a) Identification of heat-stable A-factor from *Myxococcus xanthus*. *J Bacteriol* **174**: 3319-3326.

Kuspa, A., L. Plamann & D. Kaiser, (1992b) A-signalling and the cell density requirement for *Myxococcus xanthus* development. *J Bacteriol* **174**: 7360-7369.

Laemmli, U.K., (1970) Cleavage of structural proteins during the assembly of the head of bacteriophage T4. *Nature* **227**: 680-685.

Lau, I.F., S.R. Filipe, B. Soballe, O.A. Okstad, F.X. Barre & D.J. Sherratt, (2003) Spatial and temporal organization of replicating Escherichia coli chromosomes. *Mol Microbiol* **49**: 731-743.

Laub, M.T., S.L. Chen, L. Shapiro & H.H. McAdams, (2002) Genes directly controlled by CtrA, a master regulator of the *Caulobacter* cell cycle. *Proc Natl Acad Sci U S A* **99**: 4632-4637.

LeDeaux, J.R., N. Yu & A.D. Grossman, (1995) Different roles for KinA, KinB, and KinC in the initiation of sporulation in *Bacillus subtilis*. *J Bacteriol* **177**: 861-863.

Lee, B., C. Holkenbrink, A. Treuner-Lange & P.I. Higgs, (2012) *Myxococcus xanthus* developmental cell fate production: heterogeneous accumulation of developmental regulatory proteins and reexamination of the role of MazF in developmental lysis. *J Bacteriol* **194**: 3058-3068.

Lee, B., P. Mann, V. Grover, A. Treuner-Lange, J. Kahnt & P.I. Higgs, (2011) The *Myxococcus xanthus* spore cuticula protein C is a fragment of FibA, an extracellular metalloprotease produced exclusively in aggregated cells. *PLoS One* **6**: e28968.

Lenarcic, R., S. Halbedel, L. Visser, M. Shaw, L.J. Wu, J. Errington, D. Marenduzzo & L.W. Hamoen, (2009) Localisation of DivIVA by targeting to negatively curved membranes. *EMBO J* **28**: 2272-2282.

Leslie, D.J., C. Heinen, F.D. Schramm, M. Thüring, C.D. Aakre, S.M. Murray, M.T. Laub & K. Jonas, (2015) Nutritional Control of DNA Replication Initiation through the Proteolysis and Regulated Translation of DnaA. *PLoS Genet* **11**: e1005342.

Letek, M., E. Ordonez, M. Fiuza, P. Honrubia-Marcos, J. Vaquera, J.A. Gil, D. Castro & L.M. Mateos, (2007) Characterization of the promoter region of *ftsZ* from *Corynebacterium glutamicum* and controlled overexpression of FtsZ. *International microbiology : the official journal of the Spanish Society for Microbiology* **10**: 271-282.

Levin, P.A., I.G. Kurtser & A.D. Grossman, (1999) Identification and characterization of a negative regulator of FtsZ ring formation in *Bacillus subtilis*. *Proc Natl Acad Sci U S A* **96**: 9642-9647.

Levin, P.A. & R. Losick, (1996) Transcription factor Spo0A switches the localization of the cell division protein FtsZ from a medial to a bipolar pattern in *Bacillus subtilis*. *Genes & development* **10**: 478-488.

Li, Y., K. Sergueev & S. Austin, (2002) The segregation of the *Escherichia coli* origin and terminus of replication. *Mol Microbiol* **46**: 985-996.

Lim, H.C., I.V. Surovtsev, B.G. Beltran, F. Huang, J. Bewersdorf & C. Jacobs-Wagner, (2014) Evidence for a DNA-relay mechanism in ParABS-mediated chromosome segregation. *eLife* **3**: e02758.

Liu, Z., A. Mukherjee & J. Lutkenhaus, (1999) Recruitment of ZipA to the division site by interaction with FtsZ. *Mol Microbiol* **31**: 1853-1861.

Livny, J., Y. Yamaichi & M.K. Waldor, (2007) Distribution of centromere-like parS sites in bacteria: insights from comparative genomics. *J Bacteriol* **189**: 8693-8703.

Lobedanz, S. & L. Sogaard-Andersen, (2003) Identification of the C-signal, a contact-dependent morphogen coordinating multiple developmental responses in *Myxococcus xanthus*. *Genes & development* **17**: 2151-2161.

Loose, M. & T.J. Mitchison, (2014) The bacterial cell division proteins FtsA and FtsZ self-organize into dynamic cytoskeletal patterns. *Nature cell biology* **16**: 38-46.

Lopez, D. & R. Kolter, (2010) Extracellular signals that define distinct and coexisting cell fates in *Bacillus subtilis*. *FEMS microbiology reviews* **34**: 134-149.

Lu, C., M. Reedy & H.P. Erickson, (2000) Straight and curved conformations of FtsZ are regulated by GTP hydrolysis. *J Bacteriol* **182**: 164-170.

Lyons, N.A. & R. Kolter, (2015) On the evolution of bacterial multicellularity. *Curr Opin Microbiol* **24**: 21-28.

Manoil, C. & D. Kaiser, (1980a) Accumulation of guanosine tetraphosphate and guanosine pentaphosphate in *Myxococcus xanthus* during starvation and myxospore formation. *J Bacteriol* **141**: 297-304.

Manoil, C. & D. Kaiser, (1980b) Guanosine pentaphosphate and guanosine tetraphosphate accumulation and induction of *Myxococcus xanthus* fruiting body development. *J Bacteriol* **141**: 305-315.

Marston, A.L. & J. Errington, (1999) Dynamic movement of the ParA-like Soj protein of *B. subtilis* and its dual role in nucleoid organization and developmental regulation. *Mol Cell* **4**: 673-682.

Marston, A.L., H.B. Thomaides, D.H. Edwards, M.E. Sharpe & J. Errington, (1998) Polar localization of the MinD protein of *Bacillus subtilis* and its role in selection of the mid-cell division site. *Genes & development* **12**: 3419-3430.

McCleary, W.R., B. Esmon & D.R. Zusman, (1991) *Myxococcus xanthus* protein C is a major spore surface protein. *J Bacteriol* **173**: 2141-2145.

Messer, W., (2002) The bacterial replication initiator DnaA. DnaA and *oriC*, the bacterial mode to initiate DNA replication. *FEMS microbiology reviews* **26**: 355-374.

Messer, W. & C. Weigel, (1997) DnaA initiator-also a transcription factor. *Mol Microbiol* **24**: 1-6.

Mittal, S. & L. Kroos, (2009) A combination of unusual transcription factors binds cooperatively to control *Myxococcus xanthus* developmental gene expression. *Proc Natl Acad Sci U S A* **106**: 1965-1970.

Mohl, D.A. & J.W. Gober, (1997) Cell cycle-dependent polar localization of chromosome partitioning proteins in *Caulobacter crescentus*. *Cell* **88**: 675-684.

Mott, M.L. & J.M. Berger, (2007) DNA replication initiation: mechanisms and regulation in bacteria. *Nat Rev Microbiol* **5**: 343-354.

Mukherjee, A. & J. Lutkenhaus, (1994) Guanine nucleotide-dependent assembly of FtsZ into filaments. *J Bacteriol* **176**: 2754-2758.

Mukherjee, S., A.C. Bree, J. Liu, J.E. Patrick, P. Chien & D.B. Kearns, (2015) Adaptor-mediated Lon proteolysis restricts *Bacillus subtilis* hyperflagellation. *Proc Natl Acad Sci U S A* **112**: 250-255.

Müller, F.D., C.W. Schink, E. Hoiczyk, E. Cserti & P.I. Higgs, (2012) Spore formation in *Myxococcus xanthus* is tied to cytoskeleton functions and polysaccharide spore coat deposition. *Mol Microbiol* **83**: 486-505.

Müller, F.D., A. Treuner-Lange, J. Heider, S.M. Huntley & P.I. Higgs, (2010) Global transcriptome analysis of spore formation in *Myxococcus xanthus* reveals a locus necessary for cell differentiation. *BMC genomics* **11**: 264.

Munoz-Dorado, J., F.J. Marcos-Torres, E. Garcia-Bravo, A. Moraleda-Munoz & J. Perez, (2016) Myxobacteria: Moving, Killing, Feeding, and Surviving Together. *Frontiers in microbiology* **7**: 781.

Nariya, H. & M. Inouye, (2008) MazF, an mRNA interferase, mediates programmed cell death during multicellular *Myxococcus* development. *Cell* **132**: 55-66.

Ni, T., F. Ye, X. Liu, J. Zhang, H. Liu, J. Li, Y. Zhang, Y. Sun, M. Wang, C. Luo, H. Jiang, L. Lan, J. Gan, A. Zhang, H. Zhou & C.G. Yang, (2016) Characterization of Gain-of-Function Mutant Provides New Insights into ClpP Structure. *ACS chemical biology* **11**: 1964-1972.

Nogales, E., K.H. Downing, L.A. Amos & J. Lowe, (1998) Tubulin and FtsZ form a distinct family of GTPases. *Nat Struct Biol* **5**: 451-458.

Nordstrom, K., R. Bernander & S. Dasgupta, (1991) The *Escherichia coli* cell cycle: one cycle or multiple independent processes that are co-ordinated? *Mol Microbiol* **5**: 769-774.

O'Connor, K.A. & D.R. Zusman, (1991a) Behavior of peripheral rods and their role in the life cycle of *Myxococcus xanthus*. *J Bacteriol* **173**: 3342-3355.

O'Connor, K.A. & D.R. Zusman, (1991b) Development in *Myxococcus xanthus* involves differentiation into two cell types, peripheral rods and spores. *J Bacteriol* **173**: 3318-3333.

Oliva, M.A., S.C. Cordell & J. Lowe, (2004) Structural insights into FtsZ protofilament formation. *Nat Struct Mol Biol* **11**: 1243-1250.

Ossa, F., M.E. Diodati, N.B. Caberoy, K.M. Giglio, M. Edmonds, M. Singer & A.G. Garza, (2007) The *Myxococcus xanthus* Nla4 protein is important for expression of stringent response-associated genes, ppGpp accumulation, and fruiting body development. *J Bacteriol* **189**: 8474-8483.

Overgaard, M., S. Wegener-Feldbrugge & L. Sogaard-Andersen, (2006) The orphan response regulator DigR is required for synthesis of extracellular matrix fibrils in *Myxococcus xanthus*. *J Bacteriol* **188**: 4384-4394.

Pazos, M., P. Natale & M. Vicente, (2013) A specific role for the ZipA protein in cell division: stabilization of the FtsZ protein. *J Biol Chem* **288**: 3219-3226.

Pesavento, C. & R. Hengge, (2009) Bacterial nucleotide-based second messengers. *Curr Opin Microbiol* **12**: 170-176.

Pichoff, S. & J. Lutkenhaus, (2002) Unique and overlapping roles for ZipA and FtsA in septal ring assembly in *Escherichia coli*. *EMBO J* **21**: 685-693.

Pichoff, S. & J. Lutkenhaus, (2005) Tethering the Z ring to the membrane through a conserved membrane targeting sequence in FtsA. *Mol Microbiol* **55**: 1722-1734.

Piggot, P.J. & D.W. Hilbert, (2004) Sporulation of *Bacillus subtilis*. *Curr Opin Microbiol* **7**: 579-586.

Pinho, M.G. & J. Errington, (2003) Dispersed mode of *Staphylococcus aureus* cell wall synthesis in the absence of the division machinery. *Mol Microbiol* **50**: 871-881.

Pomerantz, R.T. & M. O'Donnell, (2007) Replisome mechanics: insights into a twin DNA polymerase machine. *Trends Microbiol* **15**: 156-164.

Potrykus, K. & M. Cashel, (2008) (p)ppGpp: still magical? *Annual review of microbiology* **62**: 35-51.

Ptacin, J.L. & L. Shapiro, (2010) Initiating bacterial mitosis: understanding the mechanism of ParA-mediated chromosome segregation. *Cell cycle* **9**: 4033-4034.

Radhakrishnan, S.K., M. Thanbichler & P.H. Viollier, (2008) The dynamic interplay between a cell fate determinant and a lysozyme homolog drives the asymmetric division cycle of *Caulobacter crescentus*. *Genes & development* **22**: 212-225.

Rahn-Lee, L., H. Merrikh, A.D. Grossman & R. Losick, (2011) The sporulation protein SirA inhibits the binding of DnaA to the origin of replication by contacting a patch of clustered amino acids. *J Bacteriol* **193**: 1302-1307.

Rajagopalan, R., Z. Sarwar, A. G. Garza & L. Kroos, (2014) Developmental Gene Regulation. In: Myxobacteria: Genomics, Cellular and Molecular Biology. pp.

Ramamurthi, K.S. & R. Losick, (2009) Negative membrane curvature as a cue for subcellular localization of a bacterial protein. *Proc Natl Acad Sci U S A* **106**: 13541-13545.

Raskin, D.M. & P.A. de Boer, (1999) MinDE-dependent pole-to-pole oscillation of division inhibitor MinC in *Escherichia coli*. *J Bacteriol* **181**: 6419-6424.

RayChaudhuri, D. & J.T. Park, (1992) *Escherichia coli* cell-division gene *ftsZ* encodes a novel GTP-binding protein. *Nature* **359**: 251-254.

Reyes-Lamothe, R., E. Nicolas & D.J. Sherratt, (2012) Chromosome replication and segregation in bacteria. *Annual review of genetics* **46**: 121-143.

Ring, M.W., G. Schwar, V. Thiel, J.S. Dickschat, R.M. Kroppenstedt, S. Schulz & H.B. Bode, (2006) Novel iso-branched ether lipids as specific markers of developmental sporulation in the myxobacterium *Myxococcus xanthus*. *J Biol Chem* **281**: 36691-36700.

Robinson, M., B. Son, D. Kroos & L. Kroos, (2014) Transcription factor MrpC binds to promoter regions of hundreds of developmentally-regulated genes in *Myxococcus xanthus*. *BMC genomics* **15**: 1123.

Rolbetzki, A., M. Ammon, V. Jakovljevic, A. Konovalova & L. Sogaard-Andersen, (2008) Regulated secretion of a protease activates intercellular signaling during fruiting body formation in *M. xanthus*. *Developmental cell* **15**: 627-634.

Romeo, J.M. & D.R. Zusman, (1991) Transcription of the myxobacterial hemagglutinin gene is mediated by a sigma 54-like promoter and a *cis*-acting upstream regulatory region of DNA. *J Bacteriol* **173**: 2969-2976.

Rosario, C.J. & M. Singer, (2007) The *Myxococcus xanthus* developmental program can be delayed by inhibition of DNA replication. *J Bacteriol* **189**: 8793-8800.

Rosario, C.J. & M. Singer, (2010) Developmental expression of *dnaA* is required for sporulation and timing of fruiting body formation in *Myxococcus xanthus*. *Mol Microbiol* **76**: 1322-1333.

Rosenberg, E., M. Katarski & P. Gottlieb, (1967) Deoxyribonucleic acid synthesis during exponential growth and microcyst formation in *Myxococcus xanthus*. *J Bacteriol* **93**: 1402-1408.

Roy, S. & P. Ajitkumar, (2005) Transcriptional analysis of the principal cell division gene, *ftsZ*, of *Mycobacterium tuberculosis*. *J Bacteriol* **187**: 2540-2550.

Ruban-Osmialowska, B., D. Jakimowicz, A. Smulczyk-Krawczyszyn, K.F. Chater & J. Zakrzewska-Czerwinska, (2006) Replisome localization in vegetative and aerial hyphae of *Streptomyces coelicolor*. *J Bacteriol* **188**: 7311-7316.

Rudner, D.Z. & R. Losick, (2001) Morphological coupling in development: lessons from prokaryotes. *Developmental cell* **1**: 733-742.

Rueda, S., M. Vicente & J. Mingorance, (2003) Concentration and assembly of the division ring proteins FtsZ, FtsA, and ZipA during the *Escherichia coli* cell cycle. *J Bacteriol* **185**: 3344-3351.

Ruvolo, M.V., K.E. Mach & W.F. Burkholder, (2006) Proteolysis of the replication checkpoint protein Sda is necessary for the efficient initiation of sporulation after transient replication stress in *Bacillus subtilis*. *Mol Microbiol* **60**: 1490-1508.

Ryter, A., B. Bloom & J.P. Aubert, (1966) Intracellular localization ribonucleic acids synthesized during sporulation in *Bacillus subtilis*. *Comptes rendus hebdomadaires des seances de l'Academie des sciences. Serie D: Sciences naturelles* **262**: 1305-1307.

Sass, P., M. Josten, K. Famulla, G. Schiffer, H.G. Sahl, L. Hamoen & H. Brotz-Oesterhelt, (2011) Antibiotic acyldepsipeptides activate ClpP peptidase to degrade the cell division protein FtsZ. *Proc Natl Acad Sci U S A* **108**: 17474-17479.

Scheffers, D. & A.J. Driessen, (2001) The polymerization mechanism of the bacterial cell division protein FtsZ. *FEBS letters* **506**: 6-10.

Schumacher, D., (2016) The PomXYZ cell division regulators self-organize on the nucleoid to position cell division at midcell in the rod-shaped bacterium *Myxococcus xanthus*. In., pp.

Schumacher, D., S. Bergeler, A. Harms, J. Vonck, S. Huneke-Vogt, E. Frey & L. Sogaard-Andersen, (2017) The PomXYZ Proteins Self-Organize on the Bacterial Nucleoid to Stimulate Cell Division. *Developmental cell* **41**: 299-314 e213.

Schwedock, J., J.R. McCormick, E.R. Angert, J.R. Nodwell & R. Losick, (1997) Assembly of the cell division protein FtsZ into ladder-like structures in the aerial hyphae of *Streptomyces coelicolor*. *Mol Microbiol* **25**: 847-858.

Serrano, M., A. Neves, C.M. Soares, C.P. Moran, Jr. & A.O. Henriques, (2004) Role of the anti-sigma factor SpoIIAB in regulation of sigmaG during *Bacillus subtilis* sporulation. *J Bacteriol* **186**: 4000-4013.

Shapiro, L. & R. Losick, (1997) Protein localization and cell fate in bacteria. *Science* **276**: 712-718.

Shen, B. & J. Lutkenhaus, (2009) The conserved C-terminal tail of FtsZ is required for the septal localization and division inhibitory activity of MinC(C)/MinD. *Mol Microbiol* **72**: 410-424.

Shereda, R.D., A.G. Kozlov, T.M. Lohman, M.M. Cox & J.L. Keck, (2008) SSB as an organizer/mobilizer of genome maintenance complexes. *Crit Rev Biochem Mol Biol* **43**: 289-318.

Sherratt, D.J., (2003) Bacterial chromosome dynamics. *Science* **301**: 780-785.

Shi, X., S. Wegener-Feldbrugge, S. Huntley, N. Hamann, R. Hedderich & L. Sogaard-Andersen, (2008) Bioinformatics and experimental analysis of proteins of two-component systems in *Myxococcus xanthus*. *J Bacteriol* **190**: 613-624.

Shimkets, L.J., (1990) Social and developmental biology of the Myxobacteria. *Microbiological reviews* **54**: 473-501.

Shimkets, L.J. & H. Rafiee, (1990) CsgA, an extracellular protein essential for *Myxococcus xanthus* development. *J Bacteriol* **172**: 5299-5306.

Singer, M. & D. Kaiser, (1995) Ectopic production of guanosine penta- and tetraphosphate can initiate early developmental gene expression in *Myxococcus xanthus*. *Genes & development* **9**: 1633-1644.

Singh, J.K., R.D. Makde, V. Kumar & D. Panda, (2007) A membrane protein, EzrA, regulates assembly dynamics of FtsZ by interacting with the C-terminal tail of FtsZ. *Biochemistry* **46**: 11013-11022.

Sinha, N.K. & D.P. Snustad, (1972) Mechanism of inhibition of deoxyribonucleic acid synthesis in *Escherichia coli* by hydroxyurea. *J Bacteriol* **112**: 1321-1324.

Sitnikov, D.M., J.B. Schineller & T.O. Baldwin, (1996) Control of cell division in *Escherichia coli*: regulation of transcription of *ftsQA* involves both *rpoS* and SdiA-mediated autoinduction. *Proc Natl Acad Sci U S A* **93**: 336-341.

Skotnicka, D., T. Petters, J. Heering, M. Hoppert, V. Kaever & L. Sogaard-Andersen, (2015) Cyclic Di-GMP Regulates Type IV Pilus-Dependent Motility in *Myxococcus xanthus*. *J Bacteriol* **198**: 77-90.

Skotnicka, D., G.T. Smaldone, T. Petters, E. Trampari, J. Liang, V. Kaever, J.G. Malone, M. Singer & L. Sogaard-Andersen, (2016) A Minimal Threshold of c-di-GMP Is Essential for Fruiting Body Formation and Sporulation in *Myxococcus xanthus*. *PLoS Genet* **12**: e1006080.

Sogaard-Andersen, L., F.J. Slack, H. Kimsey & D. Kaiser, (1996) Intercellular C-signaling in *Myxococcus xanthus* involves a branched signal transduction pathway. *Genes & development* **10**: 740-754.

Stricker, J., P. Maddox, E.D. Salmon & H.P. Erickson, (2002) Rapid assembly dynamics of the *Escherichia coli* FtsZ-ring demonstrated by fluorescence recovery after photobleaching. *Proc Natl Acad Sci U S A* **99**: 3171-3175.

Sudo, S.Z. & M. Dworkin, (1969) Resistance of vegetative cells and microcysts of *Myxococcus xanthus*. *J Bacteriol* **98**: 883-887.

Sugimoto, S., K. Yamanaka, S. Nishikori, A. Miyagi, T. Ando & T. Ogura, (2010) AAA+ chaperone ClpX regulates dynamics of prokaryotic cytoskeletal protein FtsZ. *J Biol Chem* **285**: 6648-6657.

Szeto, T.H., S.L. Rowland, C.L. Habrukowich & G.F. King, (2003) The MinD membrane targeting sequence is a transplantable lipid-binding helix. *J Biol Chem* **278**: 40050-40056.

Szeto, T.H., S.L. Rowland, L.I. Rothfield & G.F. King, (2002) Membrane localization of MinD is mediated by a C-terminal motif that is conserved across eubacteria, archaea, and chloroplasts. *Proc Natl Acad Sci U S A* **99**: 15693-15698.

Szwedziak, P., Q. Wang, T.A. Bharat, M. Tsim & J. Lowe, (2014) Architecture of the ring formed by the tubulin homologue FtsZ in bacterial cell division. *eLife* **3**: e04601.

Tan, I.S. & K.S. Ramamurthi, (2014) Spore formation in *Bacillus subtilis*. *Environmental microbiology reports* **6**: 212-225.

Thanbichler, M., (2010) Synchronization of chromosome dynamics and cell division in bacteria. *Cold Spring Harbor perspectives in biology* **2**: a000331.

Thanbichler, M. & L. Shapiro, (2006) MipZ, a spatial regulator coordinating chromosome segregation with cell division in *Caulobacter*. *Cell* **126**: 147-162.

Tojo, N., S. Inouye & T. Komano, (1993a) Cloning and nucleotide sequence of the *Myxococcus xanthus lon* gene: indispensability of *lon* for vegetative growth. *J Bacteriol* **175**: 2271-2277.

Tojo, N., S. Inouye & T. Komano, (1993b) The *lonD* gene is homologous to the *lon* gene encoding an ATP-dependent protease and is essential for the development of *Myxococcus xanthus*. *J Bacteriol* **175**: 4545-4549.

Treuner-Lange, A., K. Aguiluz, C. van der Does, N. Gomez-Santos, A. Harms, D. Schumacher, P. Lenz, M. Hoppert, J. Kahnt, J. Munoz-Dorado & L. Sogaard-Andersen, (2013) PomZ, a ParA-like protein, regulates Z-ring formation and cell division in *Myxococcus xanthus*. *Mol Microbiol* **87**: 235-253.

Treuner-Lange, A., L. Søgaard-Andersen, M. Singer, (2014) Cell Cycle Regulation in *Myxococcus xanthus* during vegetative growth and development: Regulatory links between DNA replication and cell division. In: Myxobateria: Genomics, Cellular and Molecular Biology. pp. 79-90.

Trusca, D., S. Scott, C. Thompson & D. Bramhill, (1998) Bacterial SOS checkpoint protein SulA inhibits polymerization of purified FtsZ cell division protein. *J Bacteriol* **180**: 3946-3953.

Tzeng, L., T.N. Ellis & M. Singer, (2006) DNA replication during aggregation phase is essential for *Myxococcus xanthus* development. *J Bacteriol* **188**: 2774-2779.

Tzeng, L. & M. Singer, (2005) DNA replication during sporulation in *Myxococcus xanthus* fruiting bodies. *Proc Natl Acad Sci U S A* **102**: 14428-14433.

Ueki, T. & S. Inouye, (2003) Identification of an activator protein required for the induction of *fruA*, a gene essential for fruiting body development in *Myxococcus xanthus*. *Proc Natl Acad Sci U S A* **100**: 8782-8787.

Ueki, T. & S. Inouye, (2005a) Activation of a development-specific gene, dofA, by FruA, an essential transcription factor for development of Myxococcus xanthus. *J Bacteriol* **187**: 8504-8506.

Ueki, T. & S. Inouye, (2005b) Identification of a gene involved in polysaccharide export as a transcription target of FruA, an essential factor for Myxococcus xanthus development. *J Biol Chem* **280**: 32279-32284.

van Baarle, S. & M. Bramkamp, (2010) The MinCDJ system in Bacillus subtilis prevents minicell formation by promoting divisome disassembly. *PLoS One* **5**: e9850.

van Vliet, S. & M. Ackermann, (2015) Bacterial Ventures into Multicellularity: Collectivism through Individuality. *PLoS biology* **13**: e1002162.

Veening, J.W., H. Murray & J. Errington, (2009) A mechanism for cell cycle regulation of sporulation initiation in *Bacillus subtilis*. *Genes & development* **23**: 1959-1970.

Viola, M.G., C.J. LaBreck, J. Conti & J.L. Camberg, (2017) Proteolysis-Dependent Remodeling of the Tubulin Homolog FtsZ at the Division Septum in *Escherichia coli*. *PLoS One* **12**: e0170505.

Viswanathan, P., T. Ueki, S. Inouye & L. Kroos, (2007) Combinatorial regulation of genes essential for Myxococcus xanthus development involves a response regulator and a LysR-type regulator. *Proc Natl Acad Sci U S A* **104**: 7969-7974.

Wang, X.D., P.A. de Boer & L.I. Rothfield, (1991) A factor that positively regulates cell division by activating transcription of the major cluster of essential cell division genes of Escherichia coli. *EMBO J* **10**: 3363-3372.

Weart, R.B., A.H. Lee, A.C. Chien, D.P. Haeusser, N.S. Hill & P.A. Levin, (2007) A metabolic sensor governing cell size in bacteria. *Cell* **130**: 335-347.

Weart, R.B., S. Nakano, B.E. Lane, P. Zuber & P.A. Levin, (2005) The ClpX chaperone modulates assembly of the tubulin-like protein FtsZ. *Mol Microbiol* **57**: 238-249.

Willemse, J., J.W. Borst, E. de Waal, T. Bisseling & G.P. van Wezel, (2011) Positive control of cell division: FtsZ is recruited by SsgB during sporulation of *Streptomyces*. *Genes & development* **25**: 89-99.

Willemse, J., A.M. Mommaas & G.P. van Wezel, (2012) Constitutive expression of *ftsZ* overrides the *whi* developmental genes to initiate sporulation of *Streptomyces coelicolor*. *Antonie Van Leeuwenhoek* **101**: 619-632.

Willemse, J. & G.P. van Wezel, (2009) Imaging of *Streptomyces coelicolor* A3(2) with reduced autofluorescence reveals a novel stage of FtsZ localization. *PLoS One* **4**: e4242.

Williams, B., N. Bhat, P. Chien & L. Shapiro, (2014) ClpXP and ClpAP proteolytic activity on divisome substrates is differentially regulated following the *Caulobacter* asymmetric cell division. *Mol Microbiol* **93**: 853-866.

Wireman, J.W. & M. Dworkin, (1977) Developmentally induced autolysis during fruiting body formation by *Myxococcus xanthus*. *J Bacteriol* **129**: 798-802.

Woese, C.R., (1958) Comparison of the x-ray sensitivity of bacterial spores. *J Bacteriol* **75**: 5-8.

Wolanski, M., D. Jakimowicz & J. Zakrzewska-Czerwinska, (2012) AdpA, key regulator for morphological differentiation regulates bacterial chromosome replication. *Open biology* **2**: 120097.

Wu, L.J. & J. Errington, (2003) RacA and the Soj-Spo0J system combine to effect polar chromosome segregation in sporulating *Bacillus subtilis*. *Mol Microbiol* **49**: 1463-1475.

Wu, L.J. & J. Errington, (2004) Coordination of cell division and chromosome segregation by a nucleoid occlusion protein in *Bacillus subtilis*. *Cell* **117**: 915-925.

Wu, L.J. & J. Errington, (2012) Nucleoid occlusion and bacterial cell division. *Nat Rev Microbiol* **10**: 8-12.

Wu, S.S., J. Wu & D. Kaiser, (1997) The *Myxococcus xanthus* pilT locus is required for social gliding motility although pili are still produced. *Mol Microbiol* **23**: 109-121.

Yang, X., Z. Lyu, A. Miguel, R. McQuillen, K.C. Huang & J. Xiao, (2017) GTPase activity-coupled treadmilling of the bacterial tubulin FtsZ organizes septal cell wall synthesis. *Science* **355**: 744-747.

Youderian, P., N. Burke, D.J. White & P.L. Hartzell, (2003) Identification of genes required for adventurous gliding motility in *Myxococcus xanthus* with the transposable element *mariner*. *Mol Microbiol* **49**: 555-570.

Zhang, H., N.N. Rao, T. Shiba & A. Kornberg, (2005) Inorganic polyphosphate in the social life of *Myxococcus xanthus*: motility, development, and predation. *Proc Natl Acad Sci U S A* **102**: 13416-13420.

Zhang, L., J. Willemse, D. Claessen & G.P. van Wezel, (2016) SepG coordinates sporulation-specific cell division and nucleoid organization in *Streptomyces coelicolor*. *Open biology* **6**: 150164.

Zusman, D. & E. Rosenberg, (1968) Deoxyribonucleic acid synthesis during microcyst germination in *Myxococcus xanthus*. *J Bacteriol* **96**: 981-986.

Zusman, D. & E. Rosenberg, (1970) DNA cycle of *Myxococcus xanthus*. *J Mol Biol* **49**: 609-619.

# 11. Acknowledgement/Danksagung

# 12. Curriculum Vitae

**List of publications:**

Schumacher, D., S. Bergeler, A. Harms, J. Vonck, **S. Huneke-Vogt**, E. Frey & L. Søgaard-Andersen, (2017) The PomXYZ Proteins Self-Organize on the Bacterial Nucleoid to Stimulate Cell Division. *Developmental cell* **41**: 299-314 e213.

**Huneke-Vogt, S.** & Søgaard-Andersen, L. (2017). Cell differentiation specific inhibition of cell division guarantees the formation of diploid spores in *Myxococcus xanthus*. (in preparation)

# 13. Erklärung

Hiermit versichere ich, dass ich die vorliegende Dissertation mit dem Titel

**“Cell differentiation specific inhibition of cell division guarantees the formation of diploid spores during development of *Myxococcus xanthus*”**

selbstständig verfasst, keine anderen als die im Text angegebenen Hilfsmittel verwendet und sämtliche Stellen, die dem Wortlaut oder dem Sinn nach aus anderen Werken entnommen sind, mit Quellenangabe kenntlich gemacht habe. Die Dissertation wurde in der jetzigen oder einer ähnlichen Form noch bei keiner anderen Hochschule eingereicht und hat noch keinem anderen Prüfungszweck gedient.

Marburg,den_____._____._____ _____

Sabrina Huneke-Vogt

# 14. Einverständniserklärung

Hiermit erkläre ich mich einverstanden, dass die vorliegende Dissertation mit dem Titel

**“Cell differentiation specific inhibition of cell division guarantees the formation of diploid spores during development of *Myxococcus xanthus*”**

in Bibliotheken zugänglich gemacht wird. Dazu gehört, dass sie

- von der Bibliothek der Einrichtung, in der meine Dissertation angefertigt wurde, zur Benutzung in ihren Räumen bereitgehalten wird;
- in konventionellen und maschinenlesbaren Katalogen, Verzeichnissen und Datenbanken verzeichnet wird;
- im Rahmen der urheberrechtlichen Bestimmungen für Kopierzwecke benutzt werden kann.

Marburg, den _____._____._____ _____

Sabrina Huneke-Vogt

_____

Prof. Dr. MD Lotte Søgaard-Andersen